OUKA
The University of Osaka
Institutional Knowledge Archive

Title	Machine-leaning Assisted Optimization for Organo-catalytic Reactions in Flow System
Author(s)	Hettiarachchige Dona, Piyumi Wathsala
Citation	大阪大学, 2021, 博士論文
Version Type	VoR
URL	https://doi.org/10.18910/85331
rights	
Note	

The University of Osaka Institutional Knowledge Archive : OUKA

https://ir.library.osaka-u.ac.jp/

The University of Osaka

Machine-learning Assisted Optimization for Organo-Catalytic Reactions in Flow System

Doctoral Thesis

By H. D. P. Wathsala

Department of Chemistry

Graduate School of Science

Osaka University

September 2021

Acknowledgment

The success of this study required the immense help of various individuals. Without them, my dream to complete this study would have remained a dream. Foremost, I would like to express my sincere gratitude to my supervisor, Prof. Hiroaki Sasai for the continuous support during my Ph.D. study and research. I take this opportunity to thank him for his patience, motivation, enthusiasm, and immense knowledge. His guidance helped me at all times of research and writing of this thesis. The author is also deeply indebted to her advisor, Associate professor Shinobu Takizawa, for his constant support, suggestions, experimental experience. His advice, encouragement, and valuable ideas extremely helped me to achieve this research. I also give special thanks to Assis. Prof. Masaru Kondo who is the co-author of the Machine learning programming part. His continuous support and advice helped me to complete this research. Additionally, I would like to appreciate Prof. Takashi Washio and the staff for their big effort in providing the programming and help us to correlate organic chemistry and machine learning together.

I would like to thank the former staff of Sasai laboratory, especially Associate Professor Assistant Professor Kazuhiro Takenaka, and Assistant Professor Makoto Sako for continuous assistance. My sincere thanks to my senior, Dr. Kishi, and Dr. Abozeid for teaching the fundamentals of organic chemistry and basic lab techniques. The author deeply appreciates the help received from the technical staff of the Comprehensive Analysis Center (CAC) at Osaka University

I would like to acknowledge all lab mates, for helping me with the analysis and interpretations. I take this opportunity to thank the team Sasai lab encouraged me and supported me throughout my research work. I would like to make a special mention of the secretary Mrs. Ayaka Honda who has enthusiastically helped with my backend work.

My sincere gratitude to my scholarships which I have during my Ph.D life. By awarding Ichikawa foundation scholarship and Rotary Yoneyama scholarship, that have lighted my financial burden, which allowed me to focus more on my research.

I would like to fondly thank my mother for having lived this dream of seeing me acquire this prestigious degree. Especially, I would like to thank my elder brother who always encourages, gave continuous advice and financial support equivalent to my father. It would be a dream if he is not in my life to obtain everything that I have today. Last but

not least I would like to thank my fiance Mr. Buddhika is my anchor and without whose caring support, I would never have completed this journey.

My degree is dedicated to my family. Without my family's blessings, this mission would never have been completed.

I thank my teachers, respondents, family, friends, and all my well-wishers who stood by me and gave me unconditional time and support.

H. D. P. Wathsala
Osaka University
2021

List of Abbreviations

Ac	acetyl
Aq	aqueous
Ar	aryl
BA	Brønsted acid
BINOL	1,1'-bi-2-naphthol
BO	Bayesian optimization
Bp	boiling point
Bz	benzoyl
Calcd.	calculated
Cat.	catalyst
Conv.	conversion
D	deuterium
dr	diastereomeric ratio
E	electrophile
Ee	enantiomeric excess
EDG	electron-donating group
Eq	equation
Equiv.	equiv, equivalent(s)
ESI	electrospray ionization
Et	ethyl
EWG	electron-withdrawing group
FG	functional group
FR	flow rate
GPR	Gaussian process regression
h	hour(s)
HPLC	high performance liquid chromatography
HRMS	high resolution mass spectrometry
IM	intermediate
i-Pr	isopropyl
IR	infrared
L	ligand
LB	Lewis base

Me	methyl
Min	minute(s)
ML	machine learning
MS	mass spectrometry or molecular sieve
Ms	mesyl (methanesulfonyl)
NMR	nuclear magnetic resonance
NOBIN	2-amino-2'-hydroxy-1,1'-binaphthyl
Ns	*p*-nitrophenyl sulfonyl group
Nu	nucleophile
PG	protecting group
Ph	phenyl
Pin	pinacolato
Pybox	pyridine bis(oxazoline)
tert-	tertiary
Ts	*p*-toluene sulfonyl

Contents

Chapter 1

General Introduction

Chapter 2

Exploration of Flow Reaction Conditions Using Gaussian Process Regression (GPR) for Enantioselective Organocatalyzed Rauhut–Currier and [3+2] Annulation Sequence.

Chapter 3

Bayesian Optimization-Assisted Multi-Parameter (Numerical and Categorical) Screening for an Organocatalytic Flow Synthesis of Highly Functionalized Biaryls.

Chapter 4

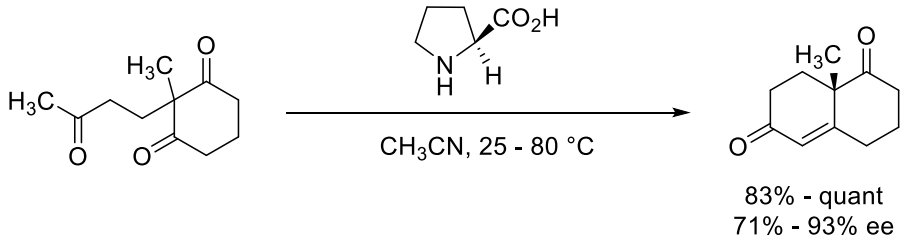
Conclusion

General Introduction

1.1. Organocatalysis

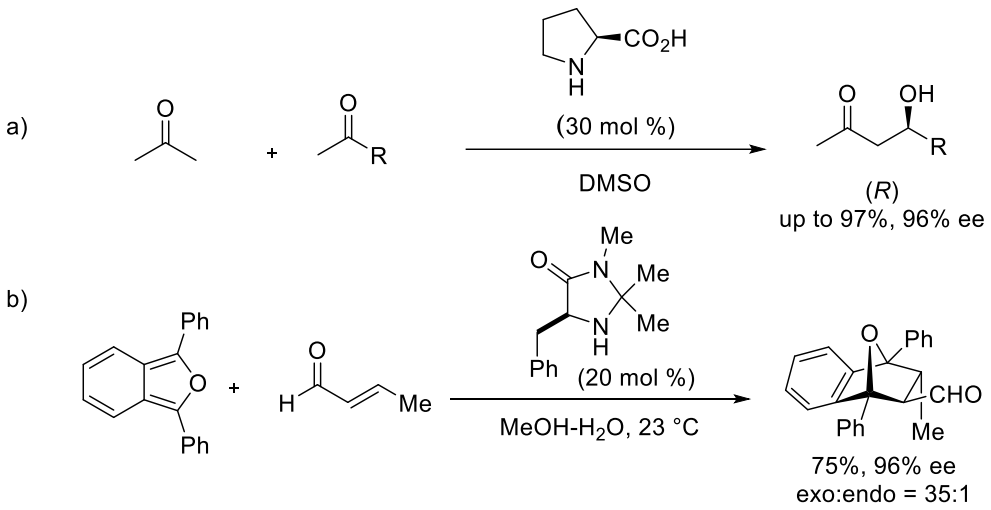
The birth of organocatalysis was in the 1910s by a mimic of biocatalytic systems in nature.[1] Biocatalysts are complex molecules and show limited specific activity which resulted in narrow substrate scope in organic reactions. In contrast, transition metal catalysts and organocatalysts are comparably simple, having a few functionalities and wide substrate accessibility. The transition metal holds the strongest feature for asymmetric transformations. In 2001, the Nobel prize in chemistry was awarded to Knowles and Noyori for their work on enantioselective catalyzed hydrogenation reactions with Rh as a transition metal, and chiral phosphine as a ligand which was provided a chiral environment for it. And also, the 2001 Nobel prize was shared with Sharpless for asymmetric epoxidation catalyzed by titanium tetra(isopropoxide) complex.[2] Between those transition metals and enzymatic catalysts, the new concept for organocatalysis which has been made from optically pure chiral organic molecules has been disclosed. Organocatalysts are purely organic molecules, consist of carbon, hydrogen, nitrogen, sulfur, and phosphorus atoms. Organocatalysts have a lot of advantages in contrast to transition metal catalysts and enzymes. Such as, they are usually robust, inexpensive and readily available, non-toxic, stable under moisture and oxygen. They have become a widely used catalyst in the domains such as natural product synthesis,[3] drug discovery,[4] and fine chemicals production.[5]

In early 1912, Bredig and Fiske reported the first example of an asymmetric organocatalytic reaction.[1a] A pioneering work was done by Pracejus in 1960 using alkaloid as a catalyst. He achieved the synthesis of (-)-α-phenyl methyl propionate in 74% ee.[6] Further, high enantioselectivities were achieved in the 1970s and 1980s. The outstanding discovery of the Hajos-Parrish-Eder-Sauer-Wiechert reaction was introduced.[7] (**Scheme 1.1.**)



Scheme 1.1. Elegant work of organocatalysis promoted by (*S*)-proline

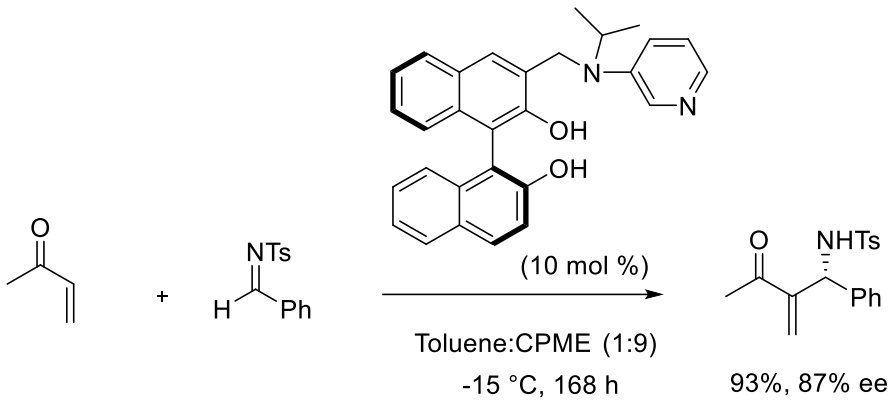
Moreover, the proline catalyzed reactions have been once again recognized; in 2000, the first direct aldol[8] reaction using an organocatalyst was reported by List and Barbas III (**Scheme 1.2a**).[9] At the same time, Macmillan reported proline-inspired catalyst for the Diels-Alder reaction of α,β-unsaturated aldehyde with high enantioselectivity (up to 96% ee)[10] (**Scheme 1.2.b**).



Scheme 1.2. Early examples of organocatalysis transformations

In addition, cinchona alkaloid which can act as a chiral base has been used for many transformations for the last 35 years.[11] Also, chiral DMAP by Fu and Kawabata was extremely selective for several nucleophilic addition reactions.[12] Thiourea-based hydrogen bond donor catalysts were introduced by Takemoto and Jacobsen independently, for the highly stereoselective Michael and Diels-Alder reaction.[13] Furthermore, the quaternary ammonium salt as a phase transfer catalyst[14] was redisclosed by Maruoka for many successful transformations.[14c-g]

Our group also reported on a bifunctional organocatalyst for the enantioselective Aza-Morita-Baylis-Hillman reaction (**Scheme 1.3**). This catalyst consists of Brønsted acid unit and Lewis base unit, where activates the generating nucleophile in site, to promote the enantioselective addition to imine. The catalyzed reaction of methyl vinyl ketone with aldimine provided the aza-MBH adduct in up to quantitative yield with 95% ee.[15]



Scheme 1.3. Aza-MBH reaction by our group

Subsequently, there are many publications were made by our group using a variety of organocatalysts to aza-MBH reaction,[16a,b,c] [2+2] cycloaddition,[16d] umpolong reaction[16e] Friedel-craft type reaction,[16f,g] Rauhut-currier reaction,[15h,i] for facile synthesis of a lot of optically active heterocycles bearing chiral tetrasubstituted carbon stereogenic centers.

Unless otherwise noted, those organocatalytic works stated above have been studied extensively, but the applicability of these synthetic methodologies is likely to be limited to small-scale synthesis. Therefore, it has not been so reliable for systems with large-scale practicality. Due to this remarkable limitation, the flow system is an efficient process to enhance the reaction's scale-up ability and reproducibility.

1.2 Introduction to Flow chemistry

Flow chemistry acts a significant job in organic synthetic chemistry the last two decades. In past, flow equipment was utilized in crude material and petrochemical changes. The advantages of flow chemistry are clear when reaction involves unsafe intermediates, and restrictions in mass and heat transfer processes.[17] Various flow chemistry research has been made in as far as synthetic transformation, multistep reactions and reaction optimization.[18]

In the flow process, adjusting flow rate enables to save the precious reagent and control the reaction time. By dividing the reactor volume by the total flow rate through the reactor system, "residence time" is obtained which is equivalent to the reaction time.
There are benefits of flow system over the conventional batch mode:

- Large surface region to volume proportion

Tubing-based reactors have a bigger surface region to volume proportion contrasted with the round bottom flask which gives more effective warm transfer.[19] These efficient heat and cool transfers avoid dangerous, unexpected exothermic reaction at any scale. Since the flow system can supply efficient heat transfer, an exothermic reaction can be performed safely and diminished the by-product formation on it. Additionally, a flow system can control the homogenous temperature distribution process and better mass transfer processing than a batch process.

- Pressurization

Many flow systems can be worked as a compressed system of low volume through the joining of a back-pressure regulator (BPR). Performing reaction under pressure allows to increase their boiling point and it resulted to optimize reaction conditions with the more prominent scope of solvents and temperatures.[20]

- Reactive intermediates

When the reaction involves highly reactive or hazardous reagents (e.g. phosgene, diazomethane, etc.), it is hard to deal with in batch systems.[21] In contrast, a reactive intermediate can be in situ can promptly be transformed with reagents to give the desired product in a flow process.[22] Productive mixing and mass exchange properties of continuous flow measures prompt a uniform concentration of product at a particular point in the reactor, and just little amounts of conceivably risky responsive intermediates

remained.

- In-line-monitoring

The incorporation of detectors (IR, Mass, HPLC, *etc.*) into the setup for monitoring the reaction stream in-line has been one of the most attractive features in the flow process. These detectors give moment, quantitative data concerning the degrees of product.[23] Moreover, mechanistic study [24] and kinetics studies[25] can likewise be directed with the guide of these instruments.

- Multistep synthesis

In late many years, numerous chemical reactions under batch conditions have been converted into a single-step flow process, and continue these cycles are joined to produce more complex products in multistep sequences.[26] As a result, the multi-step synthesis can altogether diminish the number of important unit tasks, like washing, extraction, purification, drying, and therefore the time and the work needed to play out a response succession.

- Automation

Software automation and assisted flow are becoming famous recently which gives benefits to scientific experts to have better control of the development of the multi-step flow process.[27] Performing multistep combination in the flow system requires various manual tasks, for example, sample loading, programming of reaction parameter, control of pumps. Having computerized control of these tasks would prompt a superior administration of the framework in any event, when a single specialist is performing the continuous multistage process. Additionally, Automation can likewise be utilized for library generation[28] and is considered to be a significant component in the improvement of self-upgrading reactor systems.[29]

1.3. Illustration of the flow system

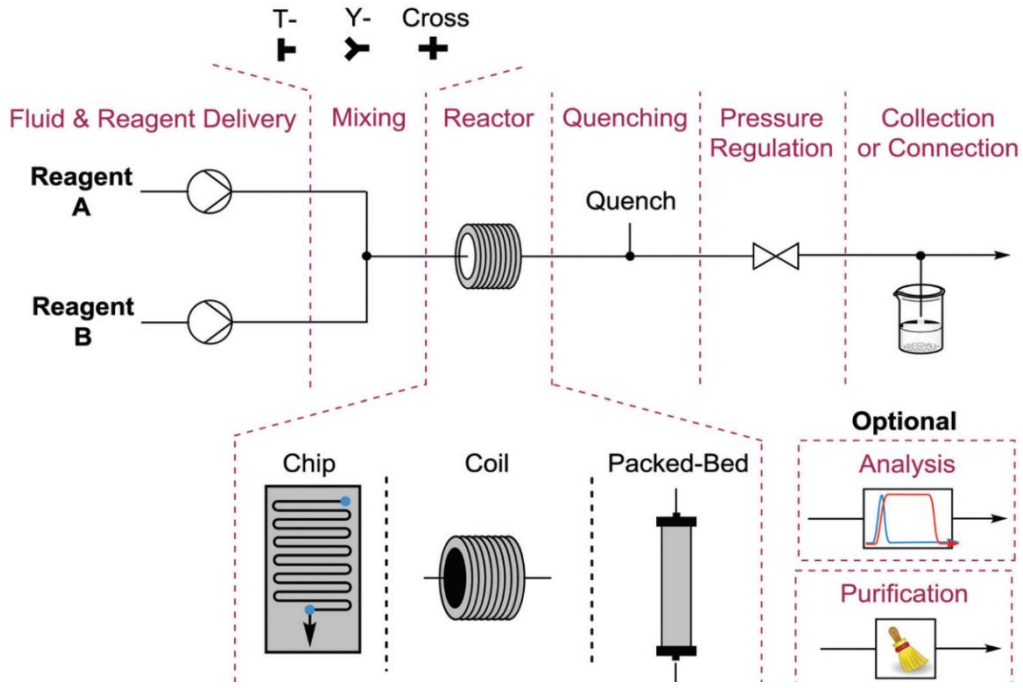
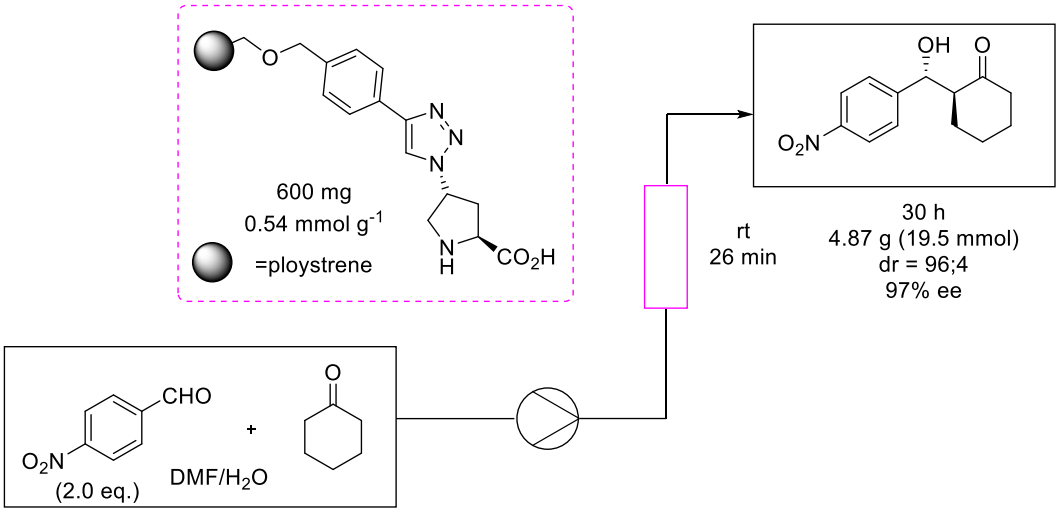


Figure 1.3. Anatomy of the flow system

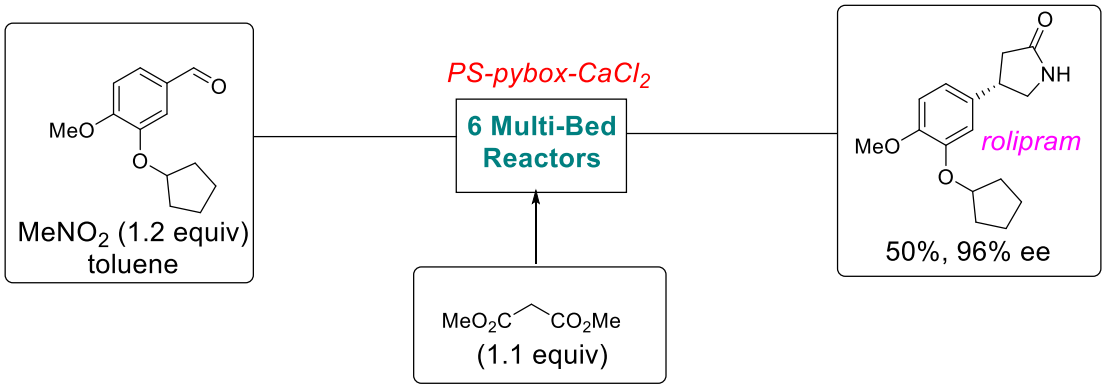
Flow system reaction requires a bit more planning than that of the batch process. The first part is the input of fluid and reagents by pump (syringe pump or HPLC pump). This reagent can be input as a neat or a solution with appropriate solvent. Then, the reagents meet together and mix before the chemical reaction has occurred. This mixing unit has characterized as T shape, Y shape, and cross shape, according to their appearance. Next, the reaction mixture enters the core unit which is called a microreactor. The core unit controls the residence time of the reaction and it can be kept in pre-set conditions such as heating, cooling, light, electricity, *etc*.). It can give several kinds of benefits such as efficient mixing, efficient heat transfers to maintain appropriate reaction conditions.[30] In addition, several types of equipment for analysis (HPLC, IR, Mass),[31] as well as continuous purification modules also can be attached.[32] The unique feature of the flow system is these individual parts can be arranged interchangeably and repetitively, resulting in an infinite number of possible modifications.

1.4 Examples in flow synthesis



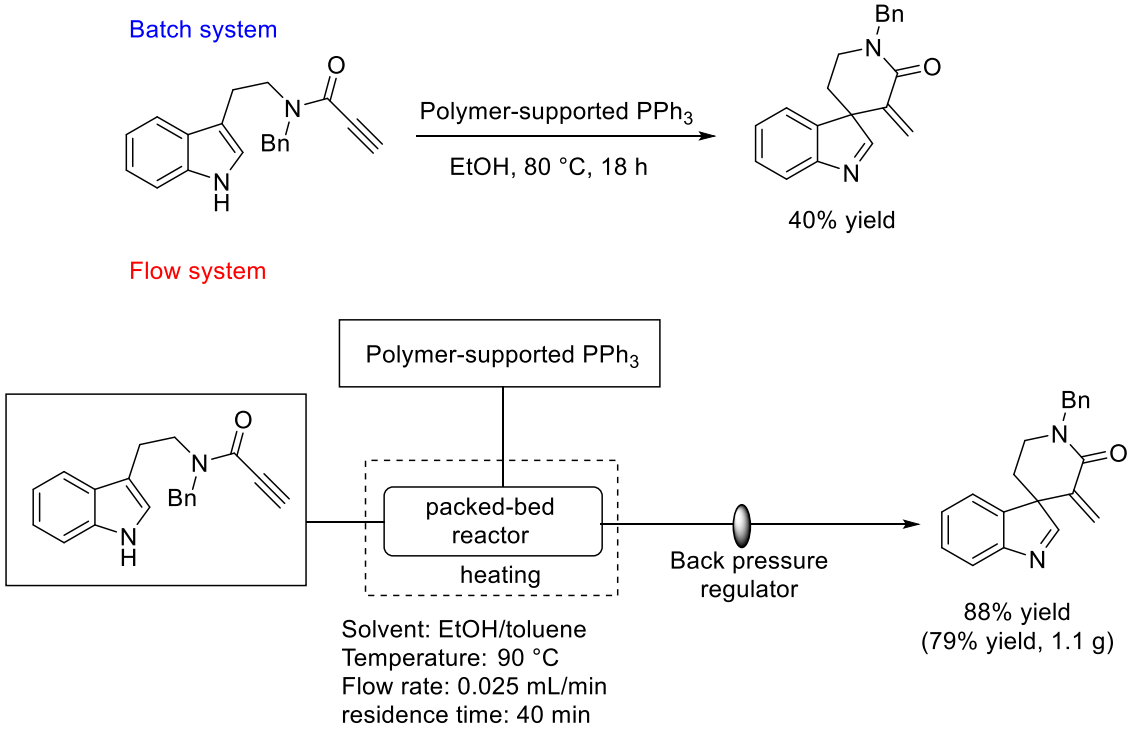
Scheme 1.4. Asymmetric aldol reaction using an immobilized proline catalyst

As shown in **Scheme 1.4**, Pericàs developed the aldol reaction of benzaldehyde derivatives and cyclohexanone.[33a] A proline derivative was immobilized on a resin that was functionalized with 4-ethynylbenzyl chloride. Water was recognized as a crucial solvent for selectivity from an initial trial. The author successfully achieved gram scale synthesis; under optimized flow conditions, the aldol reaction of *p*-nitrobenzaldehyde and cyclohexanone was monitored over 45 hours allowing for the production of 4.87 g of the chiral aldol product. In 2015, Kobayashi developed an immobilized calcium catalyst for the continuous, asymmetric 1,4-addition of 1,3-dicarbonyl compounds and nitroalkanes.[34] Chiral pybox ligand was immobilized on polystyrene to perform the asymmetric 1,4-additions with malonate and mixed with $CaCl_2 \cdot 2H_2O$ and Celite. They developed a fully continuous synthesis of enantiomerically pure rolipram (anti-inflammatory drug) in a continuous flow approach involving exclusively heterogeneously catalyzed steps (**Scheme 1.5**).[35] Overall, 50% of the target compound was isolated in high enantiomeric excess, and the system was continuously operated for 1 week. Although, this achievement consists of many flow systems and each of their optimization process might take a long time, it has resulted in many unsuccessful reactions. Therefore, when it comes to multi-step synthesis, efficient optimization is highly desired and it is the most challenging part even in up to date.



Scheme 1.5. Fully continuous synthesis of (*S*)-rolipram using several consecutive packed bed reactors

In 2019, Sharma and Eycken reported triphenyl phosphine-promoted intramolecular α-umpolung Michael addition on alkynes of the spiroindolines and spiroindolenines in batch as well as continuous-flow heterogeneous conditions to achieve the synthesis of spiroindolenine derivatives (**Scheme 1.6**).[36]



Scheme 1.6. Synthesis of spiroindolenines by PPh_3-catalyzed α-umpolung Michael addition

Recyclable polymer-supported triphenylphosphine was prepared and used as a heterogeneous organocatalyst for both batch and continuous-flow (packed bed reactor)

spirocyclization of propargylamides. A model reaction in batch mode was demonstrated and the yield was 40%. As a comparison, continuous flow experiments (EtOH/toluene, 90 °C, FR = 0.025 mL min−1, τ = 40 min) gave markedly better results, the target compound was obtained in 88% yield (79% on the gram scale). In this reaction, the advantage of the flow system on a large scale is proven by using polymer-supported catalysts even up to the gram scale. The reaction simplicity and lack of an asymmetric version of this reaction are still demanding.

As summarized above, various achievements were reported in the flow systems. But still, optimization of these flow reaction conditions is not an easy task. It may consist of a lot of trials and errors reaction including long process optimization. Therefore, the author is interested to focus on an improvement of the time-consuming optimization process in flow systems as the motivation for this doctoral thesis.

1.5. Conventional Optimization

Although, there are numerous successful reports regarding flow synthesis,[37] a common way for chemists to optimize reactions is to change a single experimental condition at a time while fixing all the others. This approach will often miss the optimal conditions. It is based on many trials and errors in a flask or flow system. It causes a lot of time-consuming, labor-intensive, expensive processes with large material consumption.

When developing a new reaction, the chemists have to consider the main factors which are directly affecting the reaction, such as:

- Stoichiometry of reagent
- Temperature of reaction
- Catalyst loading
- Concentration of solvent

In addition, the flow reaction development let chemists consider additional factors like:

- Flow rate
- Type of micromixer

In detail, the two factors were selected to be a representative example for conventional optimization. Temperature and reagent amount only can generate a minimum of 25 screening of reaction as shown in **Figure 1.4**. In addition, optimization trials are always increasing when many factors are affecting the reaction that might result in a huge number of trial experiments. Therefore, minimum trials are highly desired in the field of new reaction development.

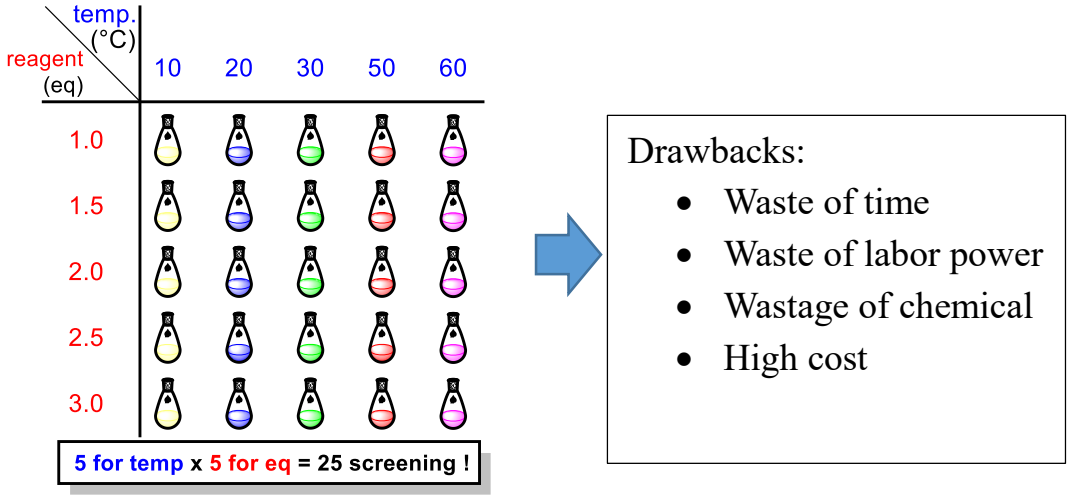


Figure 1.4: Representation of the conventional optimization

1.6 Efficient optimization in the flow system

1) Automated optimization in a flow system

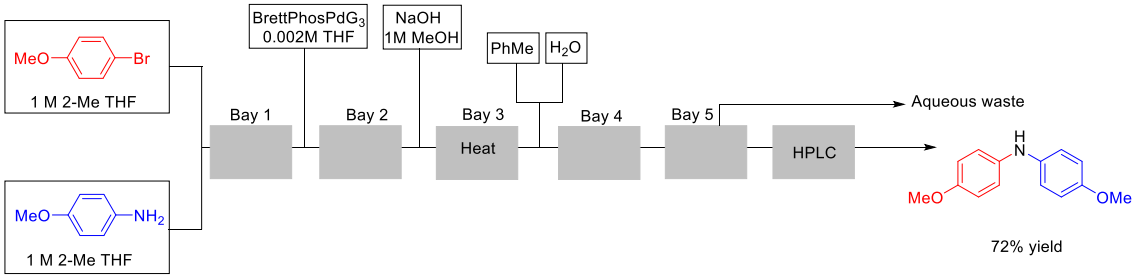
Taking advantage of flow systems such as efficient heat transfer, mass transfer, hazardous intermediate handling, scientists can overcome the batch system drawbacks by flow system when developing a new reaction. Moreover, automation is readily achieved into flow systems via in-line monitoring, offering a greater degree of reliability and reaction control.[38] Continuous flow chemistry is an ideal technology for the computer-controlled optimization of chemical reactions due to its quality of benefits, such as precise control of reaction times, temperatures, and stoichiometry of reagents.[39]

Automation in flow reaction steps are:

- Loading of reagent
- Selection of parameters (time, temperature, cat. Loading)
- Monitoring system by HPLC, Mass, or IR, *etc.*
- Automated optimization according to the monitoring system

Recently, Jensen and Jamison have disclosed the system plug-and-play, continuous-flow chemical synthesis system combined with hardware, software, and analytics to a capable of self-optimizing of reported chemical reactions[40] including Buchwald–Hartwig cross-coupling, Horner–Wadsworth–Emmons olefination, reductive amination, Suzuki–Miyaura cross-coupling, nucleophilic aromatic substitution (SNAr), and a visible light

photo redox reaction. The Buchwald-Hartwig amination is the main to chemical research, including the discovery and development of pharmaceuticals and agricultural chemicals.[41]The palladium-catalyzed coupling of 1-bromo-4-methoxybenzene with 4-methoxyaniline under basic conditions was investigated using the recently reported BrettPhos Pd G3 pre-catalyst (commercially available).[42] The setup of the reaction platform is shown in **Scheme 1.7**.



Scheme 1.7. Fully automated Buchwald-Hartwig amination

Bays 1 and 2 were used for reagent addition and mixing, and the amination itself was performed in Bay 3 using a heated reactor. Introduction of toluene and water in Bay 4 then enabled a continuous liquid-liquid separation in bay 5. A 60-nl sample of the organic layer was analyzed directly by an in-line HPLC system, with the conversion of aniline assayed relative to an internal standard. The desired secondary amine (Amination product) was obtained in a 72% yield after a few screenings. The whole optimization process took 21 h to get optimized results. An automated reaction system is always better than classical optimization since it is quick and has no involvement of humans. But this each system has to be programmed and controlled by computer. As a result, it will be complex and expertise is required to obtain and maintain this automation. A simple and efficient optimization method is essentials for everyone who is not an expert in programming.

2) Machine Learning Assisted Optimization

A common way for the chemist to optimize a chemical reaction is a complex, multi-dimensional challenge that requires experts to evaluate various reaction parameters, such as substrate, catalyst, reagent, additive, solvent, concentration, temperature, and reactor type. Reaction optimization is still often a difficult and time-consuming task for chemists.

Machine learning (ML) is one of the most promising tool to find the appropriate parameters such as reaction conditions by using a black-box optimizer.[43] ML optimization so far used in many fields. Those are drug discovery,[44] catalyst design,[45] design of experiments,[46] and retrosynthesis.[47] Additionally, as an important part, ML has also been used in continuous flow systems due to its accuracy, precise control of reaction parameters, and high reproducibility.[48]

In 2019, Mase and Takeda reported rapid optimization of reaction conditions using comprehensive reaction analysis of a flow of microwave reactors.[49] In their study, a microwave flow reactor was selected for more effective optimization of reaction conditions.[50] This comprehensive optimization method is formulated on the optimization techniques called the "9+4+1" method. The irradiation and flow rate are the variable parameters. (**Figure 1.5a**)

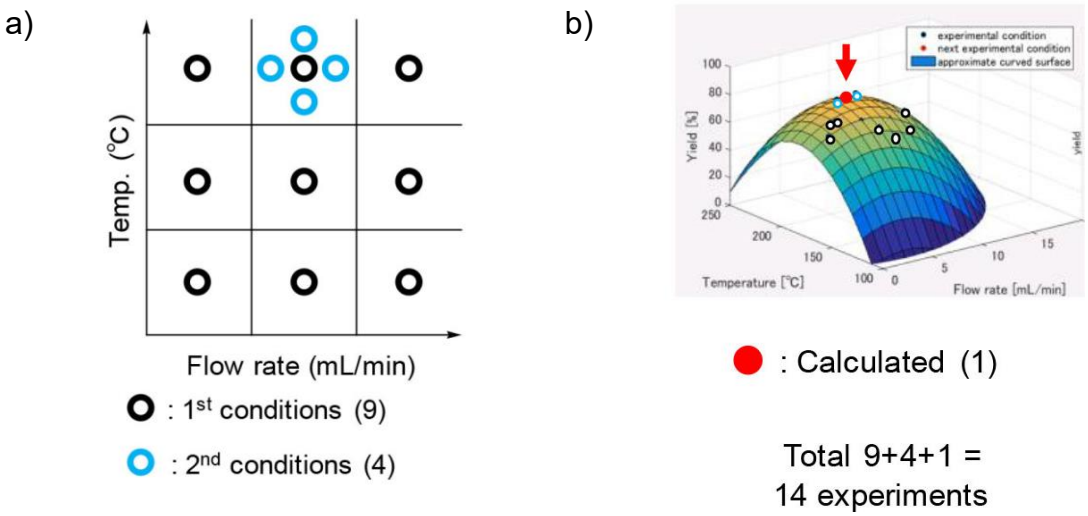


Figure 1.5. 9+4+1 method of rapid optimization

After analyzing the nine samples by nine experiments trials, the point affording the best yield was divided into four, and four more experiments were carried out. A three-dimensional approximate surface was created from the 13 points of experimental data and a 14th experiment was performed according to the expected optimal condition to give 99% yield of the desired product. They have tested this method to acetylation, Fisher indole, and Diels-Alder reaction respectively. (**Figure 1.5b**)

As described above, the ML optimization in the flow system shows a high affinity to introduce the precious reaction condition screening process. There are recent examples reported in ML assisted optimization process in batch[51] as well as flow[48a,52] respectively. But the ML efficient optimization systems are still highly desired in the community of synthetic organic chemistry.

1.7 This work

ML-assisted Optimization for Organocatalytic Reactions in the Flow System

Inspired by the advantages of a flow system (accuracy and high reproducibility), the author focused on an efficient and rapid optimization for reaction parameters via a ML approach. This ML-assisted optimization overcomes many trials and errors experiments in conventional strategies. (**Figure 1.6**)

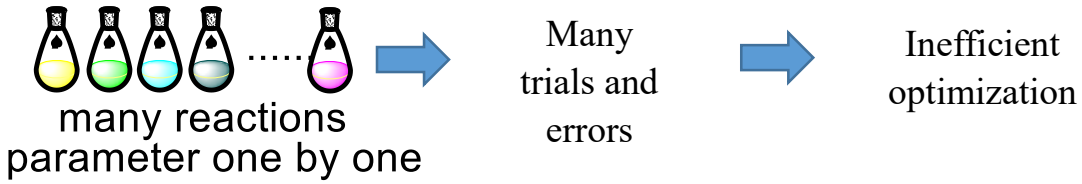


Figure 1.6. Conventional optimization

This approach: ML prediction method for appropriate reaction parameters

1) Understand the reaction parameters that are crucial for the desired function (chemical yield)

2) Multiple parameters can be simultaneously varied.

3) Performing an initial experiment set to initiate the ML process.

Examples of these parameters are reaction temperature, the ratio of reagents, flow rate, concentration, *etc*.

4) After obtaining the initial training data set, the ML prediction regression model is calculated.

5) ML-assisted screening will predict the optimum reaction conditions rapidly by visualization from the regression model even up to multi-dimensional arrangement.

In this method, the organic chemist can efficiently solve complex high-dimensional optimization, saving time, labor, and cost by minimizing reaction trials and errors. Hence, it can be described as a sustainable process considering the low wastage of chemicals and energy during optimization. (**Figure 1.7**)

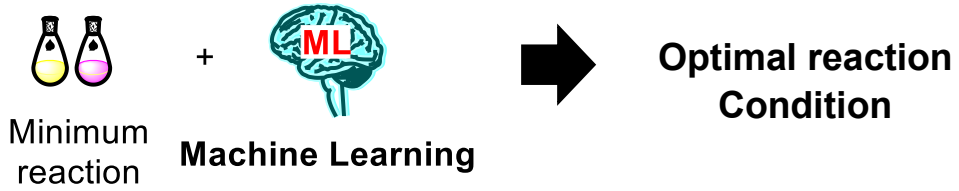
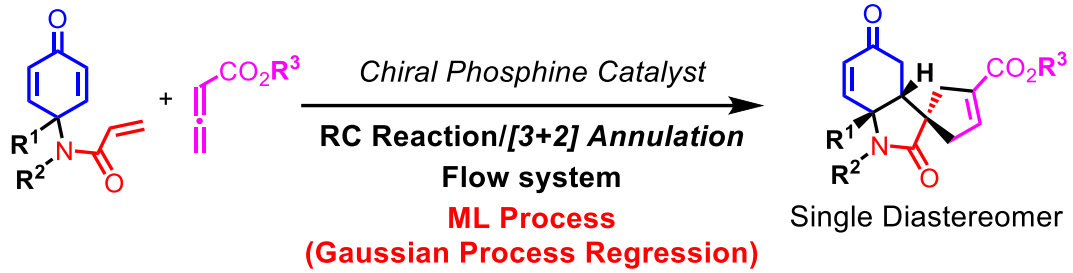


Figure 1.7. This ML optimization approach

1.8 Contents of this Thesis

Chapter 2:

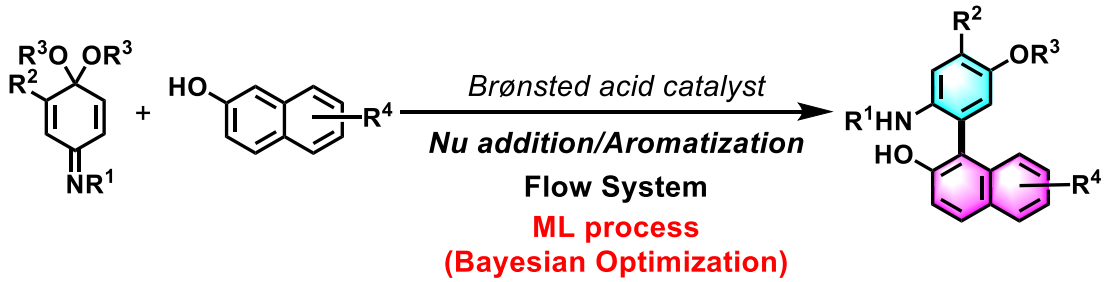
Exploration of Flow Reaction Conditions Using Gaussian Process Regression (GPR) for Enantioselective Organocatalyzed Rauhut–Currier and [3+2] Annulation Sequence



In this chapter, the development of sequential reaction in which content of Rauhut-Currier and [3+2] annulation sequence for facile synthesis of spirooxinodole analogue is described. Sprioxindole derivatives were synthesized by chiral phosphine organocatalyst. Also, the author could successfully apply the ML optimization to it by utilizing the Gaussian process regression (GPR) as the computerized algorithm to find the optimal reaction conditions by carrying a minimum number of reactions. Additionally, the two parameters were changed simultaneously to predict the maximum reaction yield of spirooxindole analogue with high enantioselectivity.

Chapter 3:

Bayesian Optimization-assisted Multi-parameter (numerical and categorical) Screening for an Organo-catalytic Flow Synthesis of Highly Functionalized Biaryls



In **Chapter 3**, the author discovered a domino reaction that includes Nu addition, followed by aromatization to afford highly functionalized biaryls derivatives in a flow system is reported. Moreover, the ML-assisted optimization was interestingly applied

with multi-parameters which are affecting the chemical yield. The appropriate reaction conditions were predicted by the Bayesian optimization process with a high-dimensional system by few experimental trials. It resulted that, the target biaryl derivatives were obtained in high yield with a few experimental trials.

1.9 Reference

1. a) G. Bredig, W. S. Fiske, *Biochem. Z*. **1912**, 7. b) W. Langenbeck, *Angew. Chem*. **1928**, *41*, 740. c) W. Langenbeck, *Angew. Chem*. **1932**, *45*, 97. d) F. G. Fischer, *Ber*. 1931, *64*, 2825. e) W. Langenbeck, *ibid*., **1942**, 75B, 951. f) Y. Tu. Z. Wang, Y. Shi, *J. Am. Chem., Soc*. **1996**, *118*, 9806. g). D. Yang, Y. Yip, M. Tang, M. Wong, J. Zheng, K. Cheung, *J. Am. Chem. Soc*. **1996**, *118*, 491. h) S. E. Denmark, Z. Wu, C. Crudden, H. Matsuhashi, *J. Org. Chem*. **1997**, 62, 8288.

2. https://www.nobelprize.org/prizes/chemistry/2001/summary/

3. a) C. Grondal, M. Jeanty, D. Enders, *Nat. Chem*. **2010**, *2*, 167. b) E. Marque´s-Lo´pez, R. P. Herrera, M. Christmann, *Nat. Prod. Rep*. **2010**, *27*, 1138. c) M. Rueping, J. Dufour, F. R. Schoepke, *Green Chem*. **2011**, *13*, 1084. d) M. E. Abbasov, D. Romo, *Nat. Prod. Rep*. **2014**, *31*, 1318. e) G. J. R-Rodríguez, N. M. Rezayee, A. V. Albalat, K. A. Jørgensen, *Chem. Rev*. **2019**, *119*, 4221.

4. J. Alemán, S. Cabrera, *Chem. Soc. Rev*. **2013**, *42*, 774. b) D. L. Hughes, *Org. Process Res. Dev*. **2018**, *22*, 574.

5. a) I. R. Shaikh, *J. Catal.* **2014**, *2014*, 1. b) P. Chauhan, S. Mahajan, U. Kaya, D. Hack, D. Enders, *Adv. Synth. Catal*. **2015**, *357*, 253. c) L.-W. Xu, *Chem. Cat. Chem.* **2015**, *5*, 2775. d) C. Yang, *Chem. Soc. Rev*. **2021**, *50*, 1522. e) J. Wang, Y. Liu, X. Ni, X. Li, J. P. Cheng, *Chem. Eur. J*. **2017**, *23*, 5488.

6. H. Pracejus, *Justus Liebigs Ann. Chem*. **1960**, *634*, 23.

7. a) Z. G. Hajos, D. R. Parrish, *J. Org. Chem*. **1974**, *39*, 1615. b) U. Eder, G. Sauer, R. Wiechert, *Angew. Chem. Int. Ed*. **1971**, *10*, 496.

8. Y. M. A. Yamada, N. Yoshikawa, H. Sasai, M. Shibazaki, *Angew. Chem. Int. Ed. Engl*., **1997**, *36*, 1871.

9. B. List, R. A. Lerner, C. F. Barbas III, *J. Am. Chem. Soc*. **2000**, *58*, 5573.

10. K. A. Ahrendt, C. J. Borths, D. W. C. Macmillan, *J. Am. Chem. Soc*. **2000**, *122*, 4243.

11. G. S. Singh, E. M. Yeboah, *Rep. Org. Chem.* **2016**, *6*, 47.

12. a) J. C. Ruble, H. A. Latham, G. C. Fu, *J. Am. Chem. Soc*., **1997**, *119*, 1492. b) T. Kawabata, M. Nagata, K. Takasu, K. Fuji, *J. Am. Chem. Soc*., **1997**, *119*, 3169.

13. a) T. Okino, Y. Hoashi, Y Takemoto, *J. Am. Chem. Soc.* **2003**, *125*, 12672. b) M. S. Taylor, E. N. Jacobsen, *Angew. Chem. Int. Ed*. **2006**, *45*, 1520.

14. a) M. J. O'Donnell, W. D. Bennett, S. Wu, *J. Am. Chem. Soc.* **1989**, *111*, 2353. b) E. J. Corey, F. Xu, M. C. Noe, *J. Am. Chem. Soc.* **1997**, *119*, 12414. c) T. Ooi, D. Ohara, M. Tamura, K. Maruoka, *J. Am. Chem. Soc*. **2004**, *126*, 6844. d) T. Ooi, K. Maruoka, *Angew. Chem. Int. Ed*. **2007**, *46*, 4222. e) K. Maruoka, T. Ooi, T. Kano, *Chem. Commun*. **2007**, 1487. f) T. Ooi, K. Maruoka, *Aldrichmica Acta* **2007**, *40*, 77. g) T. Hashimoto, K. Maruoka, *Chem. Rev*. **2007**, *107*, 5656.

15. a) K. Matsui, S.Takizawa, H. Sasai, *J. Am. Chem. Soc.* **2005**, *127*, 3680. b) K. Matsui, S. Takizawa, H. Sasai, *Synlett* **2006**, *5*, 761.

16. a) S. Takizawa, N. Inoue, S. Hirata, H. Sasai, *Angew. Chem. Int. Ed.* **2010**, *49*, 9725. b) S. Takizawa, A. Horii, H. Sasai, *Tetrahedron: Asymmetry* **2010**, *21*, 891. c) S. Takizawa, K. Kiriyama, K. Ieki, H. Sasai, *Chem. Commun.* **2011**, *47*, 9227. d) S. Takizawa, F. A. Arteaga, Y. Yoshida, M. Suzuki, H. Sasai, *Org. Lett*. **2013**, *15*, 4142. e) S. Takizawa, K. Kishi, Y. Yoshida, S. Mader, F. A. Arteaga, S. Lee, M. Hoshino, M. Rueping, M. Fujita, H. Sasai, *Angew. Chem. Int. Ed.* **2015**, *54*, 15511. f) S. Takizawa, S. Hirata, K. Murai, H. Fujioka, H. Sasai, *Org. Biomol. Chem.* **2014**, *12*, 5827. g) S. Takizawa, M. Sako, M. A. Abozeid, K. Kishi, H. D. P. Wathsala, S. Hirata, K. Murai, H. Fujioka, H. Sasai, *Org. Lett.* **2017**, *19*, 5426. h) S. Takizawa, T. M.-N. Nguyen, A. Grossmann, D. Enders, H.

Sasai, *Angew. Chem., Int. Ed.* **2012**, *51*, 5423. i) K. Kishi, F. A. Arteaga, S. Takizawa, H. Sasai, *Chem. Commun.* **2017**, *53*. 7724.

17. a) R. L. Hartman, J. P. McMullen, K. F. Jensen*, Angew. Chem. Int. Ed*. **2011**, *50*, 7502. b) A. C. Bédard, A. R. Longstreet, J. Britton, Y. Wang, H. Moriguchi, R. W. Hicklin, W. H. Green, T. F. Jamison, *Bioorg. Med. Chem*. **2017**, *25*, 6233.

18. a) B. Gutmann, D. Cantillo, C. O. Kappe, *Angew. Chem. Int. Ed*. **2015**, *54*, 6688. b) V. Hessel, D. Kralisch, N. Kockmann, T. Noël, Q. Wang, *ChemSusChem* **2013**, *6*, 746. c) K. F. Jensen, *AIChE. J*. **2017**, *63*, 858. d) S. V. Ley, D. E. Fitzpatrick, R. J. Ingham, R. M. Myers, *Angew. Chem. Int. Ed*. **2015**, *54*, 3449. e) S. V. Ley, D. E. Fitzpatrick, R. M. Myers, C. Battilocchio, R. J. Ingham, *Angew. Chem. Int. Ed*. **2015**, *54*, 10122.

19. a) R. L. Hartman, J. P. McMullen, K. E. Jensen., *Angew. Chem. Int. Ed.* **2011**, *50*, 7502. b) K. D. Nagy, B. Shen, T. F. Jamison, K. F. Jensen, *Org. Process Res. Dev.* **2012**, *16*, 976.

20. a) F. Benito-López, R. J. M. Egberink, D. N. Reinhoudt, W. Verboom, *Tetrahedron* **2008**, *64*, 10023. b) J. T. Hodgkinson, W. R. J. D. Galloway, S. Saraf, I. R. Baxendale, S. V. Ley, M. Ladlow, M. Welch, D. R. Spring, *Org. Biomol. Chem.* **2011**, *9*, 57.

21. a) J. C. Brandt, T. Wirth *Beilstein J. Org. Chem.* **2009**, doi: 10.3762/bjoc.5.30 b) M. Grafton, A. C. Mansfield, M. J. Fray, *Tetrahedron Lett.* **2010**, *51*, 1026.

22. a) H. E. Bartrum, D. C. Blakemore, C. J. Moody, C. J. Hayes., *Chem. Eur. J.* **2011**, *17*, 9586. b) S. Hübner, U. Bentrup, U. Budde, K. Lovis, T. Dietrich, A. Freitag, L. Küpper, K. Jähnisch, *Org. Process Res. Dev.* **2009**, *13*, 952. c) C. B. McPake, C. B. Murray, G. Sanford, *Tetrahedron Lett.* **2009**, *50*, 1674.

23. a) H. Lange, C. F. Carter, M. D, Hopkin, A. Burke, J. G. Goode, I. R. Baxendale, S. V. Ley, *Chem. Sci.* **2011**, *2*, 765. b) Z. Qian, I. R. Baxendale, S. V. Ley, *Chem. Eur. J.* **2010**, *16*, 12342. c) J. P. McMullen, K. F. Jensen, *Annu. Rev. Anal. Chem.* **2010**, *3*, 19.

24. L. Malet-Sanz, J. Madrzak, S. V. Ley, I. R. Baxendale, *Org. Biomol. Chem.* **2010**, *8*, 5324.

25. S. Mozharov, A. Nordon, D. Littlejohn, C. Wiles, P. Watts, P. Dallin, J. M. Girkin, *J. Am. Chem. Soc.* **2011**, *133*, 3601.

26. a) S. Newton, C. F. Carter, C. M. Pearson, L. de C Alves, H. Lange, P. Thansandote, S. V. Ley, *Angew. Chem. Int. Ed*. **2014**, 53, 4913. b) D. Webb, T. F. Jamison, *Chem. Sci*. **2010**, 1, 675.

27. M. D. Hopkin, I. R. Baxendale, S. V. Ley, *Chim. Oggi.* **2011**, *29*, 28.

28. C. J. Smith, N. Nikbin, S. V. Ley, H. Lange, I. R. Baxendale, *Org. Biomol. Chem*. **2011**, *9*, 1938.

29. a) A. Kirschning, W. Solodenko, K. Mennecke *Chem. Eur. J.* **2006**, *12*, 5972. b) D. E. Fitzpatrick, S. V. Ley, *React. Chem. Eng.* **2016**, *1*, 629. c) D. E. Fitzpatrick, C. Battilocchio, S. V. Ley, *Org. Prcoess Res. Dev.* **2016**, *20*, 386.

30. J. Britton, T. F. Jamison, *Nat. Protoc*. **2017**, *12*, 2423.

31. B. J. Reizman, K. F. Jensen, *Acc. Chem. Res*. **2016**, *49*, 1786. b) A. Chanda, A. M. Daly, D. A. Foley, M. A. LaPack, S. Mukherjee, J. D. Orr, G. L. Reid, D. R. Thompson, H. W. Ward, *Org. Process Res. Dev*. **2015**, *19*, 63. c) J. Yue, J. C. Schouten, T. A. Nijhuis, *Ind. Eng. Chem. Res*. **2012**, *51*, 14583. d) D. C. Fabry, E. Sugiono, M. Rueping, *React. Chem. Eng.* **2016**, *1*, 129. d) V. Sans, L. Cronin, *Chem. Soc. Rev*. **2016**, *45*, 2032.

32. L. Hohmann, S. K. Kurt, S. Soboll, N. Kockmann, *J. Flow Chem*. **2016**, *6*, 181.

33. a) A. H. C. Ayats, Henseler, M. A. Pericàs, *ChemSusChem* **2012**, *5*, 320. b) T. D. Machajewski, C-H. Wong, *Angew. Chem. Int. Ed.* **2011**, *50*, 7502.

34. T. Tsubogo, Y. Yamashita, S. Kobayashi, *Chem. Eur. J*. **2012**, *18*, 13624.

35. T. Tsubogo, H. Oyamada, S. Kobayashi, *Nature* **2015**, *520*, 329.

36. P. Ranjan, G. M. Ojeda, U. K. Sharma, E. V. Van der Eycken, *Chem. Eur. J.* **2019**, *25*, 2442.

37. M. B. Plutschack, B. Pieber, K. Gilmore, P. H. Seeberger, *Chem. Rev*. **2017**, *117*, 11796.

38. a) V. Sans, L. Cronin, *Chem. Soc. Rev*. **2016**, *45*, 2032. b) D. C. Fabry, E. Sugiono, M. Rueping, *React. Chem. Eng.* **2016**, *1*, 129.

39. D. C. Borda, K. V. Kutonova, C. Jamet, M. E. Trusova, F. Zammattio, C. Truchet, M. R. Zubiri, F.X. Felpin, *Org. Process Res. Dev*. **2016**, *20*, 1979. b) B. J. Reizman, Y. M. Wang, S. L. Buchwald, K. F. Jensen, *React. Chem. Eng*. **2016**, *1*, 658. c) B. J. Reizman, K. F. Jensen, *Chem. Commun*. **2015**, *51*, 13290. d) J. P. McMullen, K. F. Jensen, *Org. Process Res. Dev*. **2010**, *14*, 1169. e) D. E. Fitzpatrick, C. Battilocchio, S. V. Ley, *Org. Process Res. Dev*. **2016**, *20,* 386.

40. A. C. Bédard, A. Adamo, K. C. Aroh, M. G. Russell, A. A. Bedermann, J. Torosian, B. Yue, K. F. Jensen and T. F. Jamison, *Science* **2018**, *361*, 1220.

41. P. Ruiz-Castillo, S. L. Buchwald, *Chem. Rev*. **2016**, *116*, 12564.

42. N. C. Bruno, M. T. Tudge, S. L. Buchwald, *Chem. Sci*. **2013**, *4*, 916.

43. K. Terayama, M. Sumita, R. Tamura, K. Tsuda, *Acc. Chem. Res.* **2021**, *54*, 1334.

44. X. Yang, Y. Wang, R. Byrne, G. Schneider, S. Yang, *Chem. Rev*. **2019**, *119*, 10520.

45. a) K. T. Butler, D. W. Davies, H. Cartwright, O. Isayev, A. Walsh, *Nature* **2018**, 559, 547. b) A. F. Zahrt, J. J. Henle, B. T. Rose, Y.Wang, W. T. Darrow, S. E. Denmark, *Science* **2019**, *363*, 5631. c) D. J. Durand, N. Fey, *Chem. Rev*. **2019**, *119*, 6561.

46. a) S. A. Weissman, N. G. Anderson, *Org. Process Res. Dev*. **2015**, *19*, 1605. b) D. C. Borda, K. V. Kutonova, C. Jamet, M. E. Trusova, F. Zammattio, C. Truchet, M. R. Zubiri, F. X. Felpin, *Org. Process Res. Dev*. **2016**, *20*, 1979.

47. a) A. F. Almeida, R. Moreiraand, T. Rodrigues, *Nat. Rev. Chem*. **2019**, *3*, 589. b) J. S. Schreck, C. W. Coley, K. J. M. Bishop, *ACS Cent. Sci*. **2019**, *5*, 970.

48. a) A. M. S. Adam, D. C. Nicholas, H. Eric, B. Richard, A. B.Alexei, A. Lapkin, *Chem. Eng. J*. **2018**, *352*, 277. b) T. Hardwicka, N. Ahmed, *Chem. Sci*. **2020**, *11*, 11973.

49. P. Vámosi, K. Matsuo, T. Masuda, K. Sato, T. Narumi, K. Takeda, N. Mase. *Chem. Rec*. **2019**, *19*, 77.

50. J. Jacob, *Int. J. Chem*. **2012**, *4*, 29.

51. B. J. Shields, J. Stevens, J. Li, M. Parasram, F. Damani, J. I. M. Alvarado, J. M. Janey, R. P. Adams, A. G. Doyle, *Nature* **2021**, *590*, 89.

52. C. J. Taylor1, A, Baker, M. R. Chapman, W. R. Reynolds, K. E. Jolley, G. Clemens, G. E. Smith, A. J. Blacker, T. W. Chamberlain, S. D. R. Christie, B. A. Taylor, R. A. Bourne, *J Flow Chem.* **2021**, *11*, 75.

Chapter 2

Chapter 2

Exploration of Flow Reaction Conditions Using Gaussian Process Regression (GPR) for Enantioselective Organocatalyzed Rauhut–Currier and [3+2] Annulation Sequence

2.1 Introduction

Reaction optimization of a new reaction development requires plenty of time and many trial reactions to get the optimum reaction conditions. Each reaction has different parameters which are directly affecting to chemical yield. As the author described in **Chapter 1**, the classical way of reaction parameter screening performs is changing one parameter at one time and keeping others constant. As a result, there will be a lot of trial and errors experiments that are necessary to find the maximum yield.

Automational[1] and computational[2] optimizations are the so-far best achievements that scientists have discovered to overcome this tedious reaction screening process. Among both, machine learning optimization is the most reliable process in many research filed due to its resolving ability even in the complex optimization process. Over few decades, ML has been applied to various fields such as drug discovery, synthetic planning and materials, and catalyst design (also see **Chapter 1**). The author is interested in the Gaussian process regression (GPR) model as a machine learning optimization approach to estimate the appropriate parameter in a new reaction system.

GPR is a kernel-based statistical learning algorithm in theoretical and physical chemistry.[3] GPR models have been widely used[4] to predict several chemical properties in machine learning applications, because of their flexibility and constitutionally uncertainty measures over predictions as a black box optimizer under given up to data set. This model can be used for probability distribution over possible functions that fit a set of points.

As an example when we have the data set, the probability distribution over all possible functions, we can calculate the means as the function, and the variances to indicate how confident the predictions are by GPR. In regression, there is a function (f) we are trying to make a regression model (f = chemical yield) from the experimental initial training data set.

The Gaussian Process is therefore followed as:

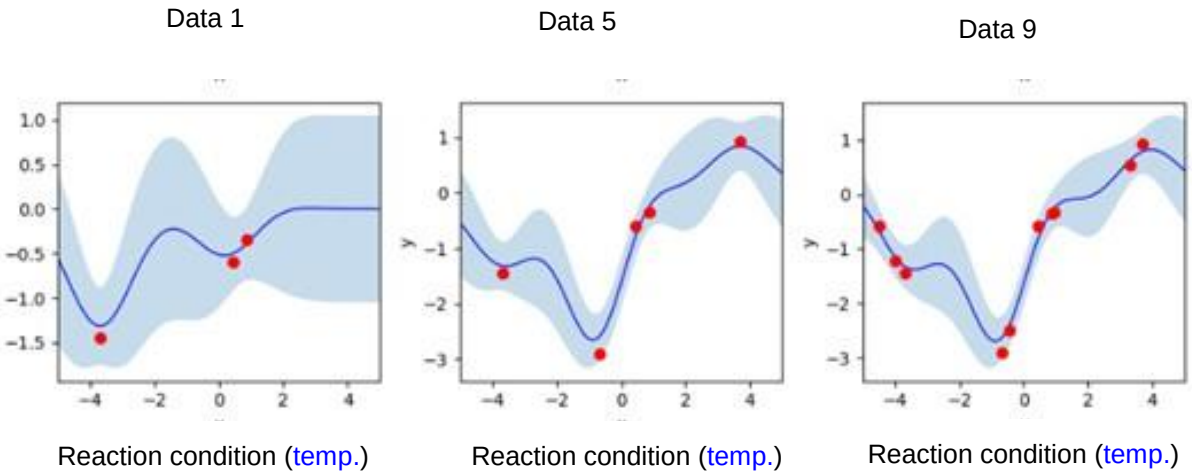
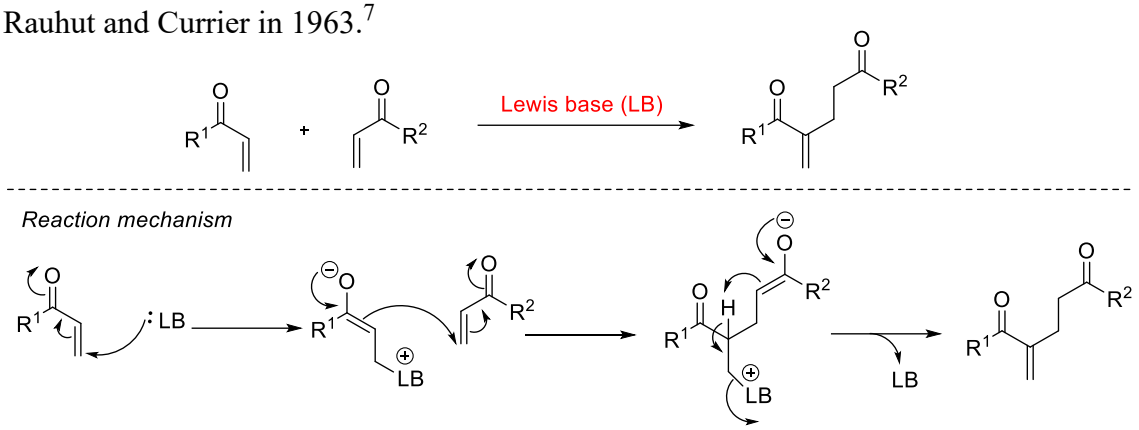


Figure 2.1. Graphical understand of GPR[5]

As shown in **Figure 2.1**, the red dots resemble experimental data by the initial training set. The blue line is the mean which is calculated by GPR. Also, the light blue band is the probability distribution band. It is known as a variance. After drawing a mean line from the initial training data set, several GPR is applied to get maximum yield prediction against reaction parameters. It has resulted that GPR can predict the maximum yield up to the 10th time of data iteration (data 9 in **Figure 2.1**). The chemist can judge the yield of the reaction by this yield vs parameter map. Therefore, we decided to use this statistical method for our new reaction development. To the best of our knowledge, this is the first report to establish the reaction parameter screening by GPR for the development of the organic flow reactions.

2.2 Rauhut-Currier reaction

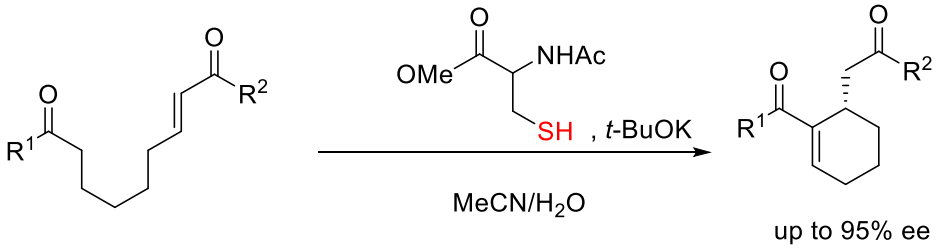
The Rauhut-Currier (RC) reaction (**Scheme 2.1**) is one of the most efficient C-C bond-forming reactions between two electron-deficient alkenes[6] because it leads to the synthesis of highly functionalized exo-methylidene compounds. It was first reported by Rauhut and Currier in 1963.[7]



Scheme 2.1. General mechanism of Rauhut-Currier reaction

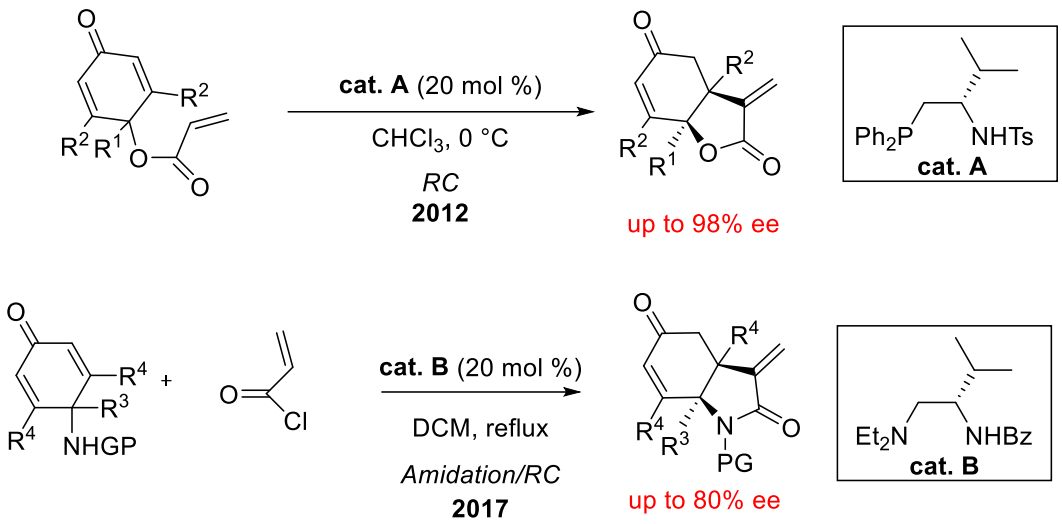
This reaction involves a conjugate addition of Lewis base (LB) to activate electron-deficient alkene, followed by a Michael addition of resulting carbonation to the second alkene (**Scheme 2.1**). The subsequent proton migration and elimination of LB are occurred to give RC adduct.

The first enantioselective RC was reported by Miller in 2007 [8] (**Scheme 2.2**). They have reported cyclo isomerization by intramolecular RC reaction promoted by thiolate catalyst to deliver the desired product in up to 95% ee.



Scheme 2.2. First enantioselective RC reaction

Subsequently, many publications in RC reaction were reported by Gladysz[9] in 2007, and Chrisrmann.[10] Also, Wu group reported the same reaction which was catalyzed by chiral organophosphine.[11]



Scheme 2.3. Catalytic enantioselective RC reaction reported by our group

In 2012,[12] our group also reported highly enantioselective RC reactions catalyzed by chiral phosphine to afford α-alkylidene-butyrolactones[13] in high enantioselectivity (**Scheme 2.3**). The chiral amine catalyzed Rauhut-Currier reaction was also reported by our group in 2017.[14] The sequential reaction consists of amidation step and asymmetric RC reaction for facile synthesis of α-methylidene-γ-lactams.[15]

2.3 This work

This time, I designed the new organocatalyzed sequential reaction[16] which was initiated with RC process. My domino reaction affords the optically active spirooixindole analogues which are important motifs that are found in many natural products and bioactive compounds (**Figure 2.2**).[17]

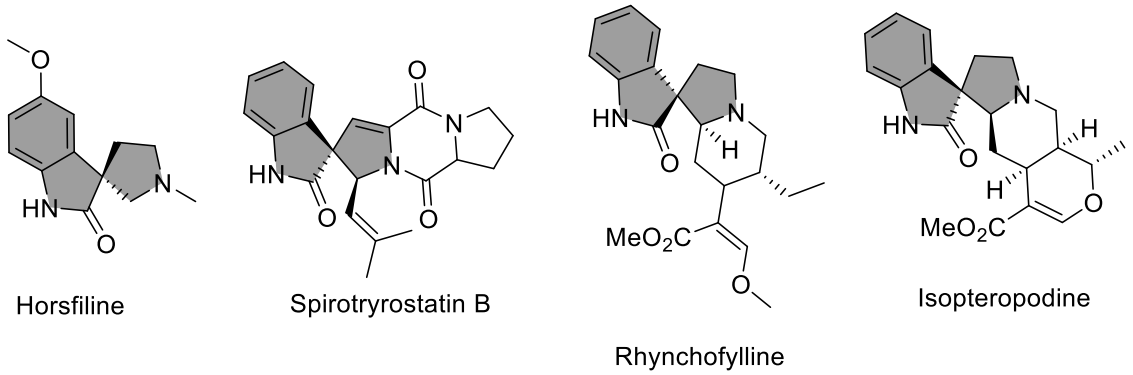
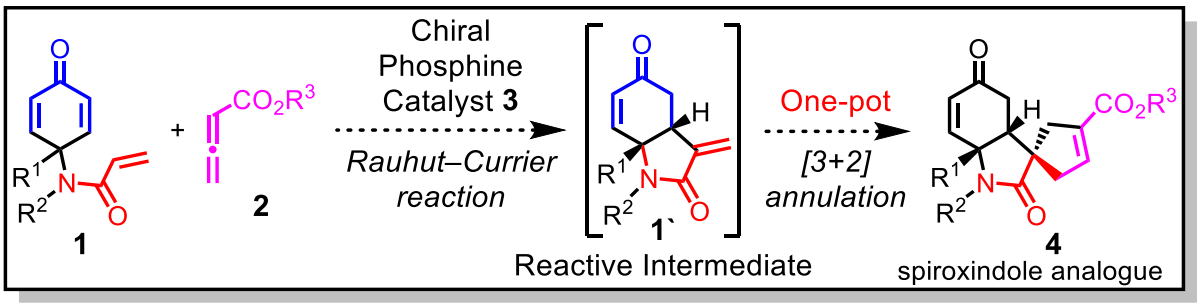


Figure 2.2. Bioactive spirooxindole derivatives

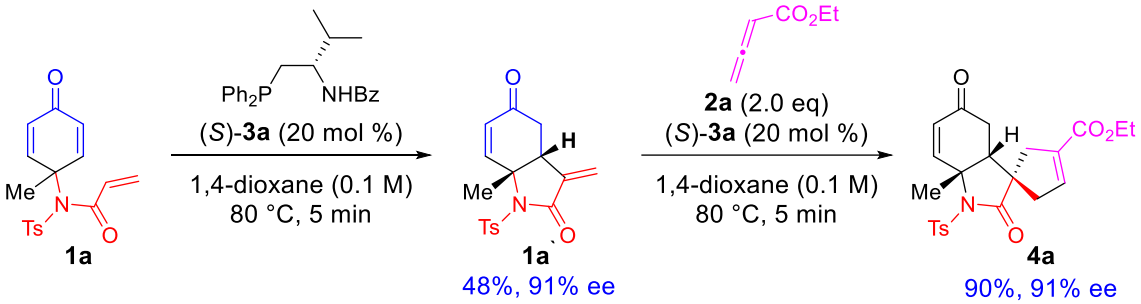
Until now, several methods have reported to afford spirooxindoles derivatives in the field of synthetic organic chemistry,[18] however, contiguous chiral centered motifs are still demanding. Hence, the author has developed a sequential organocatalysis to afford the three contiguous chiral centred analouge with a single operation.

This work:



My designed reaction consists of RC process, and sequential [3+2] annulation;[19] this organocatalyzed domino reaction is highlighted as an environmentally friendly synthetic process to afford the desired product in high yield with 100% atom economy. The reaction of dienone **1** with allenoate **2** to access the highly functionalized chiral spirooxindole analogue **4** bearing three contiguous chiral centers via the highly reactive intermediate **1`**. Among the chiral organocatalysts I tested, phosphine (*S*)-**3a** was realized as an optimum chiral organocatalyst. (optimization is explained later)

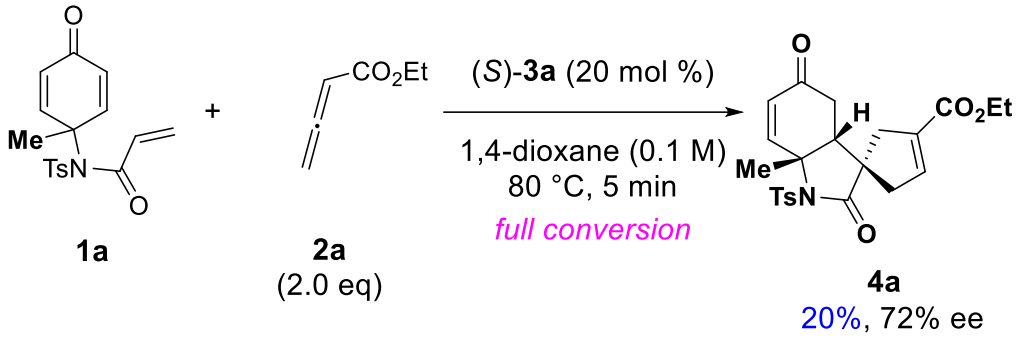
2.3.1 Initial Attempt
Stepwise reaction



Scheme 2.4. Step-wise reaction of enantioselective RC reaction and [3+2] annulation.

As an initial trial, the stepwise reaction was performed. The starting substrate **1a** gave the key intermdiate **1a'** with 48% yield with 91% ee in 1,4-dioxane at 80 ˚C through the chiral phosphine **3a** catalyzed RC process. And then [3+2] annulation of the enantioenriched reactive RC intermadiate **1a'** and alleoate **2a** was carried out. As results, the desired spirooxindole **4a** was obtained in 90% yield without loss of enantioselectivity (91% ee).

One-pot process



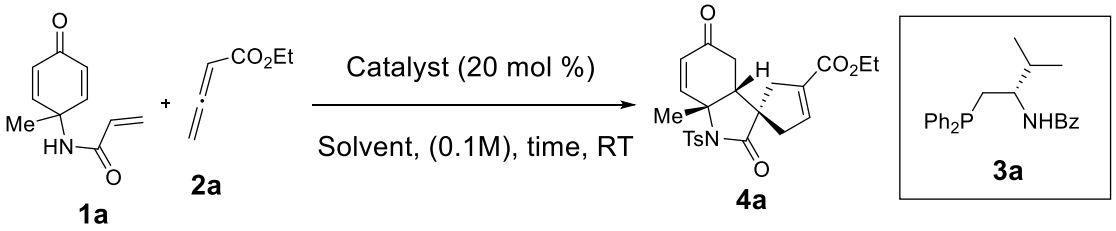
Scheme 2.5. Preliminary one-pot reaction of RC/[3+2] annulation sequence

Next, a one-pot reaction with a single operation was performed (**Scheme 2.5**). The product **4a** was obtained in quite low yield (20%) with moderate enantioselectivity (72% ee). A low chemical yield of **4a** was attributed to many undesired side reaction involvements. Therefore, further optimization study was investigated.

2.3 Batch optimization

2.3.1 Screening of solvent and temperature in batch system

Table 2.1. The solvent screening of RC/[3+2] annulation

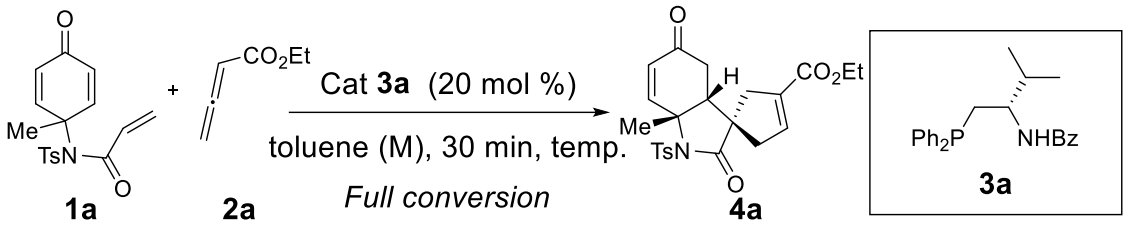


Entry	Solvent	Time (h)	Yield (%)	ee (%)
1	dioxane	0.5	20	72
2	toluene	0.5	42	86
3	DCM	0.5	36	86
4	THF	0.5	43	82
5	CH_3CN	0.5	36	72
6	MeOH	12	-	-

Among the solvents I screened (**Table 2.1**), toluene led to a formation of **4a** in 42% yield with 86% ee, but that was not sufficient enough. Other solvents in Table 2.1. did not show any improvement

2.3.2 Screening of concentration and temperature in batch system

Table 2.2. The solvent concentration and temperature screening of RC/[3+2] annulation



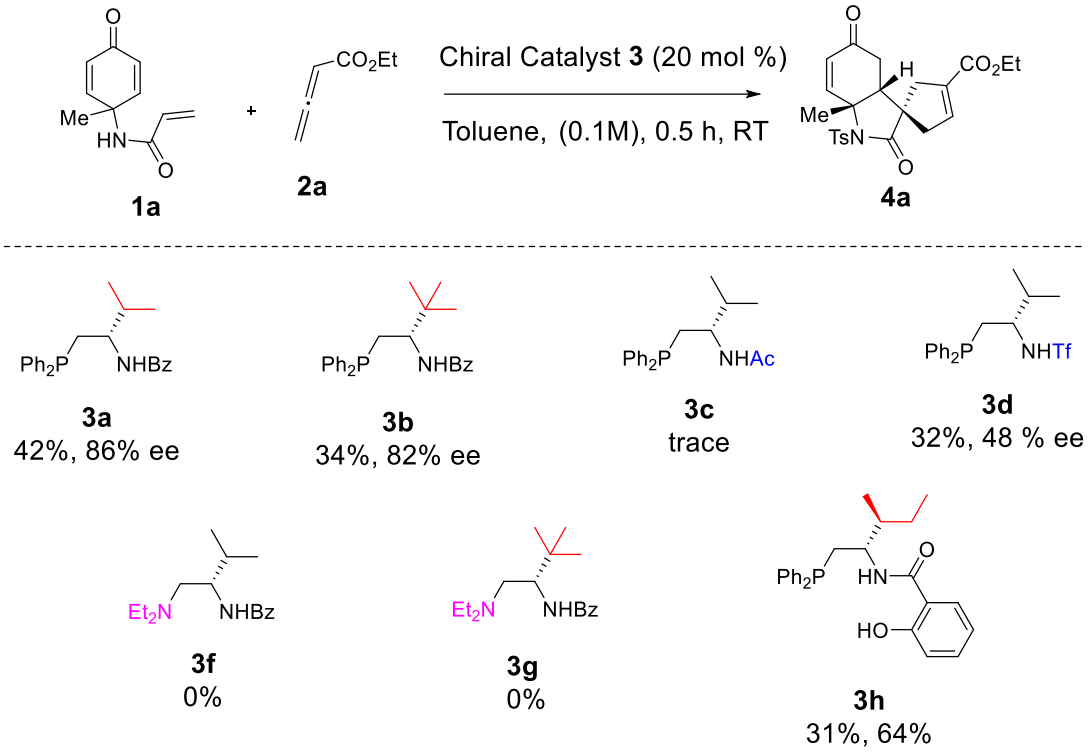
1a (0.1 mmol) **2a** (2 equiv.) **4a**

entry	temperature (°C)	concentration (M)	yield (%)	ee (%)
1	25	0.1	42	86
2	50	0.1	36	75
3	80	0.1	45	78
4	reflux	0.1	39	84
5	80	0.05	42	90
6	**80**	**0.01**	**65**	**92**
7[a]	80	0.01	44	92

a) 1 mmol scale

An optimal temperature (25 °C to reflux) was investigated in toluene as a reaction solvent (**Table 2.2**). However, no improvement of yield and ee of **4a** was achieved at various reaction temperatures. Since this reaction involves intramolecular/intermolecular manners, a various concentration of **1a** was also studied. Although the desired spiro compound **4a** was furnished in 65% yield with 92% ee, chemical yields of **4a** was decreasing from 65% to 44% when the reaction was carried out at the 10 times larger scale.

2.3.3 Screening of chiral catalyst in batch system



Scheme 2.7. Chiral catalyst screening

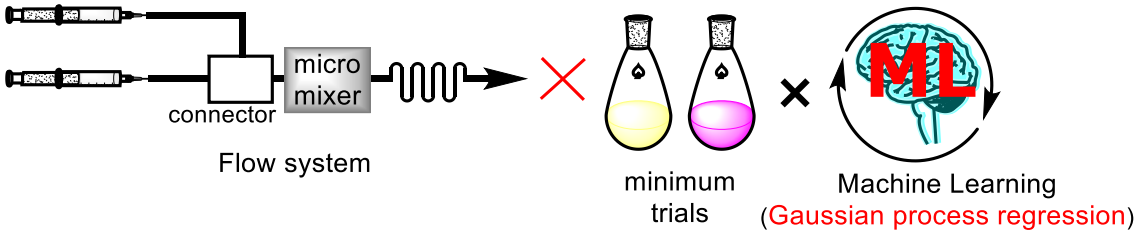
In this sequential reaction, the valine-derived catalyst **3a** showed good outcome to provide **4a** in 42% with 86% ee. A sterically hindered catalyst **3b** bearing *tert*-butyl group caused a decrease of chemical yield (**4a**: 34% yield, 82% ee). When the protecting group on nitrogen group was changed to benzoyl to acyl group only a trace amount of **4a** was obtained. It is noted that acidity of catalysts is to be crucial; a strong hydrogen bond donor catalysts **3c** and **3d** led to no formation or low enantioselectivity of the target compound **4a**. The amine catalysts as a Lewis base were unable to activate the sequential reaction to furnish the spirooxindole analogue; catalysts **3f** and **3g** provided no desired product. Huang catalyst **3h**[20] for the RC reaction gave a low amount of **4a** in 31% with 64% ee.

2.4 Problem and solution

Problem: Difficulty of controlling the highly reactive intermediate

After several screenings, I realized that an improvement of chemical yield of **4a** was extremely difficult. Because this reaction involves a highly reactive intermediate **1'**[13] that is bearing electron-deficient exo olefin. Before the intermediate **1'** reacts with an additional nucleophile **2a** in the presence of phosphine catalyst **3a**, various kinds of side reactions resulted in providing unidentified by-products and low yield of **4a**. As mentioned in **Chapter 1**, I assumed that the continuous flow reaction system might be an appropriate process to transform this reactive intermediate to stable product **4a** because of efficient mixing, heating, and mass transfer, to diminish by-product formation. In this time, ML optimization method is also applied to minimize the reaction optimization trails (**Figure 2.3**).

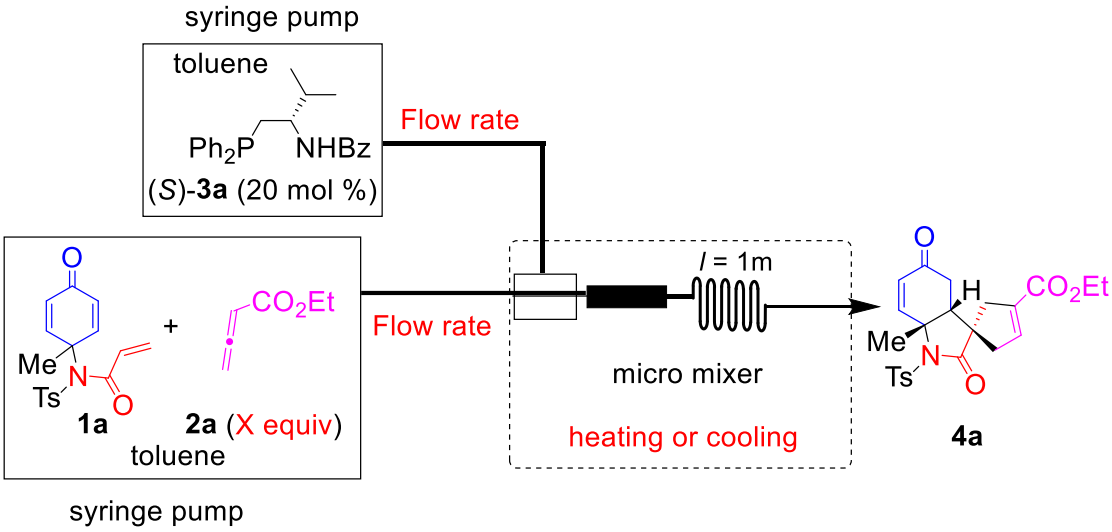
Author`s hypothesis: Solution



The reactivity of **1`** would be controlled • Efficient mixing • Rapid heating Flow reactor: Comet X-01	Apply machine learning assisted optimization • Minimum trails of experiments • Multi-parameter screening • Quick prediction of higher yield

Figure 2.3. Flow reaction system with ML assisted optimization

2.5 Flow reactor and it`s general procedure



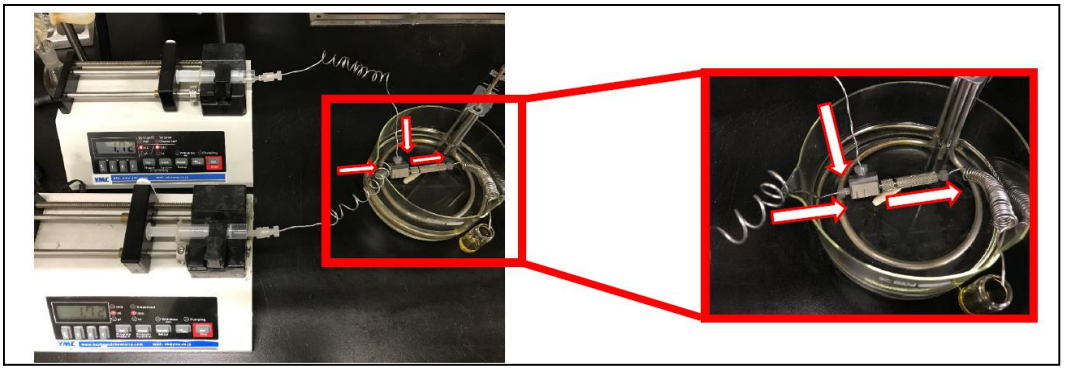


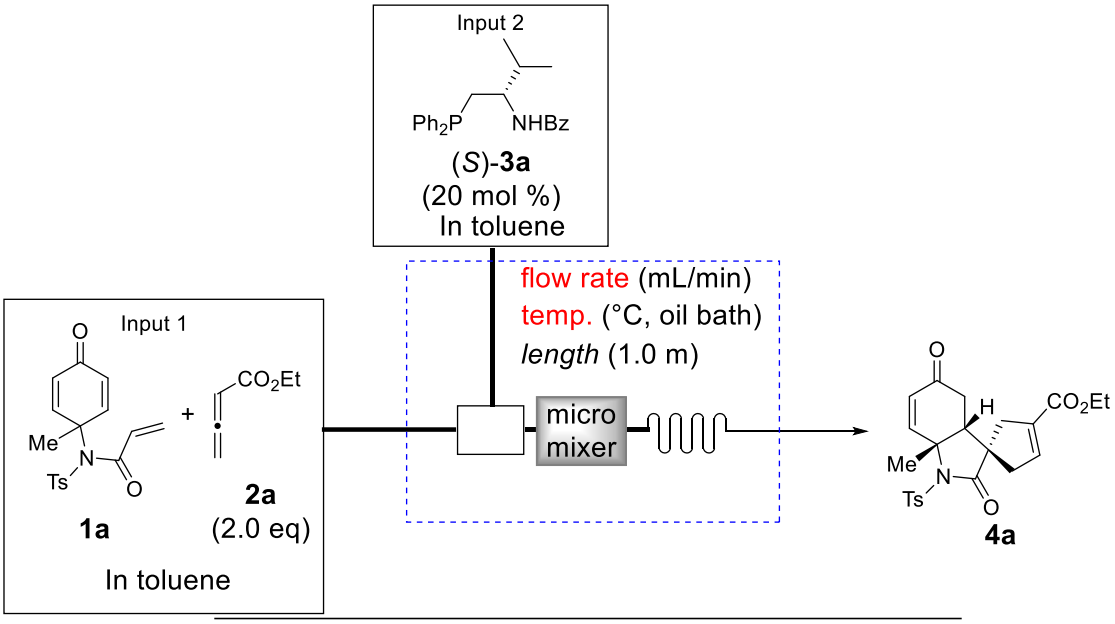
Figure 2.4: General flow reaction procedure

A flow micro-reactor system was dipped in an oil bath for heating or cooling purpose (**Figure. 2.4**). A solution of **1a** and **2a** in degassed dry toluene was input by a one syringe pump, and a solution of catalyst **3a** in degassed dry toluene was introduced by another syringe pump to the flow microreactor system. The flow rate can be changed by a syringe pump speed. After the continuous flow was kept within residence time, the reaction mixture was collected to a round bottom flask. Under an air atomosphere, an auto-oxidation of air-sensitive catalyst proceeded to stop the reaction. The reaction mixture was passed through a short silica pad with EtOAc. Removal of the solvent under reduced pressure afforded a residue, which was purified by silica gel chromatography (*n*-hexane/EtOAc) to give the product **4a**.

2.6 Machine learning assisted optimization by GPR

2.6.1 GPR for flow rate vs temperature

The first trial of the flow reaction gave **4a** in 49% NMR yield. This result motivates me to continue the reaction in a flow system. To get an initial training set, the two crucial reaction factors (flow rate and temperature) were changed simultaneously. Five experiments set were collected randomly. With these obtained outcomes in hand (**Table 2.3**), I performed ML-assisted based Gaussian process regression (GPR) searching of appropriate reaction conditions. GPR on GPy, which is a programming library for GPR, constructs a regression model by using a limited number of observed data through ML.



entry	flow rate (mL/min)	temp. (°C)	yield (%)
1	1.0	90	49
2	1.5	80	72
3	2.0	70	58
4	2.5	60	55
5	3.0	100	43

Table 2.3. Experimental set flow rate and temperature

Therefore, searches for a subsequent appropriate parameter value by using the model as a surrogate model of the flow reaction conditions. Specifically, to achieve ML prediction of the suitable flow reaction conditions, the temperature was varied from 60 ˚C to 100 ˚C.

And, the flow rate was also screened within 1.0 ml/min to 3 mL/mim. This was the first screening for GPR while keeping a constant of eq. of **2a**. (**Table 2.3**). Standardization was performed to compensate for the large difference in scale between the temperature and the flow rate. Evaluation of the observed results using GPR illustrated the estimated yield from the screening results of the flow rate and the temperature as shown in **Figure 2.5A**. Where intense yellow area shows higher yield and black area predicts lower yield. This outcome encouraged me to focus on the yellow area in **Figure 2.5A,** predicting the appropriate conditions. According to GPR, the light blue area indicates the confidence bounds in **Figure 2.5B** and **2.5C**. According to the ML prediction flow rate and the temperature was predicted as 1.7 mL/min and 77 ˚C respectively. These values were estimated from the maximum values of the upper confident bound in **Figures 2.5B** and **2.5C**. It is indicated by the red line shown there.

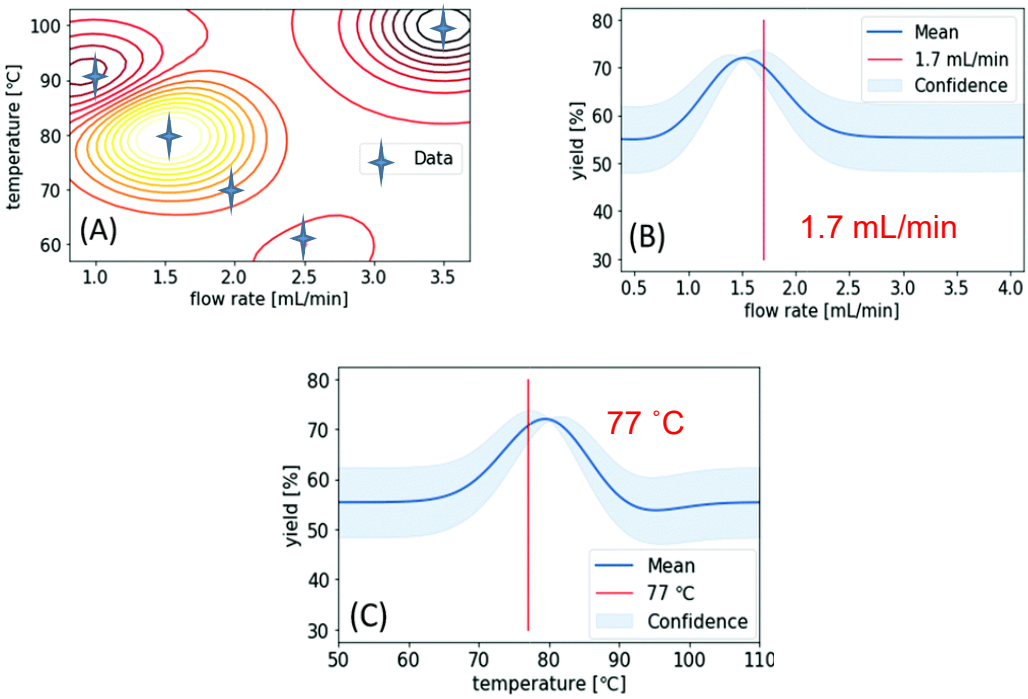
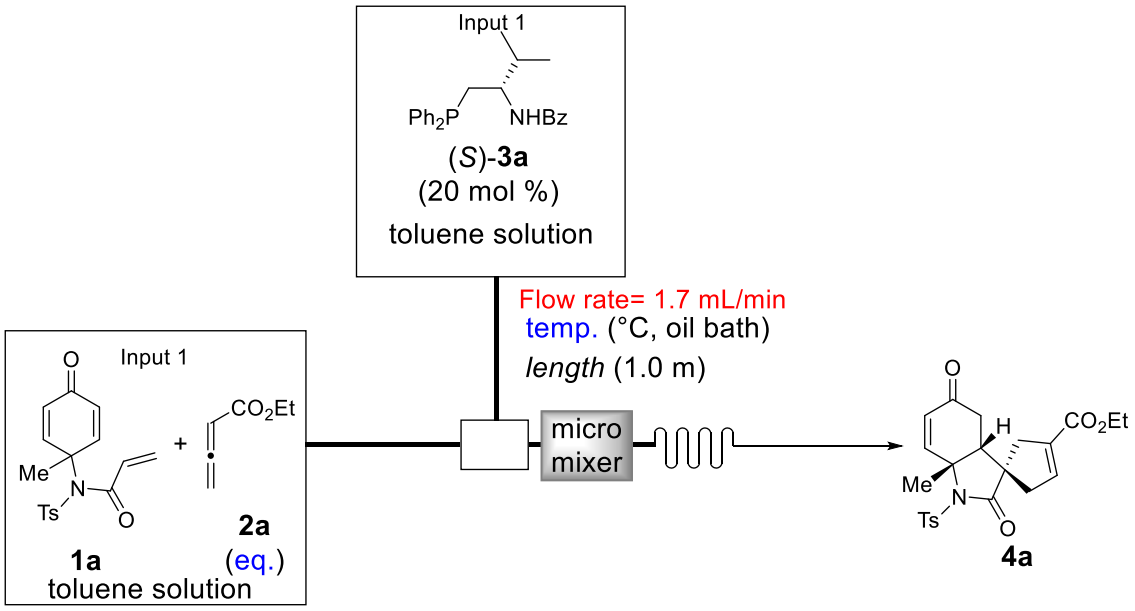


Figure 2.5: GPR with GPy. (A) Chemical yields predicted by the experimental data in **Table 2.3**, entries 1–5. (B) Predicted yields under various flow rates. (C) Predicted yields at various temperatures.

2.6.2 GPR for the equivalent of 2a versus temperature



entry	**2a** (eq.)	temp. (°C)	yield (%)
1	1.0	80	45
2	1.5	100	51
3	2.0	90	58
4	3.0	70	50
5	3.5	60	48

Table 2.4. Experimental set equiv. of **2a** and temperature

According to ML prediction, as shown in **Figure 2.5**, the flow rate was fixed as 1.7 mL/min, and temperature and equivalent of **2a** were screened randomly. The amount of **2a** varied from 1.0 eq to 3.5 eq, the temperature also changed from 60 ˚C to 100 ˚C (**Table 2.4)**. After collecting the experimental outcome of the above random screening, GPR was applied to get the prediction set as the yellow area in **Figure 2.6A**.

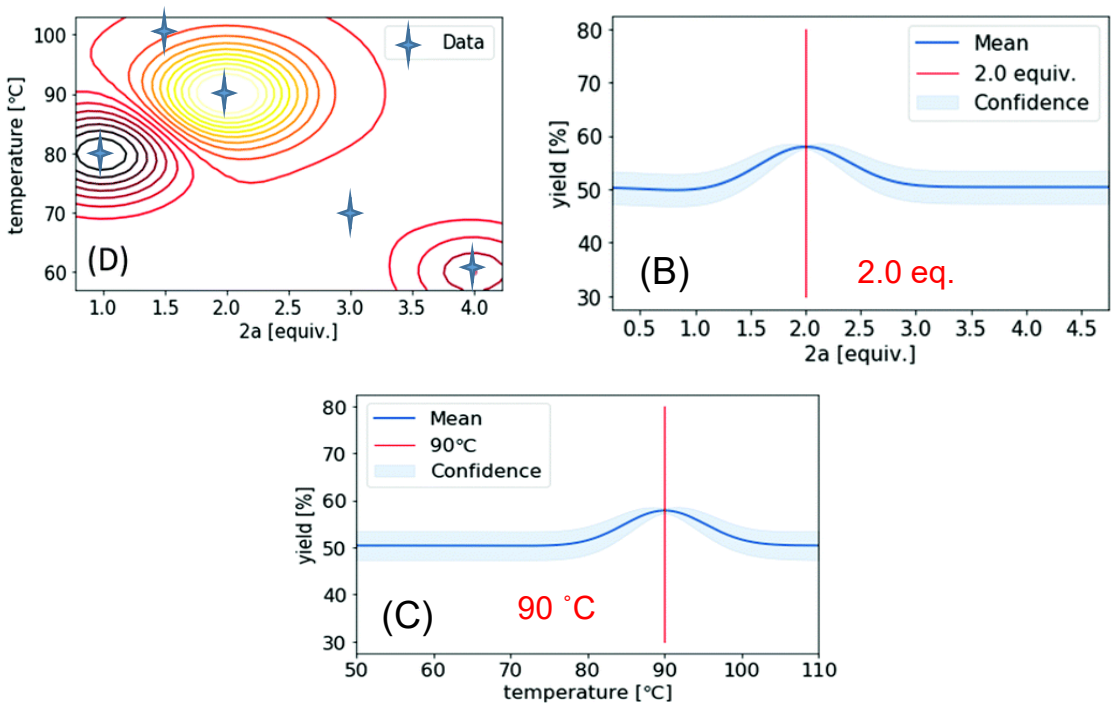
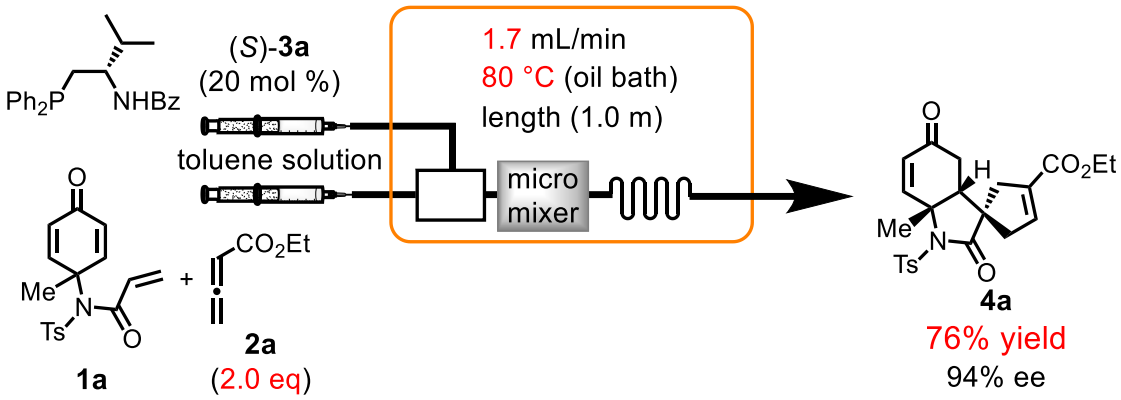


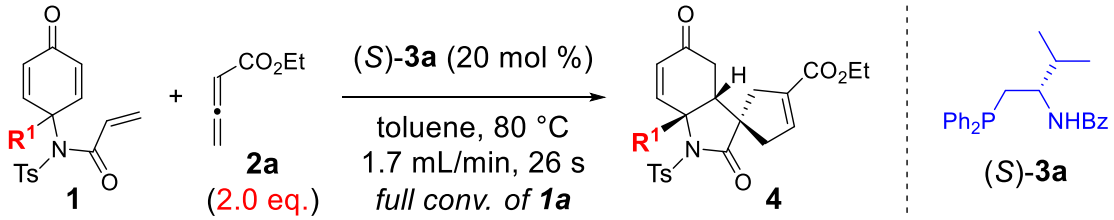
Figure 2.6. GPR with GPy. (A) Chemical yields predicted by the experimental data in **Table 2.4**, entries 1–5. (B) Predicted yields with different eq. of **2a**. (C) Predicted yields at various temperatures.

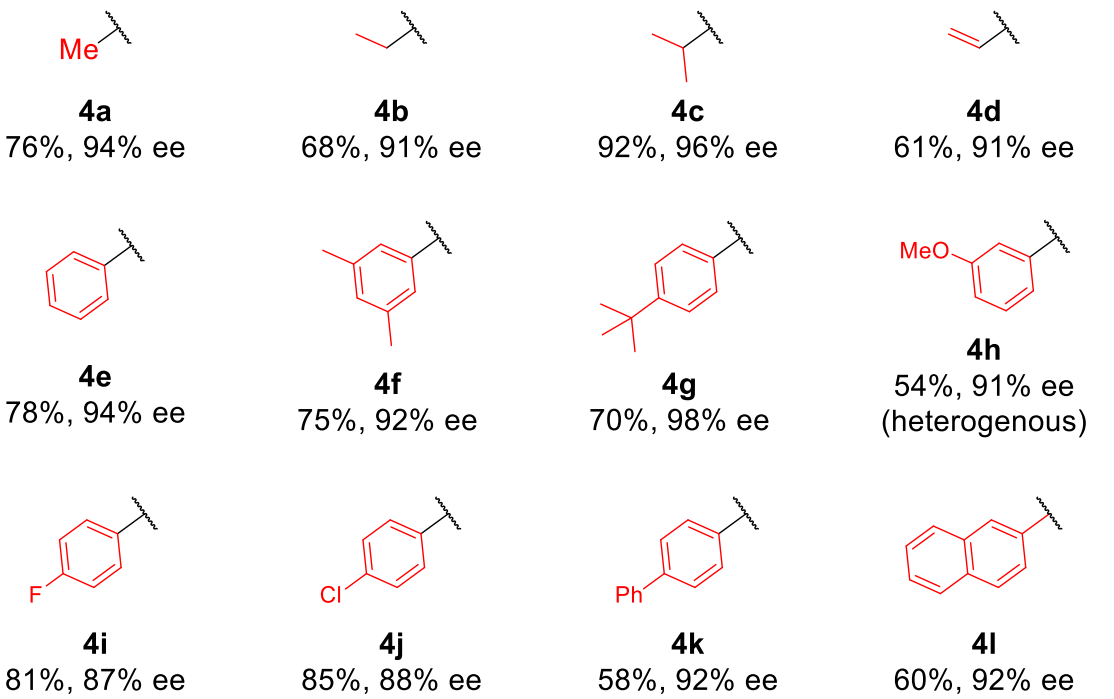
Based on ML-prediction in **Figure 2.6**, 2.0 eq of **2a** should be appropriate. (**Figure 2.6B**). And an appropriate reaction temperature was estimated as below 90 ˚C (**Figure 2.6C**) Considering all the results estimated by GPR and the experimental data in the batch system, we decided the suitable flow reaction conditions to be 2.0 eq. of **2a**, a flow rate of 1.7 mL/min, at 80 ˚C. When I applied the predicted conditions to a practical reaction, **4a** was isolated in 76% yield and 94% ee as shown in **Scheme 2.8**.



Scheme 2.8. Experimental outcome under ML-predicted reaction conditions

2.7 Substrate scope

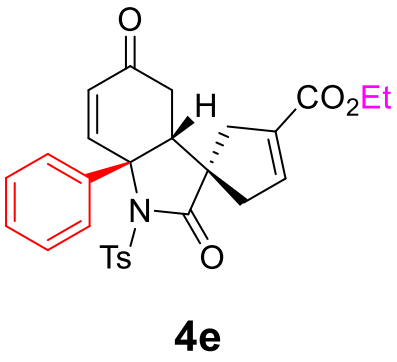




Scheme 2.9. Scope of RC and the [3+2] annulation sequence.

Under the ML-predicted reaction conditions, substrate scope was investigated. A variety of dienone starting materials **1** was tested on this domino reaction. When R^1 with aliphatic substituents **1b** (R^1 = Et) and **1c** (R^1 = iPr) afforded the corresponding products **4b** and **4c** in 68% and 92% yields with 92% and 96% ees, respectively. The reaction of **1d** bearing a vinyl group provided the corresponding spirocyclic compound **4d** in 61% yield with 91% ee. A variety of aryl group substituents on **1** were also investigated. Starting material **1e** having phenyl group afforded the product **4e** in 78% with 94% ee. Also, electron-donating groups led to **4f** (R^1 = 3,5-diMe-C_6H_3, 75% yield, 92% ee) and **4g** (R^1 = 4-tBu-C_6H_4, 70% yield, 98% ee), respectively. The electron-withdrawing substituents on the aryl group also reacted with allenoate **2a** smoothly to give the corresponding products **4i** (R^1 = 4-F-C_6H_4) and **4j** (R^1 = 4-Cl-C_6H_4) in 81% and 85% yields with 87% and 88% ees, respectively. Due to its low solubility of **1h** in toluene, spiro compound **4h** was obtained in low yield (54%) with 91% ee.

The absolute configuration of the chiral spiro compound **4e** with the catalyst (*S*)-**5** was determined to be (*S*, *R*, *R*) by single X-ray crystallographic analysis (**Figure 2.7**).



4e

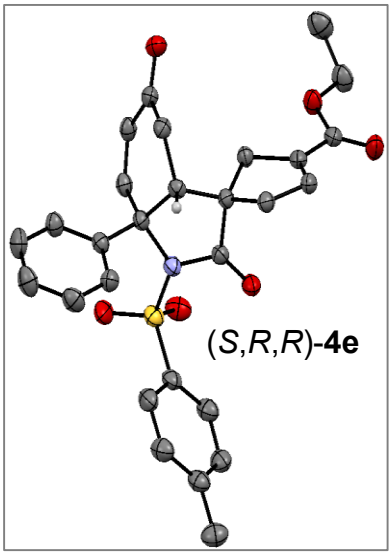


Figure 2.7. Determination of absolute cofiguration

2.9 Reaction Mechanism

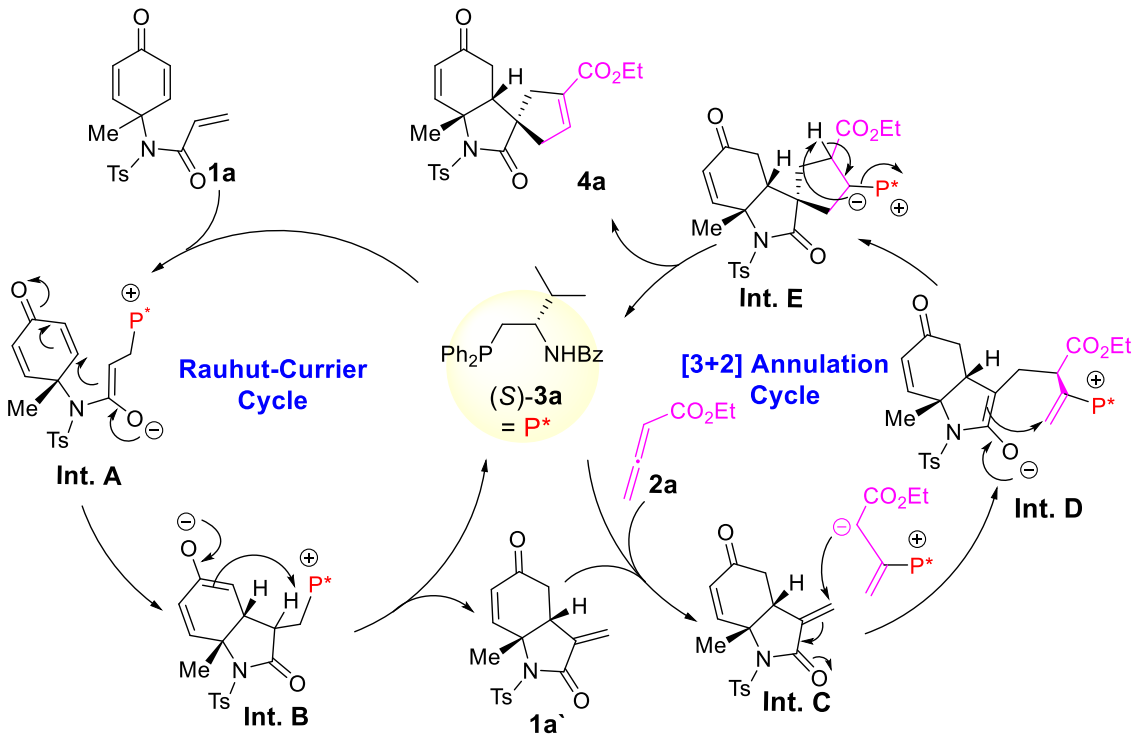


Figure 2.8. Plausible Reaction Mechanism

A plausible reaction mechanism for this sequential reaction is shown in **Figure 2.8**. Initially, the Michael addition of catalyst **3a** to the acrylamide **1a** generates the intermediate A (**Int. A**). The generating chiral enolate in **Int. A** subsequently reacts with one of the olefins on the dienone unit to afford **Int. B**. Then, deprotonation of the α-proton of the carbonyl group in **Int. B** resulted in **1a`** bearing a highly reactive exo-olefin. Then, **1a `** is subsequently trapped with allenoate **2a** by entering to [3+2] annulation cycle. In the intermolecular [3+2] annulation supported by the micro-mixing flow system, allenoate **2a** reacts with the regenerated organocatalyst **3a** to afford **Int. D**. Since this step is intermolecular and it is important to have flow reaction even in dilute conditions. Next, the electron-deficient phosphonium cation in **Int. D** prompts the conjugate addition of enolate to give **Int. E**. Finally, the desired product **4a** is formed through proton transfer and elimination of the catalyst from **Int. E**.

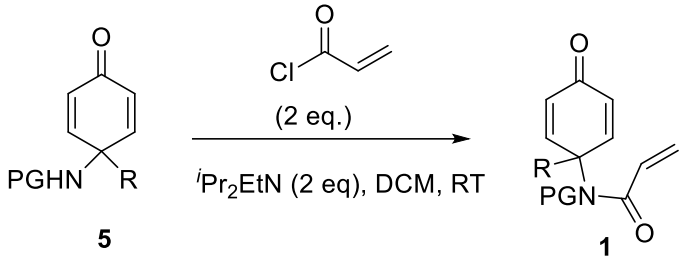
2.10 Summary

I demonstrated highly atom-economical chemo-, regio-, enantio-, and diastereoselective domino reaction consist of RC and the [3+2] annulation sequence using a chiral

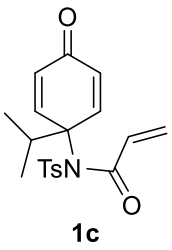
phosphine organocatalyst in a flow system. GPR was successfully applied to multi-parameter reaction screening. The present domino reaction provided chiral highly functionalized spiro heterocycles with three contiguous chiral centers in excellent results within one minute using flow reaction system.[21]

2.12 Experimental Section

1) Procedure of preparation **1**

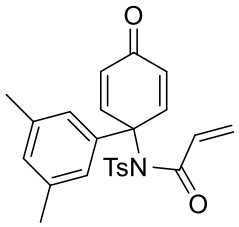


A round bottom flask was charged with a dichloromethane solution of dienone **5** (10 mL, 1.0 mmol) and DIPEA (2 eq.). Then, acrolylchloride (2.0 mmol) was added to the reaction vesicle at RT. The reaction mixture was stirred vigorously for 1 h at RT. The reaction was then quenched by a short silica pass. The combined solution was concentrated in *vacuo* and the obtained crude product was quickly purified by silica gel column chromatography using hexane/ethyl acetate as an eluent to give the desired product **1** as a yellow oil or white solid. (**1** is not so stable on silica gel)



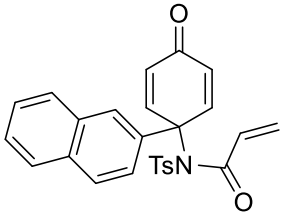
1c

1c: White solid: 40% yield; ^{1}H-NMR (400 MHz, $CDCl_3$) δ 7.54 (dd, *J* = 6.9, 1.8 Hz, 2H), 7.22 (d, *J* = 8.2 Hz, 2H), 7.06 (dd, *J* = 8.7, 1.8 Hz, 2H), 6.90 (dd, *J* = 16.9, 10.1 Hz, 1H), 6.48 (dd, *J* = 16.9, 0.9 Hz, 1H), 6.03 (dd, *J* = 8.5, 2.1 Hz, 2H), 5.90 (dd, *J* = 10.1, 1.4 Hz, 1H), 2.56-2.63 (m, 1H), 2.40 (s, 3H), 0.82 (s, 3H), 0.80 (s, 3H); ^{13}C-NMR (101 MHz, $CDCl_3$) δ 184.83, 170.82, 146.89, 145.43, 136.75, 134.68, 130.61, 130.15, 129.67, 128.67, 67.58, 32.14, 21.72, 17.15; IR (KBr) 2983, 2962, 2939, 2378, 2364, 2345, 1714, 1673, 1630, 1403, 1336, 1186, 1071, 981, 920, 663 cm^{-1}



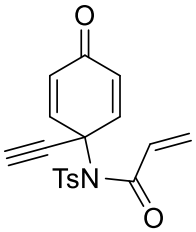
1f

1f: White solid: 64% yield; ^{1}H-NMR (400 MHz, $CDCl_3$) δ 7.54 (dd, *J* = 6.9, 1.8 Hz, 2H), 7.18-7.24 (m, 4H), 6.85 (dd, *J* = 16.7, 10.3 Hz, 1H), 6.16 (dd, *J* = 16.9, 1.4 Hz, 1H), 5.95 (dd, *J* = 8.2, 1.8 Hz, 2H), 5.72 (dd, *J* = 10.3, 1.1 Hz, 1H), 2.37 (s, 3H), 2.15 (s, 6H); ^{13}C-NMR (101 MHz, $CDCl_3$) δ 185.00, 169.69, 148.33, 145.69, 139.11, 138.22, 136.48, 133.52, 130.80, 130.50, 129.81, 128.62, 127.54, 122.98, 65.67, 21.81, 21.52; IR (KBr) 2984, 2962, 1712, 1669, 1625, 1401, 1354, 1341, 1185, 1170, 1117, 1068, 981, 666, 599 cm^{-1};



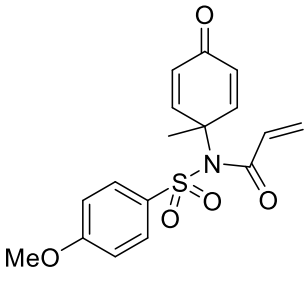
1l

1l: White solid: ^{1}H-NMR (400 MHz, $CDCl_3$) δ 7.88-7.92 (m, 2H), 7.75-7.82 (m, 5H), 7.54-7.60 (m, 2H), 7.46 (dd, J = 8.7, 1.8 Hz, 1H), 7.29 (d, J = 7.8 Hz, 2H), 6.63 (s, 1H), 6.61 (d, J = 11.0 Hz, 1H), 4.12-4.17 (m, 2H), 3.06 (d, J = 18.8 Hz, 1H), 2.95 (s, 1H), 2.61 (d, J = 2.3 Hz, 2H), 2.44-2.48 (m, 4H), 2.36 (dd, J = 18.8, 2.3 Hz, 1H), 1.26 (t, J = 7.1 Hz, 3H); ^{13}C-NMR (101 MHz, $CDCl_3$) δ 184.86, 169.47, 147.93, 145.80, 136.49, 135.72, 133.37, 133.27, 132.99, 131.07, 129.89, 129.54, 128.61, 128.25, 127.86, 127.73, 126.92, 124.53, 122.46, 65.74, 21.88; IR (KBr) 3058, 2380, 2366, 2360, 2345, 2310, 1692, 1668, 1627, 15077, 1397, 1192, 1177, 1087, 986, 865, 660 cm^{-1};



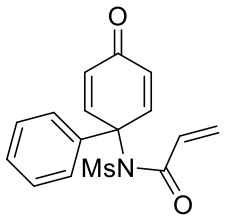
1n

1n: yellow solid: 50% yield; ^{1}H-NMR (400 MHz, $CDCl_3$) δ 7.71 (d, J = 8.2 Hz, 2H), 7.32 (d, *J* = 7.8 Hz, 2H), 7.05 (dd, *J* = 12.8, 3.2 Hz, 2H), 6.75-6.82 (m, 1H), 6.46 (dd, *J* = 16.9, 0.9 Hz, 1H), 6.13-6.17 (m, 2H), 5.91 (dd, *J* = 10.1, 0.9 Hz, 1H), 2.54 (s, 1H), 2.45 (s, 3H); ^{13}C-NMR (101 MHz, $CDCl_3$) δ 183.93, 168.20, 145.78, 144.66, 136.78, 132.27, 131.76, 130.00, 128.15, 128.11, 76.36, 76.20, 55.76, 21.79; IR (KBr) 3274, 3098, 3063, 1704, 1667, 1625, 1608, 1398, 1348, 1173, 1014, 942, 863, 811, 662 cm^{-1};



1m

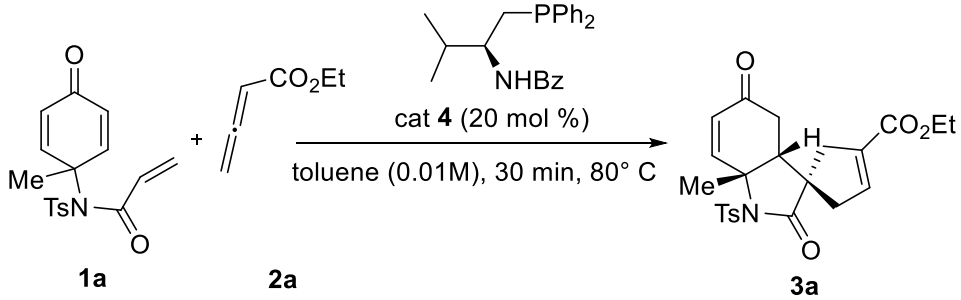
1m: yellow solid: 40% yield; ^{1}H-NMR (400 MHz, $CDCl_3$) δ 7.61-7.64 (m, 2H), 7.08-7.10 (m, 2H), 6.88 (dd, *J* = 6.9, 2.3 Hz, 2H), 6.73 (dd, *J* = 16.7, 10.3 Hz, 1H), 6.43 (dd, *J* = 16.9, 1.4 Hz, 1H), 5.96-5.99 (m, 2H), 5.91 (dd, *J* = 10.1, 0.9 Hz, 1H), 3.83 (s, 3H); ^{13}C-NMR (101 MHz, $CDCl_3$) δ 184.58, 170.73, 164.11, 150.62, 134.26, 131.70, 130.81, 130.77, 127.44, 114.38, 60.16, 55.90, 26.99; IR (KBr) 3452, 2946, 2842, 2345, 1720, 1670, 1597, 1498, 1348, 1265, 1166, 1020, 835, 805, 560 cm^{-1};



1p

1p: white solid: 75% yield; ^{1}H-NMR (400 MHz, $CDCl_3$) δ 7.47 (d, *J* = 10.1 Hz, 2H), 7.31-7.38 (m, 5H), 6.65 (dd, *J* = 16.9, 10.1 Hz, 1H), 6.28-6.39 (m, 3H), 5.80 (d, *J* = 10.1 Hz, 1H), 3.22 (s, 3H)**;** ^{13}C-NMR (101 MHz, $CDCl_3$) δ 184.59, 168.72, 148.05, 138.42, 131.83, 129.53, 128.96, 128.37, 125.39, 66.09, 44.71 (one carbon overlapped); IR (KBr) 3057, 3033, 3012, 2934, 2385, 2360, 1692, 1667, 1631, 1489, 1399, 1359, 1332, 1184, 1137, 958, 787, 765 cm^{-1}

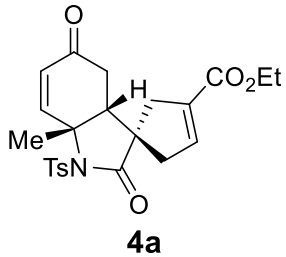
2) General procedure for the RC/[3+2] sequence (Batch)



Allenic ester **2a** (0.06 mmol, 2 eq) was added to a solution of (20 mol %), acrylic amide **1a** (0.03 mmol, 10 mg) in dry toluene 3 mL (0.01 M). Then, the reaction mixture was kept at 80 °C. Catalyst **4** was added to the mixture of **1a** and **2a**. The reaction mixture was stirred at 80 °C for 30 min. The crude mixture was filtered through the short silica pass by EtOAc. The solvent was evaporated under reduced pressure and the crude product was purified by flash chromatography on silica gel (*n*-hexane/EtOAc = 2/1) to afford the spirocyclic product **3a**.

3) General procedure for the RC/[3+2] sequence (Flow)

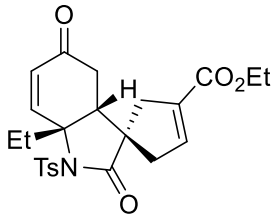
- Already explained in section 2.1



4a

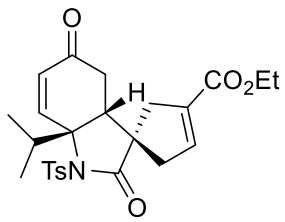
4a: 76% yield (70% yield on a 1 mmol scale of **1a**); white solid; ^{1}H-NMR (400 MHz, $CDCl_3$) δ 7.95 (d, *J* = 8.0 Hz, 2H), 7.49 (d, *J* = 10.5 Hz, 1H), 7.35 (d, *J* = 8.0 Hz, 2H), 6.62 (t, *J* = 2.1 Hz, 1H), 6.15 (d, *J* = 10.5 Hz, 1H), 4.06-4.18 (m, 2H), 2.97 (dd, *J* = 17.4 Hz, 2.2 Hz, 1H), 2.77 (dd, *J* = 18.5, 7.6 Hz, 1H), 2.56-2.60 (m, 2H), 2.37-2.49 (m, 6H), 1.96 (s, 3H), 1.24 (t, *J* = 7.1 Hz, 3H);

^{13}C-NMR (100 MHz, $CDCl_3$) δ 194.25, 176.36, 163.56, 148.22, 145.59, 140.30, 135.74, 134.12, 129.73, 128.72, 63.77, 60.61, 52.57, 49.02, 42.33, 37.62, 33.43, 27.13, 21.81, 14.27 (one carbon overlapped); HRMS (ESI) calcd for $C_{23}H_{25}NO_6SNa$: *m/z* ([M+Na$^+$]) 466.1295, found 466.1295; IR (KBr) 2963, 2926, 2854, 1738, 1719, 1710, 1686, 1678, 1362, 1304, 1263, 1172, 1086, 1015 cm^{-1}; $[\alpha]_D^{25}$ = -72.2 (*c* 1.0, $CHCl_3$ for 94% ee); HPLC conditions: Daicel Chiralpak ID column, *n*-hexane/EtOH = 2/1, 1.0 mL/min, 215 nm, tR = 24.0 min (major isomer) and 41.1 min (minor isomer).



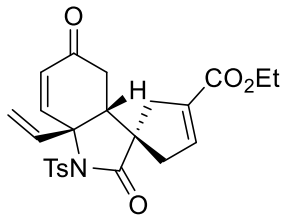
4b

4b: 68% yield; white solid; ^{1}H-NMR (400 MHz, $CDCl_3$) δ 7.93 (d, *J* = 8.4 Hz, 2H), 7.48 (d, *J* = 10.5 Hz, 1H), 7.34 (d, *J* = 8.4 Hz, 2H), 6.62 (t, *J* = 2.3 Hz, 1H), 6.22 (d, *J* = 10.5 Hz, 1H), 4.06-4.14 (m, 2H), 3.04 (dd, *J* = 18.6, 2.3 Hz, 1H), 2.66-2.75 (m, 2H), 2.47-2.56 (m, 2H), 2.40-2.45 (m, 5H), 2.26 (dd, *J* = 18.6, 2.3 Hz, 1H), 2.11-2.18 (m, 1H), 1.22 (t, *J* = 7.1 Hz, 3H), 1.10 (t, *J* = 7.3 Hz, 3H); ^{13}C-NMR (100 MHz, $CDCl_3$) δ 194.51, 176.56, 163.41, 147.37, 145.54, 140.28, 135.11, 133.86, 129.56, 129.53, 128.78, 67.66, 60.49, 52.40, 43.83, 42.51, 37.64, 34.03, 30.87, 21.71, 14.16, 8.59 (one carbon overlapped); HRMS (ESI) calcd for $C_{24}H_{27}NO_6SNa$: *m/z* ([M+Na]$^+$) 480.1451, found 480.1447; IR (KBr) 2986, 2937, 1739, 1703, 1684, 1393, 1348, 1246, 1168 cm^{-1}; $[\alpha]_D^{20}$ = -74.8 (*c* 1.0, $CHCl_3$ for 92% ee); HPLC conditions: Daicel Chiralpak ID column, *n*-hexane/EtOH = 2/1, 1.0 mL/min, 225 nm, tR = 24.6 min (major isomer) and 41.4 min (minor isomer).



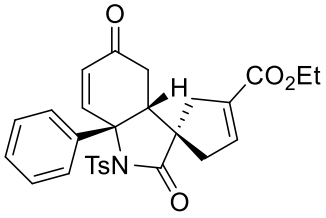
4c

4c: 92% yield; white solid; ^{1}H-NMR (400 MHz, $CDCl_3$) δ 7.83 (d, *J* = 8.4 Hz, 2H), 7.51 (d, *J* = 10.8 Hz, 1H), 7.26 (d, *J* = 8.4 Hz, 2H), 6.54 (t, *J* = 2.3 Hz, 1H), 6.28 (d, *J* = 10.8 Hz, 1H), 3.99-4.06 (m, 2H), 2.99-3.04 (m, 2H), 2.56-2.68 (m, 2H), 2.47 (d, *J* = 18.3 Hz, 1H), 2.31-2.39 (m, 5H), 1.97-2.11 (m, 1H), 1.14 (t, *J* = 7.1 Hz, 3H), 1.09 (d, *J* = 6.9 Hz, 3H), 0.97 (d, *J* = 6.9 Hz, 3H); ^{13}C-NMR (100 MHz, $CDCl_3$) δ 194.86, 176.47, 163.25, 146.73, 145.34, 140.63, 134.92, 133.49, 130.86, 129.59, 128.92, 71.21, 60.55, 52.86, 42.64, 40.32, 38.01, 36.01, 34.55, 21.78, 18.48, 16.91, 14.24; HRMS (ESI) calcd for $C_{25}H_{29}NO_6SNa$: *m/z* ([M+Na]$^+$) 494.1608, found 494.1603; IR (KBr) 2970, 1743, 1707, 1688, 1637, 1395, 1343, 1248, 1167 cm^{-1}; HPLC conditions: $[\alpha]_D^{20}$ = -113.2 (*c* 1.0, $CHCl_3$ for 96% ee); Daicel Chiralpak ID column, *n*-hexane/EtOH = 2/1, 1.0 mL/min, 250 nm, tR = 27.8 min (major isomer) and 45.9 min (minor isomer).



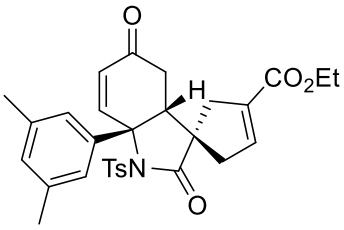
4d

4d: 61% yield; white solid; ^{1}H-NMR (400 MHz, $CDCl_3$) δ 7.96 (d, *J* = 8.2 Hz, 2H), 7.34-7.38 (m, 3H), 6.63 (t, *J* = 2.3 Hz, 1H), 6.38 (d, *J* = 10.5 Hz, 1H), 6.10 (dd, *J* = 17.4, 10.5 Hz, 1H), 5.47 (d, *J* = 10.1 Hz, 1H), 5.31 (d, *J* = 17.4 Hz, 1H), 4.10-4.17 (m, 2H), 2.98 (dd, *J* = 18.3 Hz, 2.3 Hz, 1H), 2.57-2.69 (m, 2H), 2.48-2.52 (m, 3H), 2.37-2.47 (m, 4H), 1.24 (t, *J* = 7.1 Hz, 3H); ^{13}C-NMR (100 MHz, $CDCl_3$) δ 194.63, 176.10, 163.25, 145.75, 144.57, 140.42, 138.20, 135.54, 134.32, 131.27, 129.79, 128.84, 117.63, 66.91, 60.65, 52.65, 48.12, 42.52, 37.57, 32.63, 22.08, 14.28; HRMS (ESI) calcd for $C_{24}H_{25}NO_6SNa$: *m*/*z* ($[M+Na]^+$) 478.1295, found 478.1293; IR (KBr) 2986, 2943, 1736, 1702, 1679, 1640, 1350, 1267, 1243, 1168, 1109, 1085 cm^{-1}; $[\alpha]_D^{19}$ = -138.2(*c* 0.6, $CHCl_3$ for 91% ee); Daicel Chiralpak ID column, *n*-hexane/EtOH = 2/1, 1.0 mL/min, 225 nm, tR = 26.8 min. (major isomer) and 39.0 min min. (minor isomer).



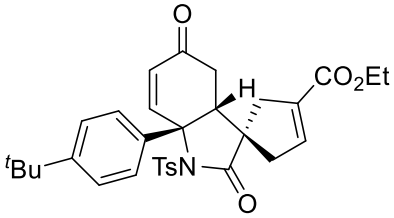
4e

4e: 78% yield; white solid; ^{1}H-NMR (400 MHz, $CDCl_3$) δ 7.78 (d, *J* = 8.2 Hz, 2H), 7.67 (d, *J* = 10.5 Hz, 1H), 7.37-7.43 (m, 5H), 7.30 (d, *J* = 8.2 Hz, 2H), 6.57-6.65 (m, 1H), 6.52 (d, *J* = 10.5 Hz, 1H), 4.11-4.17 (m, 2H), 3.00 (dd, *J* = 18.5, 2.3 Hz, 1H), 2.83-2.88 (m, 1H), 2.56 (s, 2H), 2.41-2.51 (m, 5H), 2.32 (dd, *J* = 18.5, 2.3 Hz, 1H), 1.25 (t, *J* = 7.1 Hz, 3H); ^{13}C-NMR (100 MHz, $CDCl_3$) δ 194.95, 176.90, 163.59, 145.75, 145.65, 140.59, 140.02, 135.23, 134.19, 131.15, 129.48, 129.24, 129.06, 128.84, 125.91, 68.93, 60.63, 53.16, 52.88, 42.85, 37.79, 33.43, 21.82, 14.27; HRMS (ESI) calcd for $C_{28}H_{27}NO_6SNa$: *m*/*z* ($[M+Na]^+$) 528.1451, found 528.1445; IR (KBr) 3063, 2980, 2938, 2378, 2346, 1738, 1711, 1683, 1360, 1265, 1244 cm^{-1}; $[\alpha]_D^{25}$ = -108.7 (*c* 1.0, $CHCl_3$ for 94% ee); Daicel Chiralpak ID column, *n*-hexane/EtOH = 2/1, 1.0 mL/min, 213 nm, tR = 55.0 min (major isomer) and 69.2 min (minor isomer).



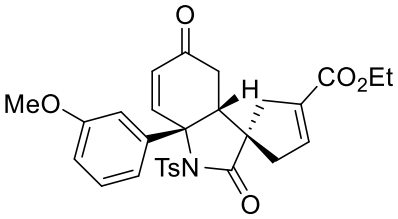
4f

4f: 75% yield; white solid; ^{1}H-NMR (400 MHz, $CDCl_3$) δ 7.76 (d, *J* = 8.2 Hz, 2H), 7.66 (d, *J* = 10.3 Hz, 1H), 7.30 (d, *J* = 8.2 Hz, 2H), 7.01 (s, 1H), 6.89 (s, 2H), 6.64 (t, *J* = 2.1 Hz, 1H), 6.51 (d, *J* = 10.3 Hz, 1H), 4.12-4.17 (m, 2H), 3.02 (dd, *J* = 18.6, 2.1 Hz, 1H), 2.81-2.83 (m, 1H), 2.54-2.63 (m, 2H), 2.46-2.51 (m, 1H), 2.43-2.45 (m, 4H), 2.37 (dd, *J* = 18.6, 2.1 Hz, 1H), 2.30 (s, 6H), 1.26 (t, *J* = 6.9 Hz, 3H); ^{13}C-NMR (150 MHz, $CDCl_3$) δ 195.13, 176.92, 163.47, 145.97, 145.52, 140.07, 138.49, 135.33, 135.18, 134.12, 130.93, 130.44, 129.31, 129.18, 123.68, 68.82, 60.65, 53.08, 52.57, 42.44, 37.81, 33.22, 21.72, 21.46, 14.20; HRMS (ESI) calcd for $C_{32}H_{35}NO_6SNa$: *m*/*z* ([M+Na]$^+$) 584.2077, found 584.2075; IR (KBr) 2986, 2931, 2367, 2312, 1744, 1717, 1708, 1688, 1638, 1599, 1507, 1362, 1245 cm^{-1}; $[\alpha]_D^{21}$ = -69.4 (*c* 1.0, $CHCl_3$ for 92% ee); Daicel Chiralpak ID column, *n*-hexane/EtOH = 2/1, 1.0 mL/min, 254 nm, tR = 16.5 min (major isomer) and 20.4 min (minor isomer).



4g

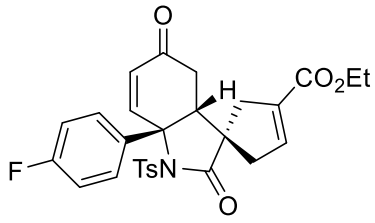
4g: 70% yield; white solid; ^{1}H-NMR (400 MHz, $CDCl_3$) δ 7.74 (d, *J* = 8.7 Hz, 2H), 7.68 (d, *J* = 10.5 Hz, 1H), 7.40 (d, *J* = 8.7 Hz, 2H), 7.27-7.31 (m, 4H), 6.62 (t, *J* = 2.1 Hz, 1H), 6.50 (d, *J* = 10.5 Hz, 1H), 4.11-4.17 (m, 2H), 3.01 (dd, *J* = 18.8, 2.1 Hz, 1H), 2.84-2.88 (m, 1H), 2.47-2.56 (m, 3H), 2.44 (s, 3H), 2.30-2.43 (m, 2H), 1.34 (s, 9H), 1.25 (t, *J* = 7.1 Hz, 3H); ^{13}C-NMR (150 MHz, $CDCl_3$) δ 195.20, 176.83, 163.68, 151.79, 145.93, 145.51, 140.10, 137.28, 135.40, 134.04, 130.95, 129.43, 129.17, 125.94, 125.67, 68.77, 60.64, 53.15, 52.72, 42.74, 37.77, 34.72, 33.48, 31.36, 21.82, 14.29; HRMS (ESI) calcd for $C_{28}H_{27}NO_6SNa$: *m*/*z* ([M+Na]$^+$) 528.1451, found 528.1445; IR (KBr) 2970, 2378, 2312, 1742, 1712, 1687, 1506, 1362, 1244, 1166 cm^{-1}; $[\alpha]_D^{25}$ = -69.5 (*c* 1.0, $CHCl_3$ for 98% ee); Daicel Chiralpak ID column, *n*-hexane/EtOH = 2/1, 1.0 mL/min, 254 nm, tR = 18.5 min (minor isomer) and 20.5 min (major isomer).



4h

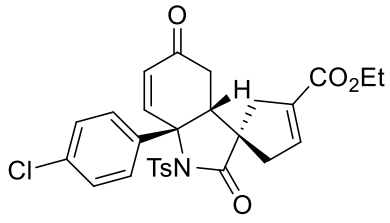
4h: 54% yield; white solid; ^{1}H-NMR (400 MHz, $CDCl_3$) δ 7.80 (d, *J* = 8.7 Hz, 2H), 7.64 (d, *J* = 10.5 Hz, 1H), 7.35 (d, *J* = 7.8 Hz, 1H), 7.31 (d, *J* = 8.7 Hz, 2H), 6.89-6.97 (m, 3H), 6.61 (t, *J* = 2.1 Hz, 1H), 6.51 (d, *J* = 10.5 Hz, 1H), 4.10-4.16 (m, 2H), 3.82 (s, 3H), 3.00 (dd, *J* = 18.5, 2.2 Hz, 1H), 2.83-2.88 (m, 1H), 2.52-2.55 (m, 2H), 2.41-2.50 (m, 5H), 2.29-2.33 (m, 1H), 1.25 (t, 3H); ^{13}C-NMR (150 MHz,

$CDCl_3$) δ 195.02, 177.03, 163.72, 159.84, 145.75, 145.51, 142.23, 140.06, 135.19, 134.15, 131.12, 130.18, 129.51, 129.23, 118.51, 114.02, 111.78, 68.90, 60.65, 55.45, 53.13, 52.69, 42.83, 37.75, 33.48, 21.76, 14.29; HRMS (ESI) calcd for $C_{29}H_{29}NO_7SNa$: *m/z* ($[M+Na]^+$) 558.1557, found 558.1552; IR (KBr) 2932, 2374, 2347, 2307, 1743, 1706, 1688, 1544, 1509, 1364, 1264 cm^{-1}; $[\alpha]_D^{20}$ = +76.2 (*c* 1.0, $CHCl_3$ for 92% ee); Daicel Chiralpak IC column, *n*-hexane/EtOH = 2/1, 1.0 mL/min, 212 nm, tR = 22.5 min (minor isomer) and 26.4 min (major isomer).



4i

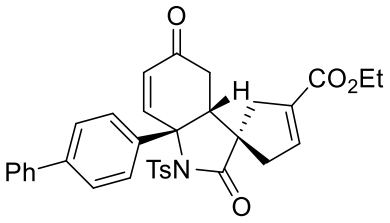
4i: 81% yield; white solid; ^{1}H-NMR (400 MHz, $CDCl_3$) δ 7.78 (d, *J* = 8.2 Hz, 2H), 7.65 (d, *J* = 10.5 Hz, 1H), 7.37-7.40 (m, 2H), 7.32 (d, *J* = 8.2 Hz, 2H), 7.10-7.14 (m, 2H), 6.62 (t, *J* = 2.3 Hz, 1H), 6.52 (d, *J* = 10.5 Hz, 1H), 4.11-4.17 (m, 2H), 3.01 (dd, *J* = 18.8, 2.3 Hz, 1H), 2.79-2.84 (m, 1H), 2.53-2.56 (m, 2H), 2.44-2.46 (m, 5H), 2.34 (dd, *J* = 18.8, 2.3 Hz, 1H), 1.25 (t, *J* = 7.1 Hz, 3H); ^{13}C-NMR (175 MHz, $CDCl_3$) δ 194.91, 177.15, 163.94, 162.98 (J_{C-F} = 284 Hz), 146.20, 145.50, 140.24, 136.68 (d, J_{C-F} = 2.6 Hz) , 135.28, 134.41, 131.57, 129.83, 129.43, 128.08 (d, J_{C-F} = 9.2 Hz), 116.35 (d, J_{C-F} = 20.8 Hz), 68.62, 60.95, 53.29, 53.16, 43.03, 38.03, 33.50, 22.12, 14.55; ^{19}F-NMR (565 MHz, $CDCl_3$) δ -113.62; HRMS (ESI) calcd for $C_{28}H_{26}FNO_6SNa$: *m/z* ($[M+Na]^+$) 546.1357, found 546.1352; IR (KBr) 3363, 2925, 2345, 1712, 1686, 1509, 1361, 1247, 1168, 1086, 866, 760, 665, 577, 560, 546 cm^{-1}; $[\alpha]_D^{22}$ = -117.83 (*c* 0.6, $CHCl_3$ for 87% ee); Daicel Chiralpak IC column, *n*-hexane/EtOH = 2/1, 1.0 mL/min, 254 nm, tR = 15.1 min. (minor isomer) and 22.3 min (major isomer).



4j

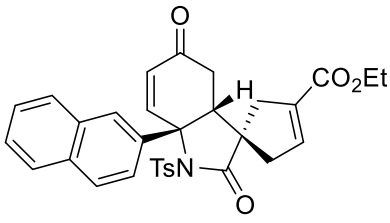
4j: 85% yield; white solid; ^{1}H-NMR (400 MHz, $CDCl_3$) δ 7.79 (d, *J* = 8.4 Hz, 2H), 7.63 (d, *J* = 10.5 Hz, 1H), 7.41 (d, *J* = 8.4 Hz, 2H), 7.32-7.36 (m, 4H), 6.62 (t, *J* = 2.3 Hz, 1H), 6.53 (d, *J* = 10.5 Hz, 1H), 4.11-4.16 (m, 2H), 3.01 (dd, *J* = 18.8, 2.3 Hz, 1H), 2.77-2.81 (m, 1H), 2.52-2.55 (m, 2H), 2.41-2.48 (m, 5H), 2.34 (dd, *J* = 18.8, 2.3 Hz, 1H), 1.25 (t, *J* = 7.1 Hz, 3H); ^{13}C-NMR (175 MHz, $CDCl_3$) δ 194.48, 176.62, 163.45, 145.92, 144.86, 139.88, 139.17, 134.87, 134.85, 131.38, 129.53, 129.22, 129.12, 127.23, 68.29, 60.62, 52.97, 52.72, 42.75, 37.70, 33.15, 21.79, 14.22 (one carbon overlapped); HRMS (ESI) calcd for $C_{28}H_{26}ClNO_6SNa$: *m/z* ($[M+Na]^+$) 562.1062, found 562.1052; IR (KBr) 2961, 2926, 2854, 1739, 1712, 1692, 1493, 1363, 1246, 1167, 1083, 664, 504, 473 cm^{-1}; $[\alpha]_D^{22}$ = -125.8 (*c* 0.45, $CHCl_3$ for 87% ee); Daicel Chiralpak IC column, *n*-

hexane/EtOH = 2/1, 1.0 mL/min, 230 nm, tR = 15.0 min (minor isomer) and 23.7 min (major isomer).



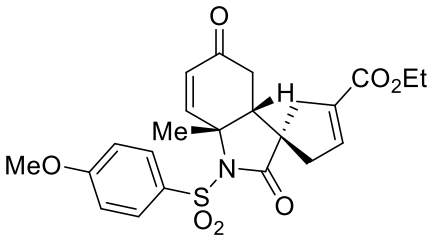
4k

4k: 58% yield; white solid; ^{1}H-NMR (400 MHz, $CDCl_3$) δ 7.81 (d, *J* = 8.2 Hz, 2H), 7.71 (d, *J* = 10.5 Hz, 1H), 7.59-7.67 (m, 4H), 7.38-7.52 (m, 5H), 7.31 (d, *J* = 8.2 Hz, 2H), 6.63 (t, *J* = 2.3 Hz, 1H), 6.55 (d, *J* = 10.5 Hz, 1H), 4.10-4.18 (m, 2H), 3.04 (dd, *J* = 18.8, 2.3 Hz, 1H), 2.87-2.92 (m, 1H), 2.44-2.61 (m, 7H), 2.36 (dd, *J* = 18.8, 2.3 Hz, 1H) 1.25 (t, *J* = 7.1 Hz, 3H); ^{13}C-NMR (150 MHz, $CDCl_3$) δ 194.94, 176.90, 163.60, 145.82, 145.56, 141.74, 140.05, 140.02, 139.50, 135.18, 134.20, 131.24, 129.54, 129.27, 129.03, 127.93, 127.72, 127.22, 126.36, 68.81, 60.67, 53.16, 52.85, 42.87, 37.81, 33.46, 21.86, 14.31; HRMS (ESI) calcd for $C_{34}H_{31}NO_6SNa$: *m*/*z* ([M+Na]$^{+}$) 604.1764, found 604.1760; IR (KBr) 2921, 2367, 2306, 1746, 1720, 1711, 1687, 1510, 1487, 1362, 1246, 1166 cm^{-1}; $[\alpha]_D^{21}$ = -34.0 (*c* 1.0, $CHCl_3$ for 93% ee) ; Daicel Chiralpak ID column, *n*-hexane/EtOH = 2/1, 1.0 mL/min, 200 nm tR = 43.5 min (major isomer) and 50.7 min (minor isomer).



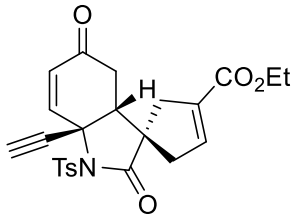
4l

4l: 60% yield; white solid; ^{1}H-NMR (400 MHz, $CDCl_3$) δ 7.88-7.92 (m, 2H), 7.75-7.82 (m, 5H), 7.54-7.60 (m, 2H), 7.46 (d, *J* = 8.7 Hz, 1H), 7.29 (d, *J* = 7.8 Hz, 2H), 6.59-6.63 (m, 2H), 4.02-4.13 (m, 2H), 3.01-3.09 (m, 1H), 2.85-2.89 (m, 1H), 2.49-2.65 (m, 2H), 2.32-2.45 (m, 5H), 2.25-2.31 (m, 1H), 1.26 (t, *J* = 7.1 Hz, 3H) (two carbons overlapped); ^{13}C-NMR (100 MHz, $CDCl_3$) δ 195.00, 177.31, 163.67, 145.79, 145.58, 140.06, 137.62, 135.21, 134.20, 133.13, 132.84, 131.38, 129.48, 129.32, 128.42, 127.78, 127.11, 125.55, 123.01, 69.14, 60.65, 53.19, 52.47, 42.90, 37.90, 33.34, 21.83, 14.28; HRMS (ESI) calcd for $C_{32}H_{29}NO_6SNa$: *m*/*z* ([M+Na]$^{+}$) 555.17, found 555.65; IR (KBr) 2926, 2374, 2310, 1745, 1712, 1688, 1364, 1244, 1167, 811, 668 cm^{1}; $[\alpha]_D^{25}$ = -74.5 (*c* 1.0, $CHCl_3$ for 96% ee); Daicel Chiralpak IE column, *n*-hexane/EtOH = 2/1, 1.0 mL/min, 230 nm, tR = 53.7 min (minor isomer) and 75.7 min (major isomer).



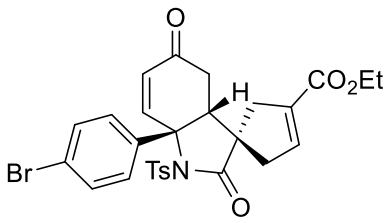
4m

4m: 54% yield; white solid; ^{1}H-NMR (400 MHz, $CDCl_3$) δ 8.01 (d, *J* = 9.2 Hz, 2H), 7.49 (dd, *J* = 10.8, 1.4 Hz, 1H), 7.00 (d, *J* = 9.2 Hz, 2H), 6.63 (t, *J* = 2.1 Hz, 1H), 6.14 (d, J = 10.8 Hz, 1H), 4.09-4.15 (m, 2H), 3.89 (s, 3H), 2.93-3.01 (m, *J* = 17.9 Hz, 1H), 2.77 (dd, *J* = 18.5, 7.6 Hz, 1H), 2.52-2.60 (m, 2H), 2.38-2.49 (m, 3H), 1.95 (s, 3H), 1.24 (t, J = 7.1 Hz, 3H); ^{13}C-NMR (100 MHz, $CDCl_3$) δ 194.28, 176.36, 164.13, 163.48, 148.35, 140.31, 134.30, 131.12, 128.70, 114.24, 63.66, 60.61, 55.85, 52.58, 49.09, 42.34, 37.64, 33.44, 27.15, 14.34 (one carbon overlapped); HRMS (ESI) calcd for $C_{23}H_{25}NO_7SNa$: *m*/*z* ([M+Na]$^+$) 482.1244, found 482.1239; IR (KBr) 2980, 2373, 2312, 1744, 1710, 1685, 1594, 1497, 1362, 1262, 1163, 1088, 1018, 675 cm^{-1}; $[\alpha]_D^{19}$ = -83.1 (*c* 1.0, $CHCl_3$ for 92% ee); Daicel Chiralpak ID column, *n*-hexane/EtOH = 2/1, 1.0 mL/min, 240 nm, tR = 40.9 min, (major isomer) and 76.3 min (minor isomer).



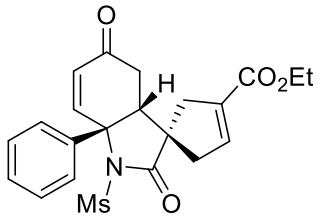
4n

4n: 45% yield; white solid; ^{1}H-NMR (400 MHz, $CDCl_3$) δ 8.03 (d, *J* = 8.2 Hz, 2H), 7.45-7.48 (m, 1H), 7.34 (d, *J* = 8.2 Hz, 2H), 6.59 (t, *J* = 2.1 Hz, 1H), 6.23 (d, *J* = 10.5 Hz, 1H), 4.15 (q, *J* = 7.0 Hz, 2H), 3.00-3.04 (m, 1H), 2.82-2.94 (m, 3H), 2.52-2.69 (m, 3H), 2.42-2.48 (m, 4H), 1.25 (t, *J* = 7.0 Hz, 3H); ^{13}C-NMR (150 MHz, $CDCl_3$) δ 193.77, 175.57, 163.52, 145.85, 143.94, 139.50, 135.03, 134.31, 129.65, 129.24, 129.04, 81.00, 76.42, 60.71, 57.32, 53.33, 49.82, 42.98, 37.04, 34.66, 21.86, 14.28; HRMS (ESI) calcd for $C_{24}H_{23}NO_6SNa$: *m*/*z* ([M+Na]$^+$) 476.1138, found 476.1135; IR (KBr) 2373, 2312, 1747, 1708, 1690, 1544, 1508, 1362, 1249, 1173 cm^{-1}; $[\alpha]_D^{20}$ = -15.4 (*c* 1.0, $CHCl_3$ for 92% ee); Daicel Chiralpak IE column, *n*-hexane/EtOH = 2/1, 1.0 mL/min, 212 nm, tR = 35.8 min. (minor isomer) and 57.8 min(major isomer).



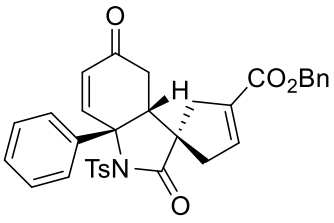
4o

4o: 76% yield; white yellowish solid; ^{1}H-NMR (400 MHz, $CDCl_3$) δ 7.80 (d, *J* = 8.2 Hz, 2H), 7.62 (dd, *J* = 10.5, 1.4 Hz, 1H), 7.56 (d, *J* = 8.7 Hz, 2H), 7.33 (d, *J* = 8.2 Hz, 2H), 7.28 (d, *J* = 8.7 Hz, 2H), 6.61 (t, *J* = 2.3 Hz, 1H), 6.53 (d, *J* = 10.5 Hz, 1H), 4.11-4.16 (m, 2H), 3.01 (dd, *J* = 18.5, 2.3 Hz, 1H), 2.77-2.79 (m, 1H), 2.52-2.55 (m, 2H), 2.43-2.45 (m, 5H), 2.34 (dd, *J* = 18.5, 2.3 Hz, 1H), 1.25 (t, *J* = 7.1 Hz, 3H); ^{13}C-NMR (150 MHz, $CDCl_3$) δ 194.51, 176.69, 163.59, 146.00, 144.87, 139.92, 139.86, 135.01, 134.15, 132.26, 131.48, 129.61, 129.21, 127.60, 123.08, 68.42, 60.60, 53.08, 52.83, 42.86, 37.87, 33.24, 21.84, 14.28; HRMS (ESI) calcd for $C_{28}H_{26}BrNO_6SNa$: *m*/*z* ([M+Na]$^+$) 606.0556, found 606.0553; IR (KBr) 2367, 2312, 1745, 1715, 1705, 1687, 1543, 1510, 1491, 1363, 1245 cm^{-1}; $[\alpha]_D^{20}$ = -105.5 (*c* 1.0, $CHCl_3$ for 86% ee); Daicel Chiralpak IC column, *n*-hexane/EtOH = 2/1, 1.0 mL/min, 245 nm, tR = 13.9 min (minor isomer) and 21.9 min (major isomer).



4p

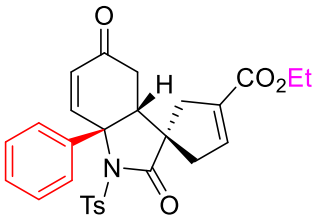
4p: 89% yield; white solid; ^{1}H-NMR (400 MHz, $CDCl_3$) δ 7.39-7.47 (m, 6H), 6.69-6.72 (m, 1H), 6.51 (d, *J* = 10.5 Hz, 1H), 4.18 (q, *J* = 7.2 Hz, 2H), 3.33 (s, 3H), 3.13-3.19 (m, 1H), 2.89-2.91 (m, 1H), 2.67-2.77 (m, 2H), 2.45-2.53 (m, 3H), 1.28 (t, *J* = 7.2 Hz, 3H); ^{13}C-NMR (150 MHz, $CDCl_3$) δ 194.66, 178.21, 163.60, 144.79, 140.45, 140.16, 134.17, 131.50, 129.31, 128.96, 125.22, 68.75, 60.79, 53.44, 52.88, 42.95, 42.83, 38.22, 33.06, 14.32; HRMS (ESI) calcd for $C_{22}H_{23}NO_6SNa$: *m*/*z* ([M+Na]$^+$) 452.1138, found 452.1135; IR (KBr) 2931, 2367, 2345, 2318, 1744, 1716, 1706, 1688, 1680, 1648, 1543, 1509, 1423, 1360, 1248, 1165 cm^{-1}; $[\alpha]_D^{20}$ = -87.0 (*c* 1.0, $CHCl_3$ for 88% ee); Daicel Chiralpak IB column, *n*-hexane/EtOH = 2/1, 1.0 mL/min, 254 nm, tR = 15.7 min (major isomer) and 19.3 min (minor isomer).



4q

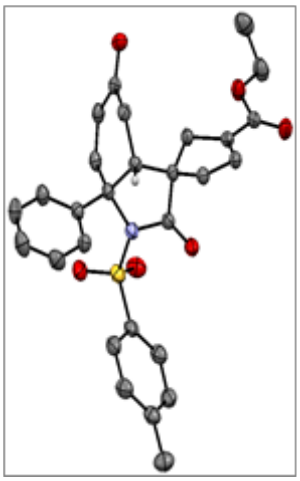
4q: 73% yield; orange solid; ^{1}H-NMR (400 MHz, $CDCl_3$) δ 7.78 (d, *J* = 7.8 Hz, 2H), 7.65 (d, *J* = 10.5 Hz, 1H), 7.29-7.41 (m, 12H), 6.66 (s, 1H), 6.51 (d, J = 10.5 Hz, 1H), 5.12 (m, 2H), 2.97-3.05 (m, 1H), 2.82-2.88 (m, 1H), 2.55-2.60 (m, 2H), 2.40-2.51 (m, 5H), 2.27-2.38 (m, 1H); ^{13}C-NMR (100 MHz, $CDCl_3$) δ 194.91, 176.83, 163.36, 145.78, 145.61, 140.74, 140.60, 135.83, 135.18, 134.87, 133.80, 131.15, 129.51, 129.22, 129.08, 128.85, 128.62, 128.29, 125.90, 68.94, 66.42, 53.12, 52.92, 42.98, 37.77, 33.47, 21.84; HRMS (ESI) calcd for $C_{33}H_{29}NO_6SNa$: *m*/*z* ($[M+Na]^+$) 590.1608, found 590.1603; IR (KBr) 2964, 2921, 2373, 2312, 1744, 1598, 1489, 1460, 1389, 1363, 1246, 1164, 1081 cm^{-1}; $[\alpha]_D^{20}$ = -60.9 (*c* 1.0, $CHCl_3$ for 90% ee); Daicel Chiralpak IC column, *n*-hexane/EtOH = 2/1, 1.0 mL/min, 217 nm, 23.7 min, (minor isomer) and 31.2 min (major isomer

2.13 X-ray Crystal Data of 4e



4e

≡



Empirical Formula	$C_{28}H_{27}NO_6S$
Formula Weight	505.58
Crystal Color	colorless, block
Crystal Dimensions	0.091 X 0.079 X 0.061 mm
Crystal System	orthorhombic
Lattice	Primitive
Primitive	a = 9.34005(17) Å
	b = 9.81274(18) Å
	c = 26.8301(19) Å
	V = 2459.01(18) Å3
Space Group	$P2_12_12_1$ (#19)
Z value	4
D_{calc}	1.366 g/cm3
F_{000}	1064.00
μ(CuKα)	2.456 cm-1
Residuals R1 (I>2.00s(I))	0.0352
Residuals R (All reflections)	0.0393
Residuals wR2 (All reflections)	0.0824
Goodness of Fit Indicator	1.041
Flack parameter (Parsons' quotients = 1625)	0.006(5)

2.14 References

1. a) G. Luo, *Netw. Model. Anal. Health Inform. Bioinform*. **2016**, *5*, 18. b) M. Feurer, F. Hutter, *Springer*, **2019**, 3. c) B. J. Reizman, K. F. Jensen, *Acc. Chem. Res*. **2016**, *49*, 1786. d) V. Sans, L. Cronin, *Chem. Soc. Rev*. **2016**, *45*, 2032. e) D. E. Fitzpatrick, T. Maujean, A. C. Evans, S. V. Ley, *Angew. Chem. Int. Ed*. **2018**, *57*, 15128. f) A.-C. Bédard, A. Adamo, K. C. Aroh, M. G. Russell, A. A. Bedermann, J. Torosian, B. Yue, K. F. Jensen, T. F. Jamison, *Science* **2018**, *361*, 1220. g) M. Trobe, M. D. Burke, *Angew. Chem. Int. Ed*. **2018**, *57*, 4192.
2. a) Z. Zhou, X. Li, R. N. Zare, *ACS Cent. Sci*. **2017**, *3*, 1337. b) H. Gao, T. J. Struble, C. W. Coley, Y. Wang, W. H. Green, K. F. Jensen, *ACS Cent. Sci*. **2018**, *4*, 1465. c) L. Häse, L. M. Roch, C. Kreisbeck, A. Aspuru-Guzik, *ACS Cent. Sci*. **2018**, *4*, 1134. d) A. M. Schweidtmann, A. D. Clayton, N. Holmes, E. Bradford, R. A. Bourne, A. Lapkin, *Chem. Eng. J*. **2018**, *352*, 277. e) P. Vámosi, K. Matsuo, T. Masuda, K. Sato, T. Narumi, K. Takeda, N. Mase, *Chem. Rec*. **2019**, *19*, 77.
3. T, Koriyama. *Acoust. Sci. & Tech*. **2020**, *41*, 2.
4. a) C. E. Rasmussen, C. K. Williams, *Gaussian processes for machine learning*, MIT Press, Cambridge, MA, USA, **2006**, 1. b) J. P. Aborzpour, D. P. Tew and S. Habershon, *J. Chem. Phys*. **2016**, *145*, 174112. c) O.-P. Koistinen, F. B. Dagbjartsdóttir, V. Ásgeirsson, A. Vehtari, H. Jónsson, *J. Chem. Phys*. **2017**, *147*, 152720.
5. https://www.bigdata-navi.com/aidrops/2925/
6. L. Wang, A. L. Luis, K. Agapiou, H. Jang, M. J. Krische, *J. Am. Chem. Soc*. **2002**, *124*, 2402.
7. M. M. Rauhut, H. Currier, U.S. Patent, **1963**, 3074999.
8. C. E. Aroyan, S. J. Miller, *J. Am. Chem. Soc*. **2007**, *129*, 256.
9. F. Seidel, J. A. Gladysz, *Synlett* **2007**, 986.
10. E. Marqus-Lpez, R. P. Herrera, T. Marks, W. C. Jacobs, D. Kçnning, R. M. de Figueiredo, M. Christmann, *Org. Lett*. **2009**, *11*, 4116.
11. J.-J. Gong, T.-Z. Li, K. Pana, X.-Y. Wu, *Chem. Commun*. **2011**, *47*, 1491.
12. S. Takizawa, T. M. Nguyen, A. Grossmann, D. Enders, H. Sasai, *Angew. Chem. Int. Ed.* **2012**, *124*, 5519.
13. a) E. Rodriguez, G. H. N. Towers, J. C. Mitchell, *Phytochemistry* **1976**, *15*, 1573. b) K. Picman, *Biochem. Syst. Ecol.* **1986**, *14*, 255. c) A. Ghantous, H. Gali-Muhtasib, H. Vuorela, N. A. Saliba, N. Darwiche, *Drug Discovery Today* **2010**, *15*, 668.
14. K. Kishi, F. A. Arteaga, S. Takizawa, H. Sasai, *Chem. Comm.* **2017**, *53*, 7724.

15. a) S. Omura, K. Matsuzaki, T. Fujimoto, K. Kosuge, T. Furuya, S. Fujita, A. Nakagawa, *J. Antibiot*. **1991**, *44*, 117. b) T. Janecki, E. Błaszczyk, K. Studzian, A. Janecka, U. Krajewska, M. Rózalski, *J. Med. Chem*. **2005**, *48*, 3516.
16. a) *Domino reactions: Concepts for efficient organic synthesis*, ed. L. F. Tietze, Wiley-VCH, Weinheim, **2014**. b) P. Chauhan, S. Mahajan, D. Enders, *Acc. Chem. Res*. **2017**, *50*, 2809. c) H. Jin, Q. Zhang, E. Li, P. Jia, N. Li, Y. Huang, *Org. Biomol. Chem*. **2017**, *15*, 7097. d) X.-Y. Chen, S. Li, F. Vetica, M. Kumar, D. Enders, *Science* **2018**, 2, 1.
17. a) C. V. Calliford, K. A. Scheidt, *Angew. Chem. Int. Ed*. **2007**, *46*, 8748. b) R. Narayan, M. Potowski, Z.-J. Jia, A. P. Antonchick, H. Waldmann, *Acc. Chem. Res*. **2014**, *47*, 1296.
18. a) G.-J. Mei, F. Shi, *Chem. Commun*. **2018**, *54*, 6607. b) S. Takizawa, K. Kishi, M. Kusaba, B. Jianfei, T. Suzuki, H. Sasai, *Heterocycles* **2017**, *95*, 761. c) W. He, J. Hu, P. Wang, L. Chen, K. Ji, S. Yang, Y. Li, Z. Xie, W. Xie, *Angew. Chem. Int. Ed*. **2018**, *57*, 3806.
19. a) C. Zhang, X. Lu, *J. Org. Chem*. **1995**, *60*, 2906. b) G. Zhu, Z. Chen, Q. Jiang, D. Xiao, P.Cao, X. Zhang, *J. Am. Chem. Soc*. **1997**, *119*, 3836.
20. H. Jin, Q. Zhang, E. Li, P. Jia, N. Lia, Y. Huang, *Org. Biomol. Chem*. **2017**, *15*, 7097.
21. M. Kondo, H. D. P. Wathsala, M. Sako, Y. Hanatani, K. Ishikawa, S. Hara, T.Takaai, Takashi Washio, S. Takizawa, H. Sasai, *Chem. Commun.* **2020**, *56*, 1259.

Chapter 3

Chapter 3

Bayesian optimization-assisted multi-parameter (numerical and categorical) screening for an organo-catalytic flow synthesis of highly functionalized biaryls

3.1. Bayesian optimization

ML-assisted optimization can always have diminished the trial and error experiments that always a huge issue when it considered conventional reaction optimization. This computer assisted optimization is currently started using in flow system,[1] electrochemical synthesis,[2] photochemical synthesis[3] and microwave reaction.[4] Among them, the flow reaction optimization system has held a huge part in automation and computational optimization, due to its unique features (high reproducibility, efficient thermal transfer, easy manipulation of unstable intermediates). In **Chapter 2**, I described GPR can efficiently predict the appropriate reaction parameters for the enantioselective sequential reaction in flow system. But that system is limited to two parameters due to its difficulty of the visualization of more than three parameters. Therefore, a much higher ML system for reaction optimization is highly demanded. Bayesian optimization (BO) is a well-established ML process where it can work as a black box optimizer even in high-dimension systems.[5] BO is a powerful probabilistic method to determine the maximum (or the minimum) of a black-box objective function based on the Bayesian approach using a dataset collected in the previous sampling and ML-modeling iteration.[6] BO does not only search around a probable maximum (exploitation) but also escape from a local maximum (or the minimum) by searching a value of the unexplored black-box objective function (exploration).[7] Furthermore, BO estimates the next parameters to search based on the Gaussian process modeling of a collected experimental dataset and the maximization of the acquisition function. Then the estimated parameters are evaluated by performing a practical experiment, subsequently, the newly obtained dataset is reapplied to the above-mentioned ML process again. Finally, the appropriate reaction parameters affording a good result are predicted through the iteration of the ML estimation and experimental evaluation.

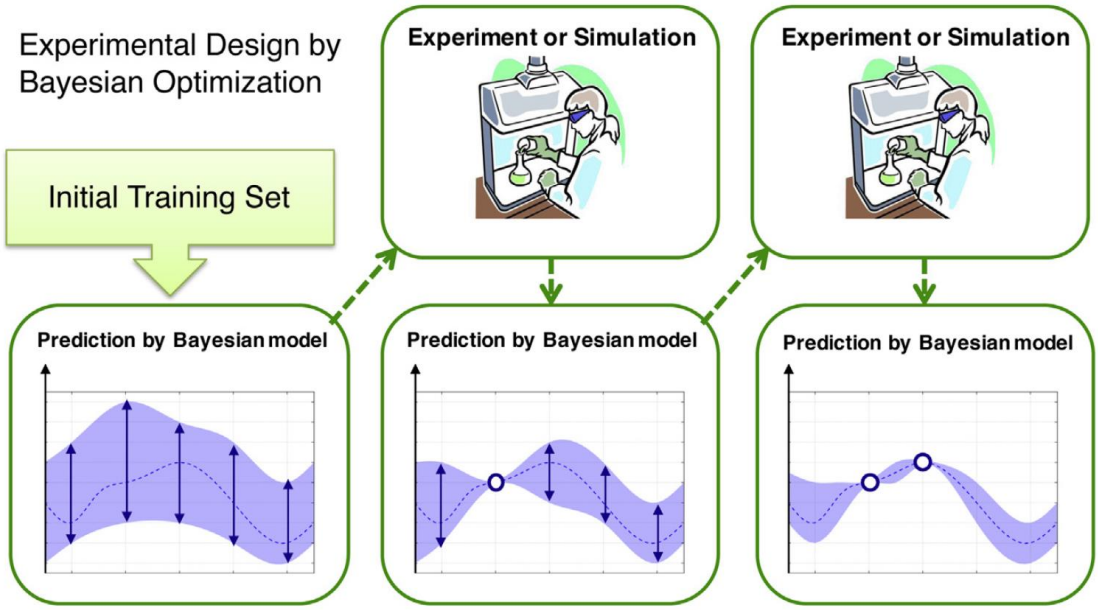
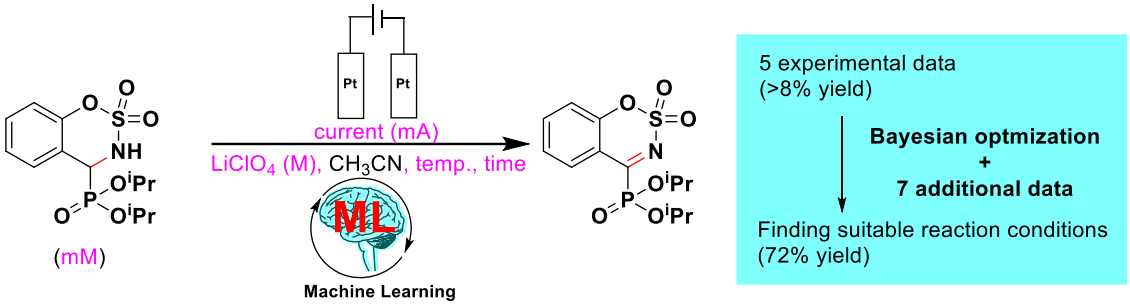


Figure 1.1. Representative figure of BO [8]

As shown in **Figure 1.1**, the BO process consists of several steps. First, several experiments were carried out to get an initial training set. Then, the calculation was performed of mean and probability (variance) by Gaussian process regression. The next parameters to perform are predicted and perform the experiments based on that ML estimation. Finally, perform the next parameter which is predicted by BO until getting the optimized results.

3.2. This work

Recently our group has investigated multi-parameter screening of electrochemical oxidation by using the Bayesian optimization process. In that work, the five parameters were simultaneously changed to get maximum yield. The optimum reaction conditions was predicted by BO within seven experimental trials (**scheme 1.1**).[2]



Scheme 1.1. Our group`s previous work

Despite our previous work, it is still difficult to optimize the parameters which have no numerical values called categorical parameters. Very recently, Doyle's group[9] also demonstrated a simultaneous multi-parameter screening based on BO. In their work, the four numerical and three categorical parameters (ligand, solvent, and base) screening by the BO platform successfully identified suitable experimental conditions Mitsunobu[10] and deoxyfluorination[11] reaction in a batch system. To use the non-numerical parameters like solvent and ligand, the steric effect and electronic properties were examined. After that, they converted these factors to numerical values by chemical descriptors, which require the construction of an appropriate model.[12] However, quantification of categorical parameters is a difficult task for chemists due to their numbering inability. Moreover, reactor type and shape (e.g. type of electrode, micro-mixer, etc) cannot be converted into numerical parameters in the absence of expertise in physics and machine engineering, while they are crucial categorical parameters to achieve good outcomes. Therefore, to demonstrate a more practical BO-assisted identification of optimal reaction conditions, my attention has focused on the direct optimization of these categorical parameters. My strategy does not involve time-consuming calculation or comprehensive knowledge of sciences. I developed the BO algorithm adopting the categorical parameter as a non-continuous numerical parameter.

To utilize a BO-assisted optimization system in multi-parameter screening, the organocatlyzed domino reaction was developed to synthesize atropoisomeric functionalized biaryls which are found in numerous natural products, and pharmaceuticals, functional materials, and chiral ligand.[13] These biaryl compounds have

been mainly synthesized by transition metal-catalyzed reactions such as cross-coupling and oxidative couplings such as Negishi, Stille, Kumada, and Suzuki reactions, of aryl compounds in regio- and stereoselective manner.[14]

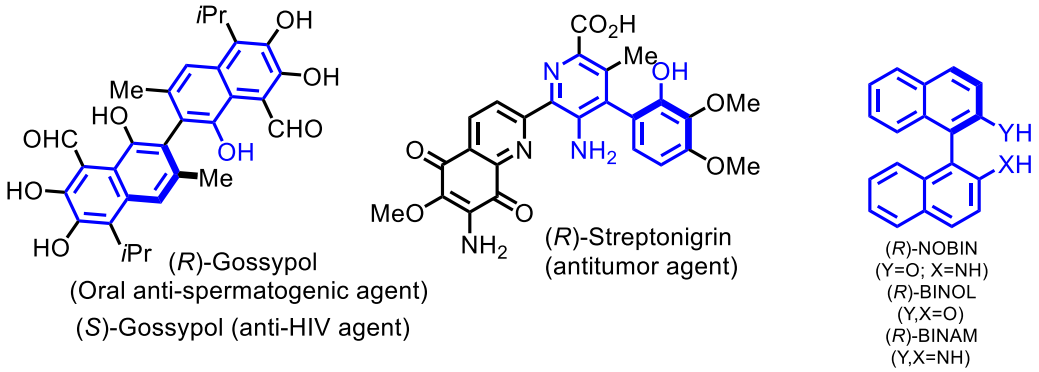
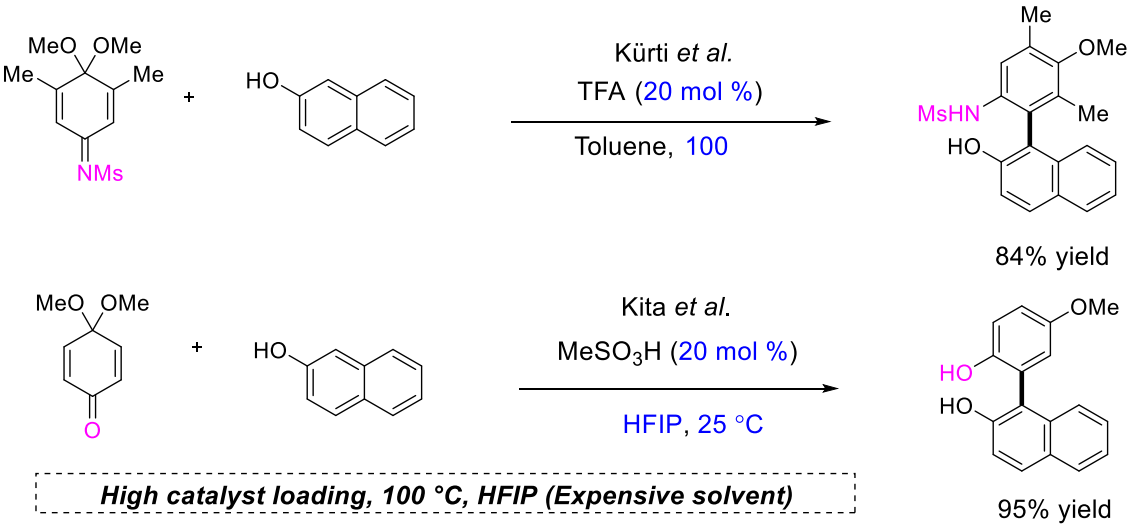


Figure 1.2. Important motifs having functionalized biaryls

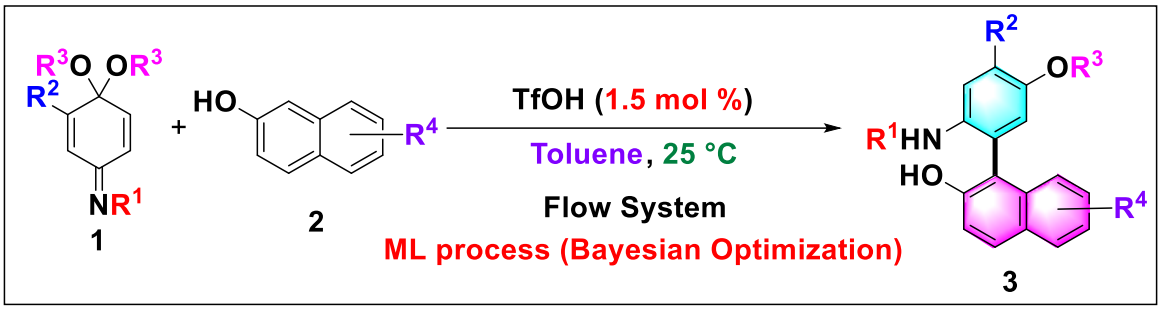
To date, organocatalyzed efficient synthesis of arenol-derived biaryls has been developed for the metal-free and operationally simple process. In 2016, Kürti's[15] and Kita's[16] groups independently reported readily available organic Brønsted acid-catalyzed cross-coupling reaction for functionalized biaryl derivatives.



Scheme 1.2. Previous examples of dienone and arenol coupling

Although these reactions showed wide substrate scope with a high yield of target biaryls, Kürti and Kita have carried out the reaction at higher temperature, high catalyst loading or expensive solvent like hexafluoro isopropanol in those reaction systems. Therefore, I tried to develop the Brønsted acid-catalyzed reaction for a facile synthesis of functionalized biarlys using low catalyst loading under mild reaction conditions.

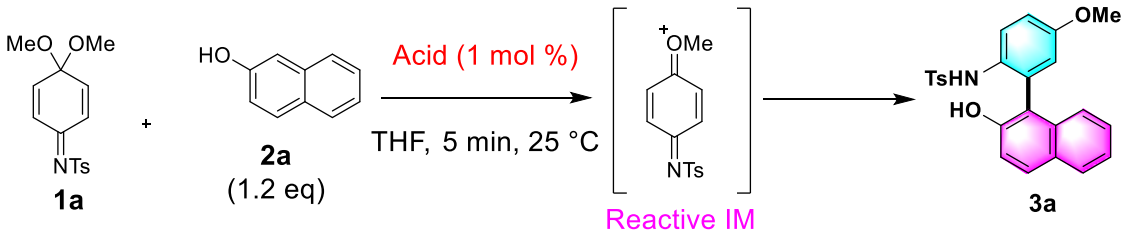
Therefore, BO-assisted optimization was applied to predict the reaction parameters from multi-parameter screening including categorical parameters.



Scheme 1.3. This work

3.3. Initial reaction screening in a batch system

To develop an efficient process in flow system, the effect of Brønsted acids for the biaryl formation was briefly investigated as shown in **Table 1.1**. When TfOH (1 mol %) was tested, the desired product **3a** was obtained in 24% yield within 5 min. These results tend me to think this reaction rate is so fast. However, monohydrate TsOH was provided trace while trifluoroacetic acid (TFA), benzoic acid and, acetic acid led to no desired biaryl due to comparatively less acidity in terms of their pKa values.

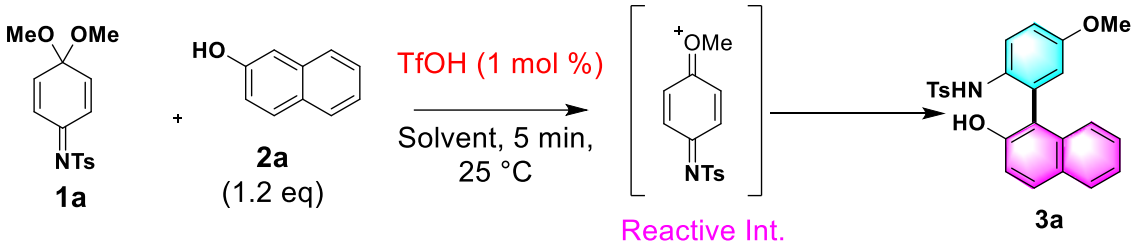


Entry	Acid	Yield (%)
1	TfOH	24
2	$TsOH.H_2O$	trace
3	TFA	0
4	Benzoic acid	0
5	Acetic acid	0

Table 1.1. Effect of acid. Reaction conditions: **1a** (0.065 mmol), **2a** (0.078 mmol), THF (0.65 mL), Acid: 6.5 µmol; Yield was determined as an NMR yield using tri-methoxy benzene as an internal standard.

3.4. Initial reaction screening in batch system

Next, various solvents were screened in a batch system. Although, a nonpolar solvent such as toluene could increase the yield up to 42%.

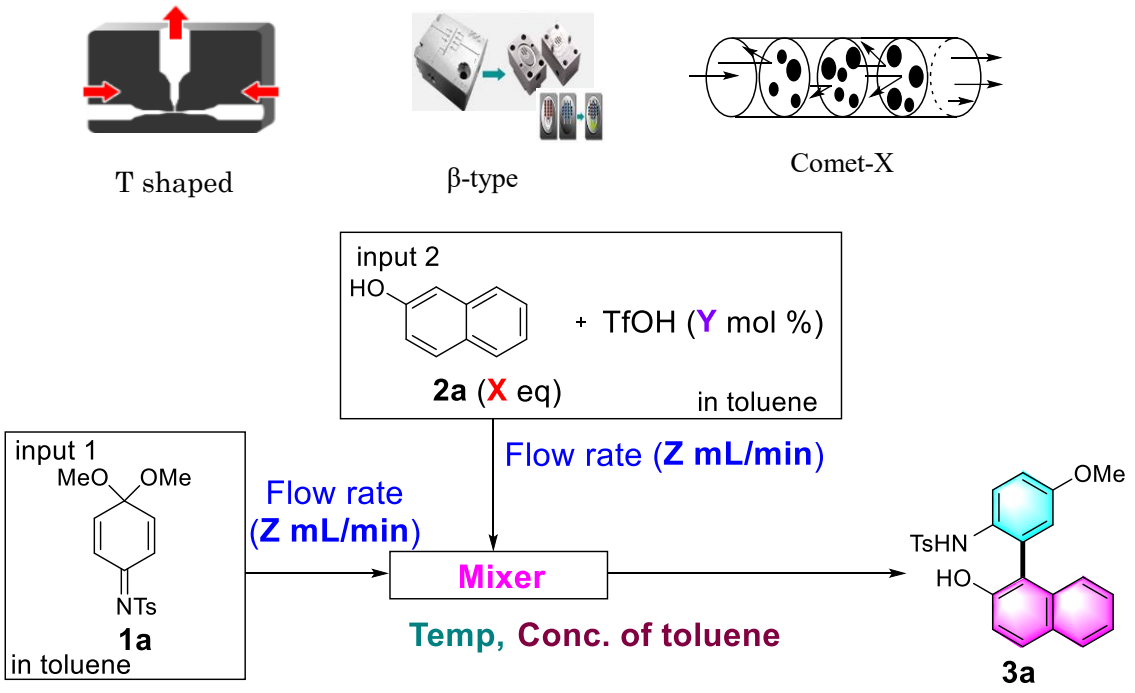


Entry	Solvent (0.01 M)	Yield (%)
1	Toluene	42
2	THF	24
3	Et_2O	23
4	Acetone	11
5	MeOH	11

Table 1.2. Optimization table of solvent screening; Reaction conditions: **1a** (0.065 mmol), **2a** (0.078 mmol), solvent (0.65 mL), TfOH (0.65 μmol); Yield was determined as an ^1H NMR yield using trimethoxy benzene as an internal standard.

3.5. BO-assisted Optimization

To improve low chemical yields in batch system, I applied the flow system for this reaction using toluene and TfOH (1 mol %). The flow system can control a highly reactive intermediate via appropriate thermal transfer and an efficient mixing process. Additionally, Bayesian optimization is also used to predict the appropriate reaction conditions efficiently minimizing the trials and error experiments. Then, six parameters (flow rate, temperature, catalyst loading, concentration, amount of reagent, and types of micro reactor) including categorical parameters were investigated. The type of flow reactor was selected as a non-numerical parameter because it is always can provide the variable ability of efficient mixing and heat transfer which is directly affecting the yield (**Scheme 1.4**). In this approach, a categorical variable can be round to the closest integer and induced to the optimal value along with the optimization of a larger number of continuous numerical parameters. (five precious numerical parameters with only one categorical parameter)



Scheme 1.4. BO-assisted multi-parameter screening in flow synthesis of functionalized biaryls under mild conditions.

3.6. BO-assisted parallel screening of flow reaction conditions

As an initial trial, the starting material **1a** and 2-naphthol (**2a**) were put into the Comet-X flow reactor with the fixed five parameters conditions (flow rate, temperature, catalyst loading, concentration, amount of reagent as shown in **Table 1.3,** entry 1. Interestingly, the desired biaryl was obtained in 68% yield. Inspired from this initial trial, 5 experiments with different parameters were carried out to obtain the initial training data set for further application of BO-ML process; equivalent of **2a** (1–3 eq.), temperature (20–60 °C), concentrations of **1a** in toluene (0.01–0.1 M), flow rate (0.05–0.2 mL/min), catalyst loading (0.5–2 mol%), and mixer type (Comet X, β-type, and T-shaped) (Table 1, entries 1–5). (**Table 1.3**)

Table 1.3. Simultaneous multi-parameter BO-assisted screening of functionalized biaryl formation in flow system.

Entry	Mixer	X Equiv of **2a**	Temp. (°C)	Conc. (M)	Flow rate (Z mLmin^{-1})	TfOH (Y mol %)	Yield **3a** (%)
1)	Comet X	2	60	0.05	0.05	1	68
2)	Comet X	3	40	0.01	0.2	0.5	73
3)	β-type	1	60	0.01	0.1	2	42
4)	β-type	3	20	0.1	0.1	0.5	28
5)	T-shaped	1	40	0.05	0.05	2	55
6)	T-shaped	2	20	0.1	0.2	1	75
			BO was applied from entry 1 to 6				
7)	T-shaped	2	20	0.1	0.15	1	81
8)	Comet X	2.3	55	0.039	0.04	1	77
9)	β-type	1.1	85	0.15	0.1	2.4	40
			BO was applied from entry 1 to 9				
10)	T-shaped	1.3	15	0.11	0.15	1.2	78
11)	T-shaped	2.1	30	0.061	0.15	1.1	76
12)	Comet X	2.8	50	0.014	0.11	1	79
			BO was applied from entry 1 to 12				
13)	Comet X	3.4	55	0.01	0.032	1.3	88
14)	Comet X	2.2	15	0.1	0.14	1.7	44
15)	Comet X	3.0	25	0.015	0.08	1.5	96

BO was applied to the first data set from entries 1 to 6. The next three parameters to evaluate were given by BO using parallel lower confidence bound which explores a maximum in parallel with batches of fixed size and avoids falling into certain parameters and local maximum. After the evaluation (entries 1-9), the yield was slightly improved to 81% under the reaction conditions in entry 7 (mixer: T-shape; equivalent of **2a**: 2 eq.; temperature: 20 °C; concentrations of **1a** in toluene: 0.1 M; flow rate: 0.15 mL/min; catalyst loading: 1 mol%). The further prediction was carried with a total of nine results (entries 1–9) and the BO estimated the three conditions using T-shaped and Comet X in entries 10–12, excluding T-shape by BO. It because there is further no improvement of the yield was expected. Finally, an additional three more experiments prediction was declared by BO from entries 1 to 12 with Comet X as a micro-mixer. To our deligt, the desired product **3a** was obtained in 96% yield within 15 min under the BO-predicted conditions as shown in **Table 1.3**, entry 15, and **Figure 1.3**; mixer: Comet X; the equivalent of **2a**: 3 eq.; temperature: 25 °C; concentrations of **1a** in toluene: 0.015 M; flow rate: 0.08 mL/min; catalyst loading: 1.5 mol%).

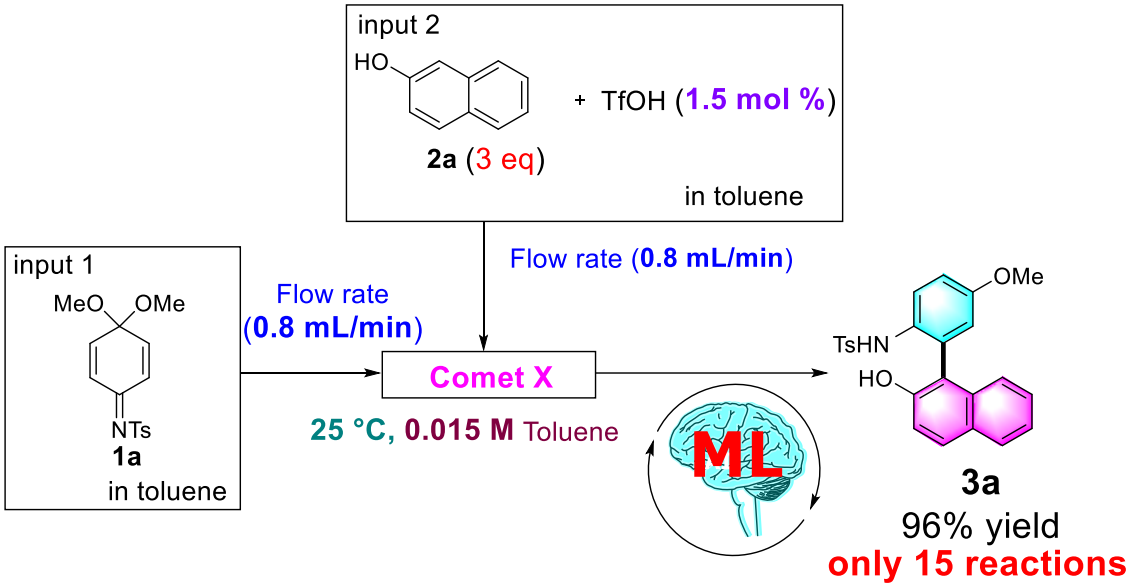
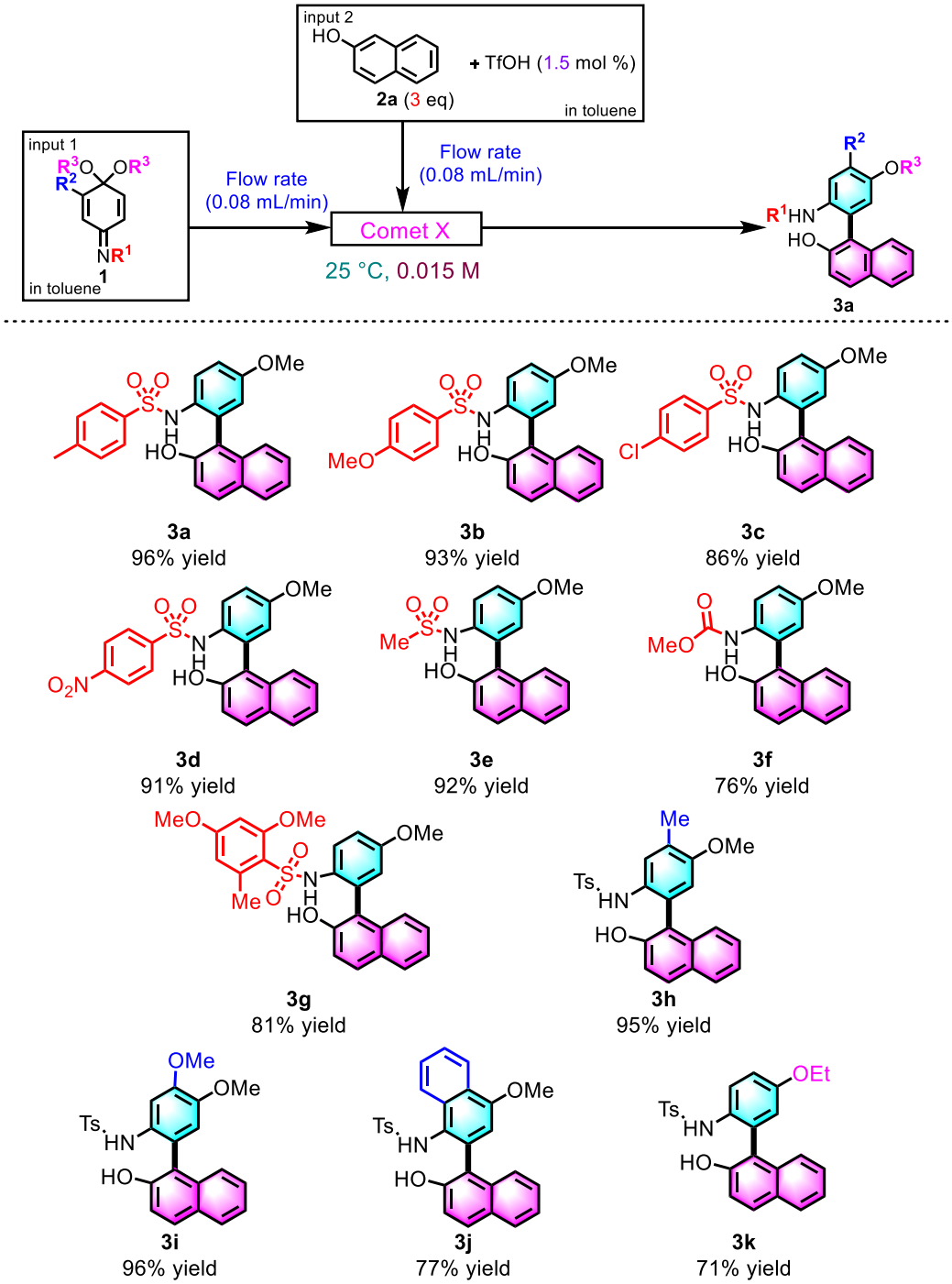


Figure 1.3. BO estimated reaction conditions and their experimental outcome.

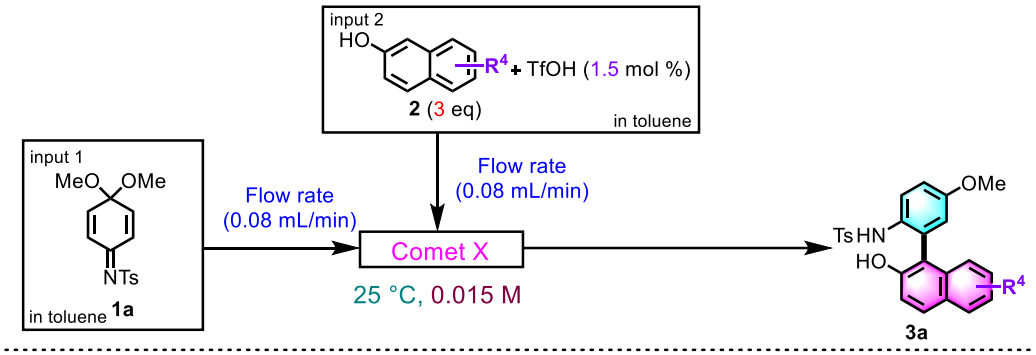
3.7. Substrate scope 1

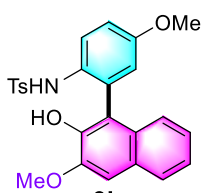


Scheme 1.4. Scope of the substrate of biaryl synthesis with **1** and arenols **2a**. Yields are those of isolated **3**. Reaction conditions: equivalent of **2**: 3 equiv.; temperature: 25 °C; concentrations of **1** in toluene: 0.015 M; flow rate: 0.08 mL/min; residence time: 15 min; catalyst loading: 1.5 mol%.

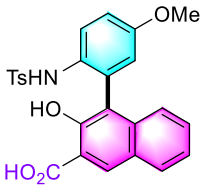
With the BO-established conditions in hand, scope and limitations of dienone **1** were examined (**Scheme 1.4**). The substituent R^1 such as 4-$MeOC_6H_4SO_2$ (**1b**), 4-$ClC_6H_4SO_2$ (**1c**), 4-$NO_2C_6H_4SO_2$ (**1d**), $MeSO_2$ (**1e**), MeOCO (**1f**), and 2,4,6-$Me_3C_6H_2SO_2$ (**1g**) led to the corresponding biaryls in up to 96% yield. When the substituent R^2 such as Me (**1h**), MeO (**1i**) were converted into the corresponding single coupling products **3h** and **3i** in 95% and 96% yields with high regio-selective manner. 1-Naphthyl-derived dienone **1j** was also suitable substrate and led to biaryl **3j** in 77% yield. In addition, diethyl acetal **1k** was found to smoothly react with **2a** to give biaryl **3k** in 71% yield.

3.8. Substrate scope 2

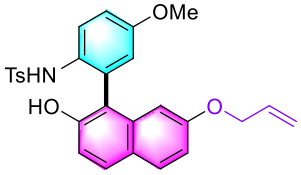




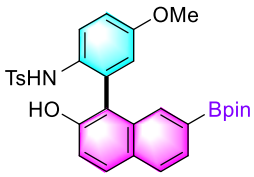
3l
68% yield



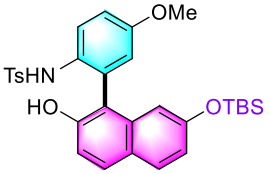
3m
83% yield



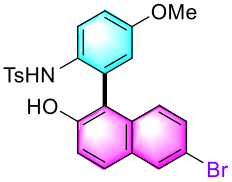
3n
80% yield



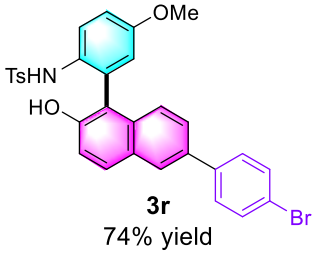
3o
82% yield



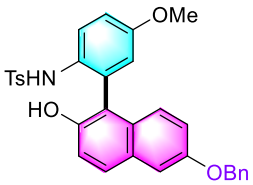
3p
82% yield



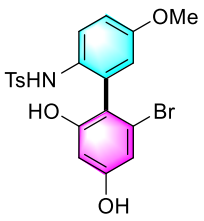
3q
74% yield



3r
74% yield



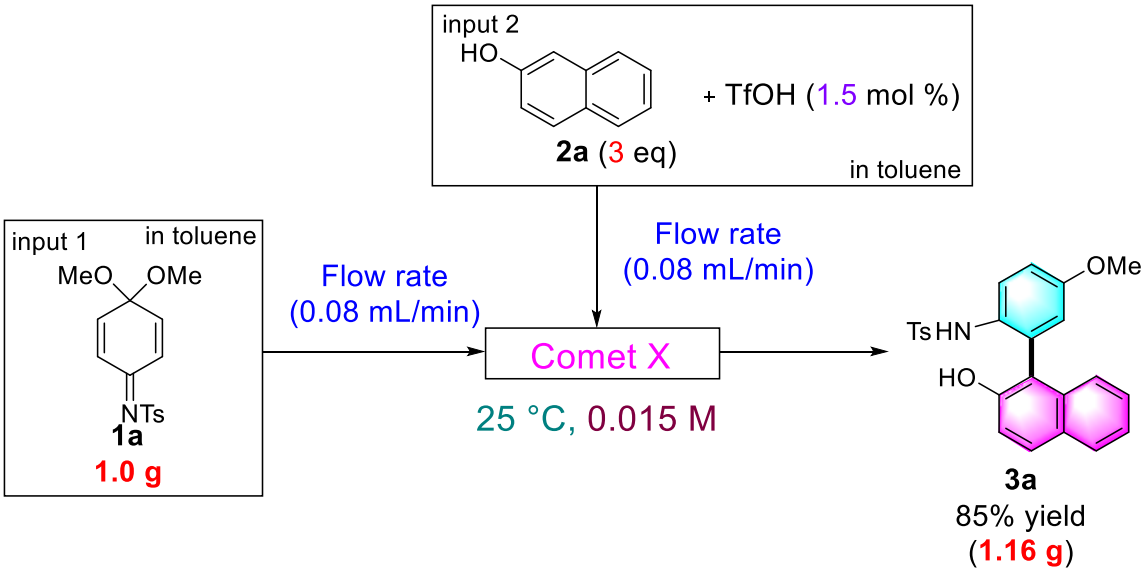
3s
85% yield



3t
67% yield

Scheme 1.5. Scope of the substrate of biaryl synthesis with **1a** and arenols **2**. Yields are those of isolated **3**. Reaction conditions: equivalent of **2**: 3 eq.; temperature: 25 °C; concentrations of **1** in toluene: 0.015 M; flow rate: 0.08 mL/min; residence time: 15 min; catalyst loading: 1.5 mol%.

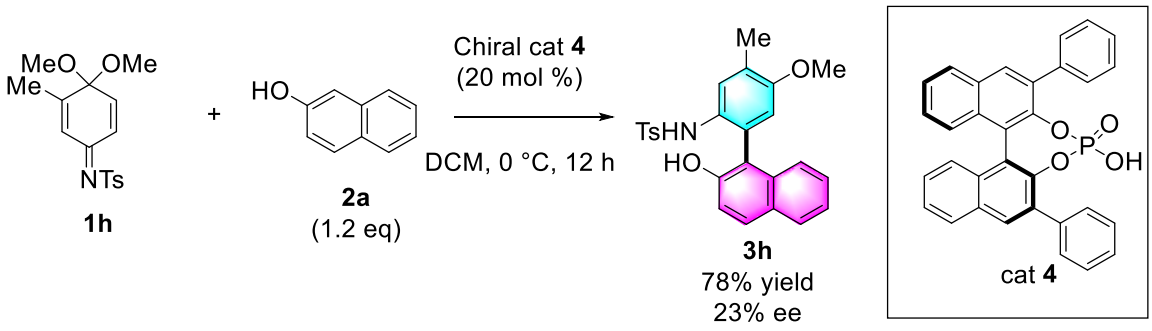
Next, the different naphthol derivatives **2** were screened. The reaction of the substituted 2-naphthols at the 3 position such as **2l** (R^4 = MeO), **2m** (R^4 = CO_2Me) afforded the coupling products **3l** and **3m** (R^4 = CO_2H) in 68% and 83% yields, respectively; a reason for low yield of **3l** was probabaly due to its low solubility in toluene. Concerning methoxy ester **2m**, the acidic conditions led to acid hydrolysis to give the carboxylic acid. The reaction of the substituted 2-naphthols at the 7 position such as **2n** (R^4 = allyl), **2o** (R^4 = pinacolatoboryl), and **2p** (R^4 = *tert*-butyl dimethyl siloxy) provided the corresponding aryls in up to 82% yield. Compound **1a** was also coupled with 2-naphthols **2q** (R^4 = Br)**,** **2r** (R^4 = 4-BrC_6H_4)**,** and **2s** (R^4 = OBn) bearing a substituent at the 6-position to afford the corresponding 2-amino-2'-hydroxy-products **3q**, **3r,** and **3s** in 74–85% yields, respectively. Using the resorcinol derivative **2t** as a substrate the coupling product **3t** was isolated in 67% yield. In addition, gram-scale synthesis was successfully performed in a flow system to get the desired highly functionalized biaryl in 85% yield (**Scheme 1.6)**.



Scheme 1.6. Gram scale synthesis of **3a** in the flow system

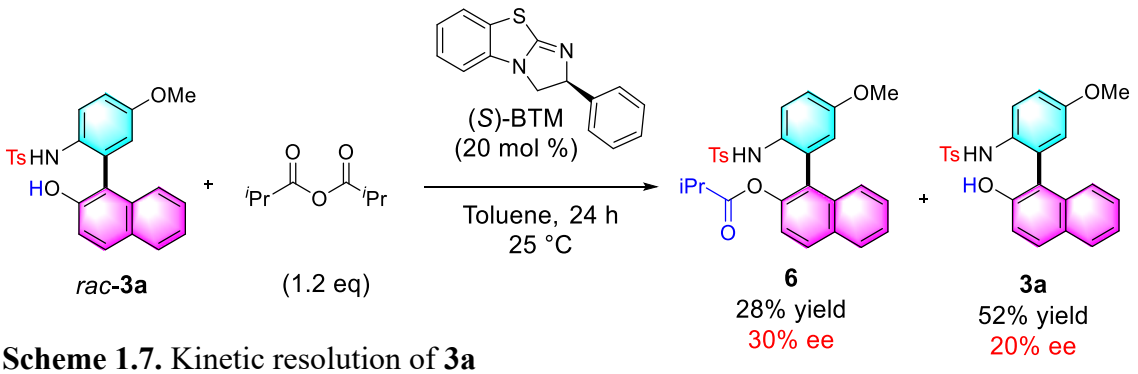
3.9. Synthesis of highly functionalized optically active biaryl

To demonstrate the enantioselective synthesis of chiral biaryl compound **3h,** axialy chiral phosphoric acid-catalyzed reaction of dienone **1h** and **2a** was carried out. The reaction in DCM for 12 h provided the optically active biaryl with but only 23% ee. No improvement of ee was observed even though using Akiyama-Therada chiral catalyst[17] having bulky substituents (naphthyl, anthracene and) at 3,3'-position on chiral binaphtyl skeltone.



Scheme 1.6. Enantioselective synthesis of chiral biaryls **3h** synthesis.

In addition, kinetic resolution of **3a** was also attempted. Organocatalyst (*S*)-BTM (2-phenyl-2,3-dihydroimidazo[2,1-b][1,3]benzothiazole) was utilized for the kinetic resolution with isobutylic anhydride.[18] Although the acylation of **3a** smoothly proceeded to give protected biaryl **6**, the optical purity of 6 was 30% ee with 28% yield.And the unreacted **3a** was recovered in 20% ee with 52% yield (**Scheme 1.7**)



Scheme 1.7. Kinetic resolution of **3a**

3.10 Plausible Mechanism

Kürti and Kita independentlly reported their plausible reaction mechanism as two possible pathways (**Figure 1.4**): (a) a formation of the mixed acetal/[3,3]-sigmatropic rearrangement, and (b) a nucleophilic substitution promoted electron donation of the oxygen atom *via* oxocarbenium intermediate to provide the desired biaryl **3a**.

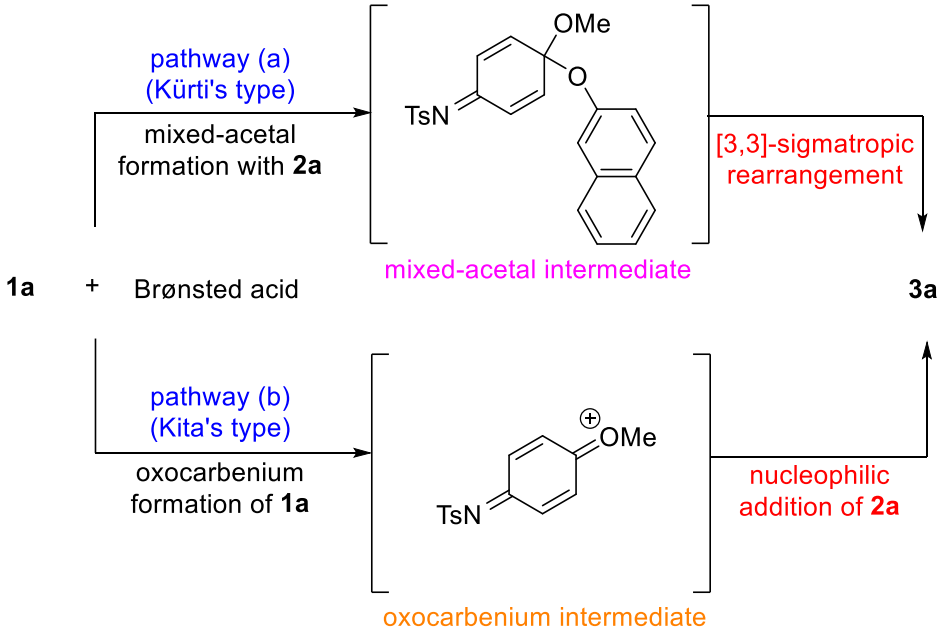
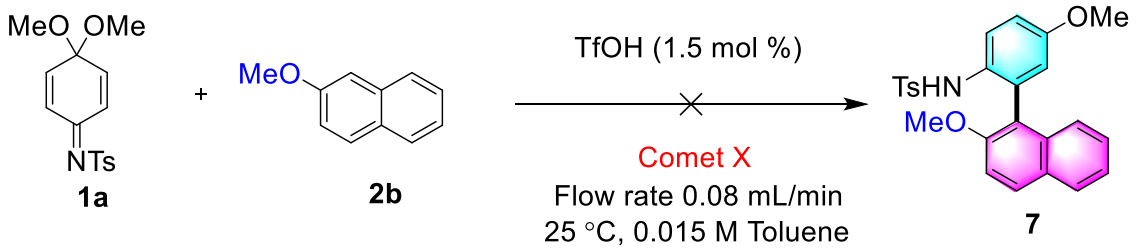


Figure 1.4. Proposed reaction mechanism

When we carried out the coupling reaction of **3a** with methyl capped 2 naphthol, the desired product **7** was not observed (**Scheme 1.8**). Therefore, we suggested that our flow reaction would proceed through the pathway (a) via *mixed-acetal intermediate*.



Scheme 1.8. Model reaction with methyl capped 2-naphthol (control experiment)

3.12 Summary

In conclusion, I demonstrated the BA catalyzed synthesis of highly functionalized biaryl in a flow reaction supported by the BO-assisted multi-parameter screening. In this screening, numeric and categorical parameters were successfully evaluated. The 6 parameters were simultaneously screened (flow rate, temperature, concentration, amount of reagent (**2**), catalyst loading, flow reactor type as a categorical parameter). Finally, within 15 trials of experiments, an appropriate condition for the synthesis was found. Under the BO-predicted conditions, the desired biaryls were obtained in up to 96% yield within 15 min residence time.

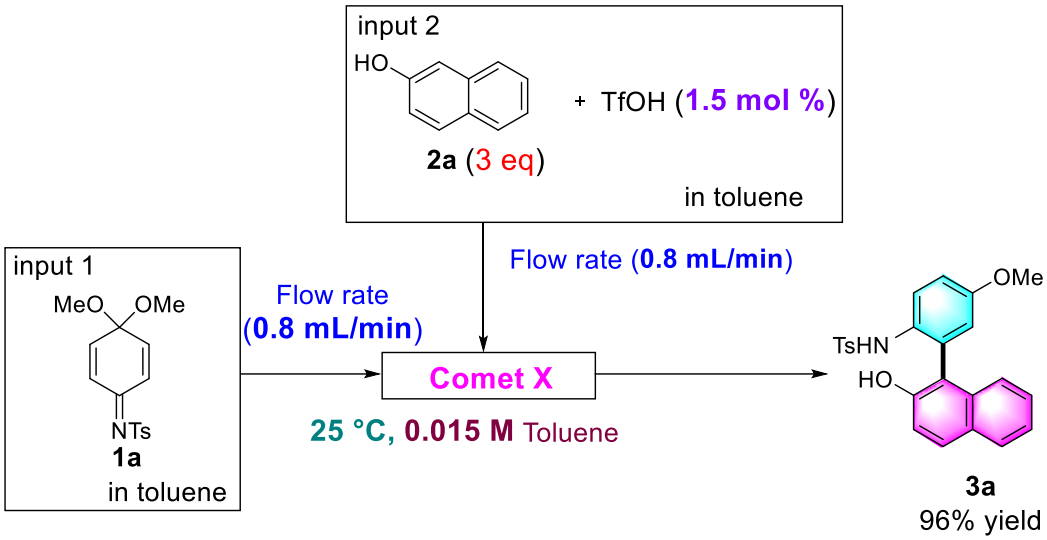
3.13 References

1. A. M. Schweidtmanna, A. D. Claytonc, N. Holmes, E. Bradford, R. A. Bournec, A. A. Lapkin, *Chem. Eng. J*., **2018**, *352*, 277. b) D. Reker, E. A. Hoyt, G. J. L. Bernardes, T. Rodrigues, *Cell Rep. Phys. Sci*. **2020**, *1*, 100247.
2. a) M. Kondo, A. Sugizaki, Md. I. Khalid, H. D. P. Wathsala, K. Ishikawa, S. Hara, T. Takaai, T. Washio, S. Takizawa, H. Sasai, *Green Chem*. **2021**, *23*, 5825. b) A. Mistry, A. A. Franco, S. J. Cooper, S. A. Roberts, V. Viswanathan, *ACS Energy Lett*. **2021**, *6*, 1422. c) K. Min, B. Choi, K. Park, E. Cho, *Sci. Rep.* **2018**, *8*, 15778.
3. a) J. Li, P. Reiser, B. R. Boswell, A. Eberhard, N. Z. Burns, P. Friederich, S. A. Lopez, *Chem. Sci*. **2021**, *12*, 5302. b) P. K. D-P. Herten, T. Buckup**,** *J. Phys. Chem. B.* **2020**, *124*, 6358.
4. P. Vámosi, K. Matsuo, T. Masuda, K. Sato, T. Narumi, K. Takeda, N. Mase, *Chem. Rec*. **2019**, *19*,77.
5. J. Snoek, H. Larochelle, R. P. Adams, *In Advances in Neural Information Processing Systems*, **2012**, *25*, 2951. b) B. Shahriari, K. Swersky, Z. Wang, R. P. Adams, N. Freitas, *Proc. IEEE*, **2016**, 104, 148.
6. a) D. R. Jones, M. Schonlau, W. J. Welch, *J. Glob. Optim*. **1998**, *13*, 455. b) J. Snoek, H. Larochelle, R. P. Adams, *Adv. Neural Inf. Process. Syst*. **2012**, 2951. c) O. Chapelle, L. Li, *Adv. Neural Inf. Process. Syst*. **2011**, 2249.
7. H. Wang, B. Stein, M. Emmerich, T. Back, *2017 IEEE International Conference on Systems, Man, and Cybernetics (SMC)* **2017**, 507, DOI: 10.1109/SMC.2017.8122656.
8. T. Uenoa, T. D. Rhone, Z. Houc, T. Mizoguchi, K. Tsudaa, *Mater. Discov*. **2016**, *4*, 18.

9. B. J. Shields, J. Stevens, J. Li, M. Parasram, F. Damani, J. I. M. Alvarado, J. M. Janey, R. P. Adams, A. G. Doyle, *Nature* **2021**, *590*, 89.
10. O. Mitsunobu, Y. Yamada, *Bull. Chem. Soc. Jpn.* **1967**, *40*, 2380.
11. W.-L. Hu, X.-G. Hu, L. Hunter, *Synthesis* **2017**, *49*, 4917.
12. a) T. Ahneman, J. G. Estrada, S. Lin, S. D. Dreher, A. G. Doyle, *Science* **2018**, 360, 186. b) H. Moriwaki, Y.-S. Tian, N. Kawashita, T. Takagi, *J. Cheminform*. **2018**, *10*, 4.
13. a) G. Bringmann, T. Gulder, T. A. M. Gulder, M. Breuning, *Chem. Rev*. **2011**, *111*, 563. b) A. Zask, J. Murphy, G. A. Ellestad, *Chirality* **2013**, *25*, 265. c) S. R. LaPlante, L. D. Fader, K. R. Fandrick, D. R. Fandrick, O. Hucke, R. Kemper, S. P. F. Miller, P. J. Edwards, *J. Med. Chem*. **2011**, *54*, 7005. d) G. Bringmann, A. J. P. Mortimer, P. A. Keller, M. J. Gresser, J. Garner, M. Breuning, *Angew. Chem. Int. Ed*. **2005**, *44*, 5384.
14. G. P. McGlacken, L. M. Bateman, *Chem. Soc. Rev*. **2009**, *38*, 2447. b) J. A. Ashenhurst, *Chem. Soc. Rev*. **2010**, *39*, 540. c) A. Lei, W. Liu, C. Liu, M. Chen, *Dalton Trans*. **2010**, *39*, 10352. d) Y.-X. Su, L.-P. Sun, *Mini-Rev. Org. Chem*. **2012**, *9*, 87.
15. H. Gao, Q-L. Xu, C. Keene, M. Yousufuddin, D. H. Ess, L. Krurti, *Angew. Chem. Int. Ed*. **2016**, *55*, 566.
16. T. Kamitanaka, K. Morimoto, K. Tsuboshima, D. Koseki, H. Takamuro, T. Dohi, Y. Kita, *Angew. Chem. Int. Ed*. **2016**, *55*, 15535.
17. T. Akiyama, J. Itoh, K. Yokota, K. Fuchibe, *Angew. Chem. Int. Ed.* **2004**, *43*, 1566. b) D. Uraguchi, K. Sorimachi, M. Terada, *J. Am. Chem. Soc.* **2004**, *126*, 5365.
18. J. Lai, R. M. Neyyappadath, A. D. Smith, M. A. Pericàsa, *Adv. Synth. Catal.* **2020**, *362*, 1370– 1377.

X A Tutorial on Bayesian Optimization of Expensive Cost Functions, with Application to Active User Modeling and Hierarchical Reinforcement Learning Eric Brochu, Vlad M. Cora and Nando de Freitas December 14, 2010

3.14. Experimental section



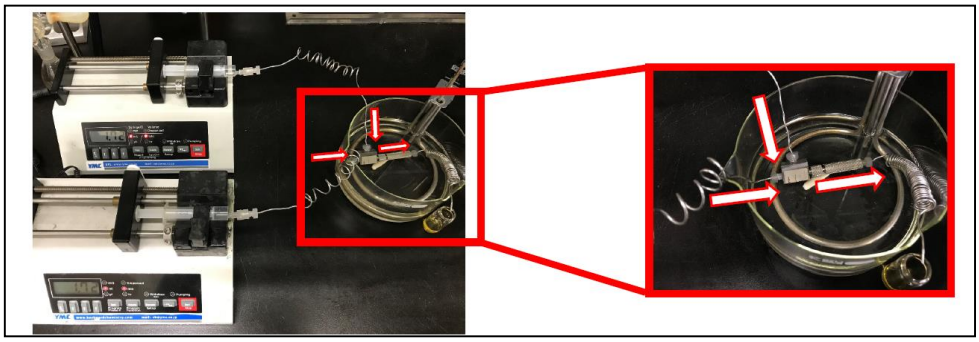
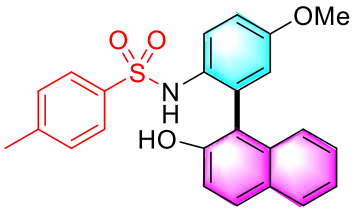


Figure S1: General procedure

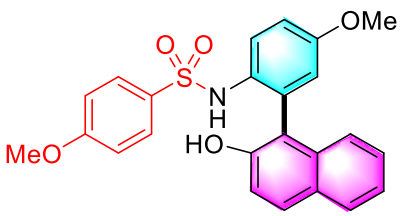
As shown in Fig. S1, a flow microreactor system is fixed with two input syringes. A solution of **1a** (0.065 mmol) in toluene (2.16 mL) was loaded in one syringe and fixed with a syringe pump as input 1. And **2a** (0.195 mmol, 3.0 eq.) in toluene (1.86 mL), was mixed in another vial. TfOH acid solution (0.00325 M) was made in toluene, and 0.3 mL of TfOH solution was taken and added to **2a** containing vial. Then **2a** with TfOH with load to syringe and fixed as input 2. The flow rate was fixed to 0.08 mL/min for both input and continuous flow was started. The outcome from continuous flow was collected and quenched with aq. $NaHCO_3$. The organic layer was extracted with EtOAc and the collected organic layer was dried in Na_2SO_4. The crude mixture was concentrated and column chromatography was performed to purify the desired **3a** as a white solid (*n*-

hexane/EtOAc).



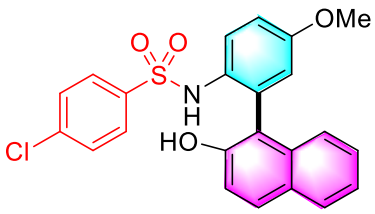
3a

3a; white solid; 96% yield; ^{1}H-NMR (400 MHz, $CDCl_3$) δ 7.77-7.83 (m, 3H), 7.31-7.35 (m, 1H), 7.24 (d, *J* = 8.2 Hz, 2H), 7.18-7.22 (m, 1H), 7.16 (d, *J* = 8.5 Hz, 1H), 7.02 (dd, *J* = 9.2, 3.2 Hz, 1H), 6.93 (d, *J* = 8.2 Hz, 2H), 6.89 (d, *J* = 8.7 Hz, 1H), 6.71 (d, *J* = 2.7 Hz, 1H), 6.31 (s, 1H), 5.00 (s, 1H), 3.77 (s, 3H), 2.29 (s, 3H), ^{13}C-NMR (101 MHz, $CDCl_3$) δ 157.67, 150.44, 143.57, 135.85, 132.74, 130.81, 129.42, 129.10, 128.69, 128.36, 128.29, 127.26, 126.95, 125.71, 123.87, 123.71, 55.61, 21.59; HRMS (ESI) calcd for $C_{24}H_{21}NO_4SNa$: *m/z* ([M+Na$^+$]) 442.1083, found 442.1079; IR (KBr) 3495, 3352, 2975, 2363, 2326, 1627, 1491, 1384, 1288, 1161, 1092, 1036, 999, 919, 880, 754, 556, 503, 419 cm^{-1}



3b

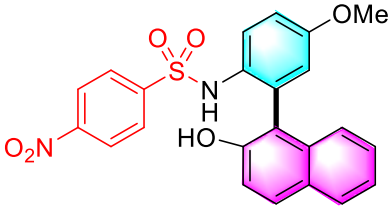
3b; white solid; 93% yield; ^{1}H-NMR (400 MHz, $CDCl_3$) δ 7.78-7.83 (m, 3H), 7.28-7.35 (m, 3H), 7.21 (td, *J* = 7.7, 1.2 Hz, 1H), 7.16 (d, *J* = 9.2 Hz, 1H), 7.03 (dd, *J* = 8.9, 3.0 Hz, 1H), 6.90 (d, *J* = 8.2 Hz, 1H), 6.72 (d, *J* = 3.2 Hz, 1H), 6.62 (dd, *J* = 6.9, 1.8 Hz, 2H), 6.23 (s, 1H), 4.85 (s, 1H), 3.79 (s, 3H), 3.77 (s, 3H), ^{13}C-NMR (101 MHz, $CDCl_3$) δ 162.97, 157.66, 150.48, 132.73, 130.83, 130.42, 129.09, 128.85, 128.27, 128.05, 127.35, 125.55, 123.80, 117.68, 116.94, 115.73, 115.61, 114.00, 55.62, 55.50; HRMS (ESI) calcd for $C_{24}H_{21}NO_5SNa$: *m/z* ([M+Na$^+$]) 458.1033, found 458.1029; IR (KBr) 3474, 3249, 2964, 2833, 1594, 1573, 1496, 1381, 1330, 1267, 1153, 1092, 1041, 1030, 951, 817, 682 cm^{-1}



3c

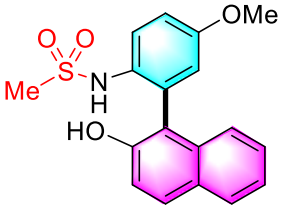
3c; 86% yield; white solid; ^{1}H-NMR (400 MHz, $CDCl_3$) δ 7.78-7.83 (m, 3H), 7.36 (td, *J* = 7.4, 1.2 Hz, 1H), 7.14-7.24 (m, 4H), 7.00-7.06 (m, 3H), 6.84 (d, *J* = 8.2 Hz, 1H), 6.74 (d, *J* = 2.7 Hz, 1H), 6.37 (s, 1H), 4.90 (s, 1H), 3.78 (s, 3H), ^{13}C-NMR (101 MHz, $CDCl_3$) δ 158.08, 150.10, 139.26, 137.34, 132.66, 130.84, 129.15, 129.07, 128.99, 128.33, 128.19, 127.96, 127.54, 124.02, 123.61, 117.51, 117.11, 115.94, 115.54, 55.64; HRMS (ESI) calcd for $C_{23}H_{18}ClNO_4SNa$: *m/z* ([M+Na$^+$]) 462.0537, found 462.0541; IR (KBr) 3491, 3249, 3085, 3011, 2941, 2837, 1613, 1490,

1331, 1286, 1204, 1163, 1093, 1037, 955, 883, 755 cm^{-1}



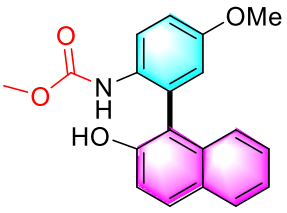
3d

3d; 91% yield; yellow solid; ^{1}H-NMR (400 MHz, $CDCl_3$) δ 7.79 (d, *J* = 8.7 Hz, 2H), 7.68 (q, *J* = 8.4 Hz, 3H), 7.29 (d, *J* = 8.7 Hz, 2H), 7.23 (t, *J* = 7.6 Hz, 1H), 7.06-7.14 (m, 3H), 6.90 (d, *J* = 8.7 Hz, 1H), 6.75 (t, *J* = 3.4 Hz, 2H), 5.10 (s, 1H), 3.80 (s, 3H), ^{13}C-NMR (101 MHz, $CDCl_3$) δ 158.61, 149.22, 149.05, 144.46, 132.57, 131.44, 130.80, 129.84, 129.14, 128.24, 127.34, 127.13, 126.65, 124.08, 124.00, 123.61, 117.50, 117.39, 116.86, 115.23, 55.68; HRMS (ESI) calcd for $C_{23}H_{18}N_2O_6SNa$: *m/z* ([M+Na^+]) 473.0778, found 473.0079; IR (KBr) 3545, 3321, 2953, 1606, 1525, 1343, 1162, 856, 740, 680, 544 cm^{-1}



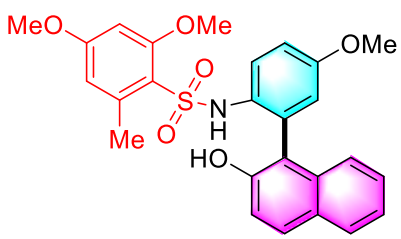
3e

3e; 92% yield; white solid; ^{1}H-NMR (400 MHz, $CDCl_3$) δ 7.85-7.90 (m, 2H), 7.75 (d, *J* = 9.2 Hz, 1H), 7.39-7.42 (m, 2H), 7.28 (d, *J* = 1.8 Hz, 1H), 7.25 (d, *J* = 3.2 Hz, 1H), 7.09 (dd, *J* = 9.2, 3.2 Hz, 1H), 6.90 (d, *J* = 2.7 Hz, 1H), 5.92 (s, 1H), 5.24 (s, 1H), 3.84 (s, 3H), 2.60 (s, 3H), ^{13}C-NMR (101 MHz, $CDCl_3$) δ 158.23, 150.66, 132.91, 131.13, 129.31, 129.06, 128.76, 127.78, 126.23, 124.24, 123.63, 117.92, 117.18, 116.07, 115.67, 55.74, 39.46; HRMS (ESI) calcd for $C_{18}H_{17}NO_4SNa$: *m/z* ([M+Na^+]) 366.0770, found 366.0770; IR (KBr) 3386, 3307, 3006, 2925, 2838, 1615, 1577, 1494, 1373, 1150, 1038, 981, 821, 750, 688, 586, 472 cm^{-1}



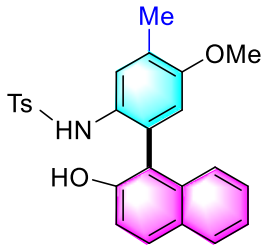
3f

3f; 76% yield; white solid; ^{1}H-NMR (400 MHz, $CDCl_3$) δ 8.11 (s, 1H), 7.86 (d, *J* = 9.2 Hz, 1H), 7.84 (t, *J* = 2.1 Hz, 1H), 7.37 (d, *J* = 4.6 Hz, 2H), 7.28 (d, *J* = 9.2 Hz, 1H), 7.24-7.25 (m, 1H), 7.09 (dd, *J* = 9.2, 2.7 Hz, 1H), 6.82 (d, *J* = 3.2 Hz, 1H), 6.24-5.99 (1H), 3.81 (s, 3H), 3.59 (s, 3H); HRMS (ESI) calcd for $C_{19}H_{17}NO_4Na$: *m/z* ([M+Na^+]) 346.1050, found 346.1051; IR (KBr) 3412, 3308, 2958, 2922, 2375, 1713, 1624, 1517, 1460, 1341, 1244, 1173, 1100, 1036, 955, 820, 750, 687, 614, 580, 551, 421 cm^{-1}



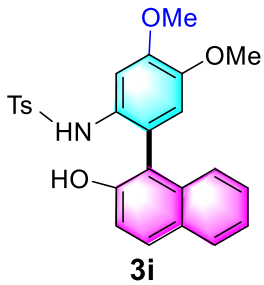
3g

3g; 81% yield; white solid; ^{1}H-NMR (400 MHz, $CDCl_3$) δ 7.81 (dd, J = 9.2, 3.7 Hz, 2H), 7.76 (d, J = 8.2 Hz, 1H), 7.35 (d, J = 8.7 Hz, 1H), 7.31 (s, 1H), 7.27-7.29 (m, 1H), 7.12-7.16 (m, 1H), 7.01 (dd, J = 8.9, 3.0 Hz, 2H), 6.95 (d, J = 8.7 Hz, 1H), 6.62 (d, J = 2.7 Hz, 1H), 6.02 (s, 1H), 5.60 (s, 1H), 3.73 (s, 3H), 3.67 (s, 3H), 3.18 (s, 3H), 1.99 (s, 3H), ^{13}C-NMR (101 MHz, $CDCl_3$) δ 162.28, 157.46, 156.05, 150.63, 133.41, 131.02, 130.18, 129.33, 128.92, 128.56, 127.55, 127.04, 126.59, 124.54, 123.53, 117.84, 117.67, 116.82, 116.46, 115.41, 93.95, 55.57, 55.55, 55.33, 15.26; HRMS (ESI) calcd for $C_{26}H_{25}NO_6SNa$: *m/z* ([M+Na$^+$]) 502.1295, found 502.1290; IR (KBr) 3413, 3304, 2948, 1606, 1495, 1433, 1320, 1287, 1269, 1214, 1138, 1033, 817, 653, 553 cm^{-1}



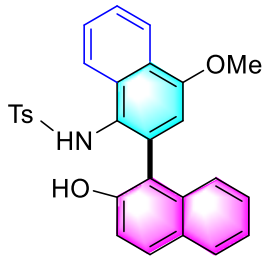
3h

3h; 95% yield; white solid; ^{1}H-NMR (400 MHz, $CDCl_3$) δ 7.81 (t, J = 8.2 Hz, 2H), 7.66 (s, 1H), 7.33 (t, J = 7.3 Hz, 1H), 7.27 (s, 1H), 7.14-7.22 (m, 2H), 6.94 (dd, J = 23.4, 8.2 Hz, 3H), 6.58 (s, 1H), 6.19 (s, 1H), 4.76 (s, 1H), 3.72 (s, 3H), 2.31 (s, 6H), ^{13}C-NMR (101 MHz, $CDCl_3$) δ 155.97, 150.56, 143.53, 135.86, 132.89, 130.67, 129.42, 129.08, 128.76, 128.31, 128.15, 127.22, 126.96, 126.69, 124.81, 123.95, 123.67, 117.60, 116.02, 112.88, 55.65, 21.63, 16.47; HRMS (ESI) calcd for $C_{25}H_{23}NO_4SNa$: *m/z* ([M+Na$^+$]) 456.1240, found 456.1237; IR (KBr) 3401, 3290, 3066, 2980, 1627, 1504, 1376, 1267, 1155, 1092, 914, 816, 746, 673 cm^{-1}



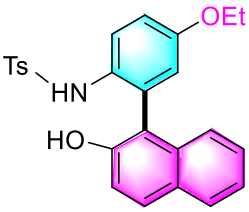
3i

3i; 96% yield; white solid; ^{1}H-NMR (400 MHz, $CDCl_3$) δ 7.81 (t, J = 8.7 Hz, 2H), 7.47 (s, 1H), 7.32-7.35 (m, 1H), 7.28 (d, J = 8.2 Hz, 2H), 7.15-7.22 (m, 2H), 6.98 (d, J = 7.8 Hz, 2H), 6.88 (d, J = 8.2 Hz, 1H), 6.62 (s, 1H), 6.27 (s, 1H), 4.78 (s, 1H), 4.00 (s, 3H), 3.77 (s, 3H), 2.32 (s, 3H), ^{13}C-NMR (101 MHz, $CDCl_3$) δ 150.86, 149.81, 147.14, 143.85, 135.65, 133.11, 130.81, 129.53, 129.16, 128.36, 127.30, 127.05, 123.85, 123.73, 117.55, 117.42, 115.35, 113.94, 56.28, 56.16, 21.64; HRMS (ESI) calcd for $C_{25}H_{23}NO_5SNa$: *m/z* ([M+Na$^+$]) 472.1189, found 472.1188; IR (KBr) 3403, 3348, 3062, 2969, 2844, 1512, 1344, 1202, 1158, 1012, 980, 812, 744 cm^{-1}



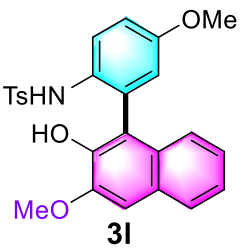
3j

3j; 77% yield: white solid; ^{1}H-NMR (400 MHz, $CDCl_3$) δ 8.30-8.39 (m, 2H), 7.82 (d, J = 8.2 Hz, 2H), 7.73 (dd, *J* = 8.1, 6.1 Hz, 2H), 7.59-7.63 (m, 3H), 7.15 (dd, *J* = 8.2, 5.5 Hz, 1H), 7.11 (d, *J* = 8.7 Hz, 1H), 7.06 (d, *J* = 8.2 Hz, 2H), 6.67 (d, *J* = 7.8 Hz, 2H), 6.65 (s, 1H), 6.56 (s, 1H), 3.95-3.89 (3H), 2.47-2.40 (3H); ^{13}C-NMR (151 MHz, $CDCl_3$) δ 155.40, 149.71, 142.52, 136.82, 133.82, 132.68, 131.39, 130.12, 129.36, 129.00, 128.21, 127.58, 126.91, 126.42, 126.31, 125.45, 124.62, 124.04, 123.58, 122.02, 119.43, 118.03, 107.13, 55.89, 21.53HRMS (ESI) calcd for $C_{28}H_{23}NO_4SNa$: *m/z* ([M+Na^+]) 492.1240, found 492.1248; IR (KBr) 3436, 3276, 3003, 2959, 1627, 1596, 1510, 1368, 1269, 1145, 767, 661, 583 cm^{-1}



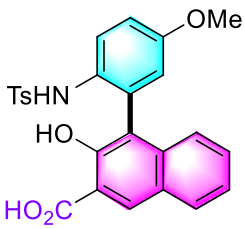
3k

3k; 71% yield; white solid; ^{1}H-NMR (400 MHz, $CDCl_3$) δ 7.77-7.81 (m, 3H), 7.38-7.30 (1H), 7.25 (s, 3H), 7.15 (d, *J* = 8.7 Hz, 1H), 7.04-6.99 (1H), 6.97 (d, *J* = 8.2 Hz, 2H), 6.92-6.81 (1H), 6.70 (d, *J* = 2.7 Hz, 1H), 6.26-6.15 (1H), 4.78-4.61 (1H), 4.07-3.90 (2H), 2.32 (s, 3H), 1.38 (t, *J* = 6.9 Hz, 3H), ^{13}C-NMR (101 MHz, $CDCl_3$) δ 157.07, 150.51, 143.62, 135.87, 132.67, 130.83, 129.46, 129.08, 128.62, 128.34, 127.80, 127.35, 127.01, 125.40, 123.79, 123.76, 117.66, 117.39, 116.17, 115.67, 63.88, 21.61, 14.84; HRMS (ESI) calcd for $C_{25}H_{23}NO_4SNa$: *m/z* ([M+Na^+]) 456.1240, found 456.1239; IR (KBr) 3469, 3257, 2980, 2925, 1608, 1573, 1494, 1386, 1308, 1283, 1268, 1199, 1162, 1091, 935, 916 cm^{-1}



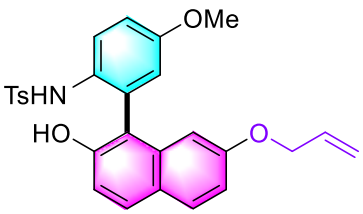
3l

3l; 68% yield; white solid; ^{1}H-NMR (400 MHz, $CDCl_3$) δ 7.77 (d, J = 8.7 Hz, 1H), 7.65 (d, *J* = 8.2 Hz, 1H), 7.28-7.30 (m, 1H), 7.16 (s, 1H), 7.05 (d, *J* = 8.2 Hz, 2H), 6.98-7.02 (m, 2H), 6.83 (d, *J* = 8.2 Hz, 1H), 6.67-6.70 (m, 2H), 6.62 (d, *J* = 7.8 Hz, 2H), 6.11 (s, 1H), 4.10 (s, 3H), 3.75 (s, 3H), 2.12 (s, 3H); HRMS (ESI) calcd for $C_{25}H_{23}NO_5SNa$: *m/z* ([M+Na^+]) 472.1189, found 472.1183; IR (KBr) 3423, 3358, 3072, 3017, 2971, 2946, 2841, 2363, 1608, 1577, 1510, 1492, 1387, 1282, 1174, 1019, 868, 744, 549, 418 cm^{-1}



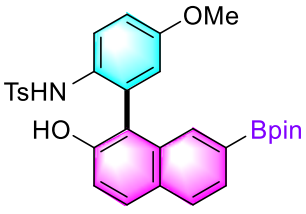
3m

3m; 83% yield; Pale yellow solid; ^{1}H-NMR (400 MHz, $CDCl_3$) δ 11.02 (s, 1H), 8.61 (s, 1H), 7.86-7.88 (m, 1H), 7.62 (d, *J* = 8.2 Hz, 2H), 7.37-7.45 (m, 2H), 7.23 (d, *J* = 8.2 Hz, 3H), 7.12 (dd, *J* = 8.7, 2.7 Hz, 1H), 6.28 (s, 1H), 5.13 (s, 1H), 4.07 (s, 3H), 2.39 (s, 3H), ^{13}C-NMR (151 MHz, $CDCl_3$) δ 169.75, 152.61, 151.90, 142.99, 135.97, 135.31, 132.99, 129.29, 129.22, 128.96, 128.26, 127.29, 126.81, 125.23, 123.81, 121.85, 116.89, 116.03, 113.19, 52.17, 20.95; HRMS (ESI) calcd for $C_{25}H_{21}NO_6SNa$: *m/z* ([M+Na$^+$]) 486.0982, found 486.0980; IR (KBr) 3518, 3419, 3249, 2948, 2373, 1683, 1509, 1449, 1322, 1218, 1158, 951, 809, 669, 528 cm^{-1}



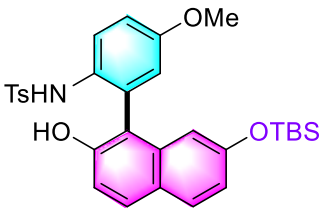
3n

3n; 80% yield; white solid; ^{1}H-NMR (400 MHz, $CDCl_3$) δ 7.79 (d, *J* = 8.7 Hz, 1H), 7.72 (dd, *J* = 14.7, 8.7 Hz, 2H), 7.21 (d, *J* = 8.2 Hz, 2H), 6.98-7.04 (m, 3H), 6.91 (d, *J* = 8.2 Hz, 2H), 6.71 (d, *J* = 2.7 Hz, 1H), 6.31 (s, 1H), 6.20 (d, *J* = 2.7 Hz, 1H), 5.96 (dq, *J* = 17.3, 5.3 Hz, 1H), 5.25-5.33 (m, 2H), 4.70 (s, 1H), 4.28 (d, *J* = 5.5 Hz, 2H), 3.77 (s, 3H), 2.29 (s, 3H); ^{13}C-NMR (101 MHz, $CDCl_3$) δ 157.76, 150.95, 143.68, 135.88, 134.13, 133.02, 130.50, 129.90, 129.33, 128.55, 128.48, 128.43, 126.98, 126.05, 125.96, 124.49, 118.15, 116.68, 116.33, 115.66, 115.02, 103.90, 68.62, 55.62, 21.53; HRMS (ESI) calcd for $C_{27}H_{25}NO_5SNa$: *m/z* ([M+Na$^+$]) 498.1346, found 498.1344; IR (KBr) 3567, 3485, 3276, 3151, 2937, 1622, 1513, 1494, 1379, 1291, 1152, 1093, 1013, 934, 838, 665, 542 cm^{-1}



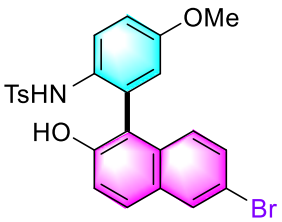
3o

3o; 82% yield; white solid; ^{1}H-NMR (400 MHz, $CDCl_3$) δ 7.71-7.78 (m, 4H), 7.52 (s, 1H), 7.14-7.17 (m, 3H), 7.04 (dd, *J* = 8.9, 3.0 Hz, 1H), 6.78 (d, *J* = 6.0 Hz, 2H), 6.74 (d, *J* = 3.2 Hz, 1H), 6.54 (s, 1H), 5.36 (s, 1H), 3.77 (s, 3H), 1.33 (d, *J* = 3.7 Hz, 12H); ^{13}C-NMR (101 MHz, $CDCl_3$) δ 157.95, 150.02, 143.30, 135.86, 131.99, 131.66, 130.74, 130.49, 129.32, 128.74, 128.37, 127.37, 118.62, 116.93, 115.92, 83.96, 55.68, 24.96, 21.59; HRMS (ESI) calcd for $C_{30}H_{32}BNO_6SNa$: *m/z* ([M+Na$^+$]) 568.1936, found 568.1931; IR (KBr) 3419, 3337, 2982, 2925, 1604, 1500, 1453, 1382, 1267, 1158, 1092, 916, 856, 733, 556 cm^{-1}



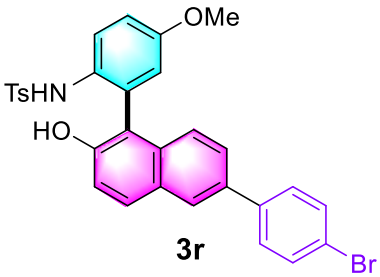
3p

3p; 68% yield; orange solid; ^{1}H-NMR (600 MHz, $CDCl_3$) δ 7.77 (d, J = 8.9 Hz, 1H), 7.71 (d, *J* = 8.2 Hz, 1H), 7.65 (d, J = 8.9 Hz, 1H), 7.19 (d, J = 7.6 Hz, 2H), 7.02 (dd, *J* = 8.9, 2.7 Hz, 1H), 6.99 (d, J = 8.9 Hz, 1H), 6.87-6.91 (m, 3H), 6.69 (d, *J* = 2.7 Hz, 1H), 6.41 (s, 1H), 6.23 (d, *J* = 2.1 Hz, 1H), 3.76 (s, 3H), 2.26 (s, 3H), 0.93 (s, 9H), 0.09 (d, *J* = 1.4 Hz, 6H); 13C-NMR (151 MHz, CHLOROFORM-D) δ 157.72, 154.95, 150.66, 143.68, 135.74, 134.24, 130.43, 129.76, 129.35, 128.56, 126.86, 126.06, 124.68, 119.80, 116.62, 115.68, 115.20, 114.70, 111.31, 55.56, 25.75, 21.54, 18.32, -4.24, -4.44; HRMS (ESI) calcd for $C_{30}H_{35}NO_5SSiNa$: *m/z* ([M+Na^+]) 572.1897, found 572.1893; IR (KBr) 3414, 3348, 2955, 2929, 2857, 1624, 1509, 1466, 1374, 1267, 1160, 1091, 903, 838, 782, 663, 540 cm^{-1}



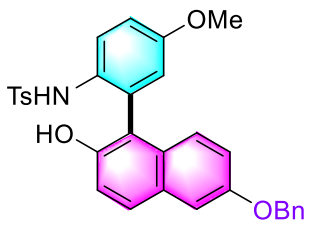
3q

3q; 74% yield; white solid; ^{1}H-NMR (400 MHz, $CDCl_3$) δ 7.92 (d, *J* = 2.3 Hz, 1H), 7.79 (d, *J* = 9.2 Hz, 1H), 7.72 (d, *J* = 9.2 Hz, 1H), 7.16-7.20 (m, 4H), 7.04 (dd, *J* = 8.9, 3.0 Hz, 1H), 6.88 (d, *J* = 8.2 Hz, 2H), 6.67-6.72 (m, 2H), 6.30 (s, 1H), 5.15 (s, 1H), 3.77 (s, 3H), 2.31 (s, 3H), ^{13}C-NMR (101 MHz, $CDCl_3$) δ 157.80, 150.53, 143.77, 135.93, 131.45, 130.29, 130.18, 130.03, 129.78, 129.34, 128.51, 128.04, 126.84, 126.37, 125.79, 118.78, 117.52, 116.99, 116.37, 115.69, 55.64, 21.79; HRMS (ESI) calcd for $C_{24}H_{20}BrNO_4SNa$: *m/z* ([M+Na^+]) 520.0189, found 520.0187; IR (KBr) 3382, 3312, 3080, 2938, 2840, 1601, 1492, 1335, 1156, 1038, 952, 891, 663, 548, 484 cm^{-1}



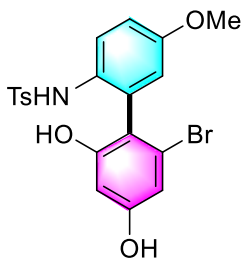
3r

3r; 76% yield; white solid; ^{1}H-NMR (400 MHz, $CDCl_3$) δ 7.87 (dd, *J* = 12.4, 8.7 Hz, 2H), 7.75 (d, *J* = 9.2 Hz, 1H), 7.53-7.58 (m, 3H), 7.33 (dd, *J* = 6.8, 1.9 Hz, 2H), 7.26 (s, 1H), 7.24 (s, 1H), 7.19 (d, *J* = 9.2 Hz, 1H), 7.11 (t, *J* = 0.9 Hz, 1H), 7.03 (dd, *J* = 8.9, 3.0 Hz, 1H), 6.81 (d, *J* = 8.2 Hz, 2H), 6.74 (d, *J* = 3.2 Hz, 1H), 6.34 (s, 1H), 4.94 (s, 1H), 3.77 (s, 3H), 2.15 (s, 3H), ^{13}C-NMR (101 MHz, $CDCl_3$) δ 157.62, 151.19, 143.70, 139.73, 138.68, 135.80, 132.92, 132.05, 130.68, 129.39, 129.26, 128.99, 128.87, 128.48, 127.23, 127.02, 125.02, 123.22, 121.98, 121.45, 118.02, 116.91, 115.92, 115.82, 55.73, 21.61; HRMS (ESI) calcd for $C_{30}H_{24}BrNO_4SNa$: *m/z* ([M+Na^+]) 596.0502, found 596.0502; IR (KBr) 3407, 3326, 3050, 2944, 1622, 1489, 1377, 1328, 1287, 1159, 1091, 823, 662, 554 cm^{-1}



3s

3s; 85% yield; yellow solid; ^{1}H-NMR (400 MHz, $CDCl_3$) δ 7.69-7.78 (m, 3H), 7.29-7.36 (m, 5H), 7.21 (d, *J* = 8.7 Hz, 2H), 7.05 (ddd, *J* = 11.2, 8.5, 2.3 Hz, 2H), 6.98 (d, *J* = 8.7 Hz, 1H), 6.91 (d, *J* = 7.8 Hz, 2H), 6.66 (d, *J* = 3.2 Hz, 1H), 6.26 (d, *J* = 2.3 Hz, 1H), 6.24 (s, 1H), 4.83 (d, *J* = 4.1 Hz, 2H), 4.79 (s, 1H), 3.75 (s, 3H), 2.26 (s, 3H), ^{13}C-NMR (101 MHz, $CDCl_3$) δ 157.85, 157.81, 151.02, 143.63, 136.65, 135.98, 134.09, 130.44, 129.93, 129.35, 128.70, 128.58, 128.51, 128.14, 127.62, 126.97, 126.08, 124.49, 116.59, 116.47, 115.67, 115.08, 104.19, 69.84, 55.61, 21.52; HRMS (ESI) calcd for $C_{31}H_{27}NO_5SNa$: *m/z* ([M+Na$^+$]) 548.1502, found 548.1501; IR (KBr) 3413, 3304, 3010, 2970, 2362, 1623, 1506, 1464, 1377, 1267, 1151, 1091, 919, 855, 811, 757, 691, 549 cm^{-1}



3t

3t; 67% yield; white solid; ^{1}H-NMR (400 MHz, $CDCl_3$) δ 7.74 (d, *J* = 8.2 Hz, 1H), 7.52 (d, *J* = 8.2 Hz, 1H), 7.42 (d, *J* = 9.2 Hz, 2H), 7.28 (s, 1H), 7.18 (d, *J* = 7.8 Hz, 1H), 6.90 (dd, *J* = 8.9, 3.0 Hz, 1H), 6.79 (d, *J* = 9.2 Hz, 1H), 6.65-6.73 (m, 1H), 6.55 (d, *J* = 15.1 Hz, 1H), 6.40 (s, 1H), 3.76 (s, 3H), 2.41 (d, *J* = 18.8 Hz, 3H); HRMS (ESI) calcd for $C_{20}H_{18}BrNO_5SNa$: *m/z* ([M+Na$^+$]) 485.9981, found 485.9978; IR (KBr) 3572, 3376, 3080, 2926, 2839, 1704, 1607, 1596, 1505, 1454, 1379, 1358, 1346, 1248, 1220, 1184, 1157, 1124 cm^{-1}

Chapter 4

Chapter 4

Conclusion

This thesis is aimed to develop new organocatalytic C–C bond-forming reactions in a flow system with efficient machine learning optimization methods. I focused on two types of organocatalytic reactions in the flow system as an efficient mixing and an efficient heat transfer process. I used the flow reaction process to the sequential reaction by controlling the reactive intermediate`s reactivity and heat transfer process to afford high chemical yield. I also achieved the efficient optimization process by ML assistance to get the appropriate reaction parameter of a particular complex reaction by carrying out the minimum number of experiments. This ML optimization process can be reduced the time and cost of achieving green and sustainable process chemistry.

In **Chapter 2**, the sequential reaction of Rauhut-Currier/[3+2] annulation was established by using a chiral phosphine catalyst in flow. This sequential reaction provided the widely used biologically active spirooxindole analogues as the optically active compound in high yield with high enantioselectivity. The flow reaction system resulted in a high yield of products by using its efficient thermal transfer and mixing process. Additionally, GPR was applied to screen this sequential reaction conditions, establishing the optimal conditions with only 10 trails.

In **Chapter 3**, I investigated the flow sequential coupling reaction of dienone with arenol catalyzed by Brønsted acid to give highly functionalized axially chiral biaryls in high yields. In this work, the BO process has been applied to find a multi-parameter screening. The 6 parameters (numerical and categorical) were simultaneously screened to find an appropriate reaction condition, within 15 experimental trials.

As a conclusion of my thesis, the achievement of new reactions and, as well as ML predictions contribute to the development of new synthetic ways with saving time and chemicals. And they will broaden the application of the ML-optimization process and it will give a new era to synthetic organic chemistry in the near future.